DEVELOPMENT OF PROTOCOL FOR 100-YEAR SERVICE LIFE OF SYNTHETIC FIBER-REINFORCED CONCRETE PIPES

By

Maziar Mahdavi

DISSERTATION

Submitted in partial fulfillment of the requirements

for the degree of Doctor of Philosophy at

The University of Texas at Arlington

August, 2019

Arlington, Texas

Supervising Committee:

Dr. Ali Abolmaali, Supervising Professor

Dr. Dereje Agonafer

Dr. Shih-Ho Chao

Dr. Andrew Kruzic

Dr. Bo p. Wang

ABSTRACT

DEVELOPMENT OF PROTOCOL FOR 100-YEAR SERVICE LIFE OF SYNTHETIC FIBER-REINFORCED CONCRETE PIPES

Maziar Mahdavi, Ph.D.

The University of Texas at Arlington, 2019

Supervising Professor: Professor Ali Abolmaali

Among different components of US highways and roads, concrete pipes are one of the most important parts of these infrastructures. Currently, most of the concrete pipes that are produced in the United States are made from steel reinforced concrete composite, and this system is prone to deterioration and steel corrosion during the service life of these pipelines. In this study, a newly developed composite at the Center for Structural Engineering Research/Simulation and Pipeline Inspection was studied for service life assessment with accelerated aging methods. This composite doesn't contain any steel reinforcement, and it is reinforced by Polypropylene fibers. At the first phase of this study, synthetic fiber reinforced concrete cylinders were tested to determine the effects of low pH and high temperatures on this material. The results showed that specimens immersed in pH2.5 solutions lost their compressive strength approximately twice of those that were soaked in pH4.2 baths. Immersion duration had a major deteriorating effect on the specimens, and they showed more than 30% compressive strength loss after four months of immersion.

At the second phase of this research, actual reinforced concrete pipes with 0.54% fiber volume fractions were immersed in low pH solutions and elevated temperatures. The D-load test results showed that specimens that were immersed in pH2 solutions lost their ultimate D-load capacity by 20% after one year, and pH4 specimens showed 18% load decrease at the same time. The shapes of the curves in these two environments were different. pH2 specimens' results converged to a steady state load decrease value after five months, and the pattern continued for two other immersion periods. For pH4, the results were still decreasing after each immersion period and based on the trend of the results; it can be anticipated that the curve of this set of tests is going to converge approximately to the same value after a longer immersion period.

Furthermore, by using SEM and EDX analysis, the chemical composition of specimens that were extracted from these pipes was analyzed. The results showed that at early stages of the immersion tests, the surface of the pipes in pH4 solution did not absorb a significant amount of sulfur, and it shows that these specimens have not deteriorated significantly. With longer immersion duration, the amount of sulfur element on the surface of the specimens increased gradually, and for pH2, the surface was mostly saturated after 5 months of immersion. For pH4, this value was constantly increasing and similar to the mechanical tests, pH4 results were converging to the same value of pH2 results.

For 100-year service life assessment of SYNFRCPs, a curve fitting approach was adopted and based on the curve fitting results it was concluded that these pipes would not lose more than 22.5% of their strength in these corrosive environments after 100 years, which is less than 33% service life criteria. This was determined based on the assumption that pH4 curve will ultimately converge to the steady state part of pH2 results. More than 100 years service life indicates that SYNFRCPs can be used in the U.S. infrastructure systems.

ACKNOWLEDGMENT

I would like to express my sincerest gratitude to my supervising professor, Professor Ali Abolmaali, for all of the time, advice, and tireless support during my career at the Center for Structural Engineering Research/Simulation and Pipeline Inspection. This research would not have been successfully completed without his supervision.

I would also like to thank my committee members, Dr. Agonafer, Dr. Chao, Dr. Kruzic, and Dr. Wang for providing me with their valuable comments. I should also thank Dr. Hozhabri and UTA NanoFab laboratory staffs for their kind help and support.

I would like to thank the American Concrete Pipe Association and the Florida Department of Transportation who supported this project technically and financially.

I would like to extend my warmest thank you to Dr. Amir Koolivand, Research Assistant Professor at the UTA Chemistry Department, for his help and collaborations during this project.

I should thank my friends and colleagues at the Center for Structural Engineering Research/Simulation and Pipeline Inspection, Arash EmamiSaleh, Dr. Masoud Ghahremannejad, Bassam Al-lami, Sina Abhaee, and Kamlesh Khatri for their help during this research.

July 2019

DEDICATION

I would like to thank my parents, my brother, and my wife, and my friends for their continuous help, support, inspiration, and encouragements throughout my career. They never let me give up, never let me lose sight of my goal, and for that, I am grateful.

TABLE OF CONTENTS

TABLE OF FIGURES

LIST OF TABLES

CHAPTER 1. INTRODUCTION

1.1.Overview

Concrete pipes are one of the oldest types of pipes, which have been widely used since mid-1800 until now. These pipes were mainly used as sewer and stormwater systems, and they are famous for their durability. Currently, concrete pipes are one the main types of sewer and drainage systems in the U.S. infrastructure. They are being used for stormwater drainage and culverts in roads and highways, (Figure 1), and they are playing a vital role in the residential and industrial sewer collection systems, (Figure 2).

Figure1. Highway drainage pipes and concrete pipes as culverts

Figure 2. Sewer concrete pipes

Considering the costly construction of these infrastructure systems, durability of these pipes is hugely important. The design service life of these pipes based on the Florida Department of Transportation (FDOT) Drainage Manual is 100 years for major systems and 50 years for minor systems [1]. After installation, these pipes should support multiple loads from different sources. These loads would be the wheel load, earth load, surcharge load, and the self-weight load. In addition to the load-bearing capacity, the durability of this material in corrosive field environments is an important factor in the service life estimation of these pipes. Florida Department of Transportation (FDOT) has developed software for pipes and culverts service life estimation. This software, which is called "Culvert Service Life Estimator" and shown in Figure 3, determines the service life-based eligibility of each pipe material according to the environmental factors and the design service life [2].

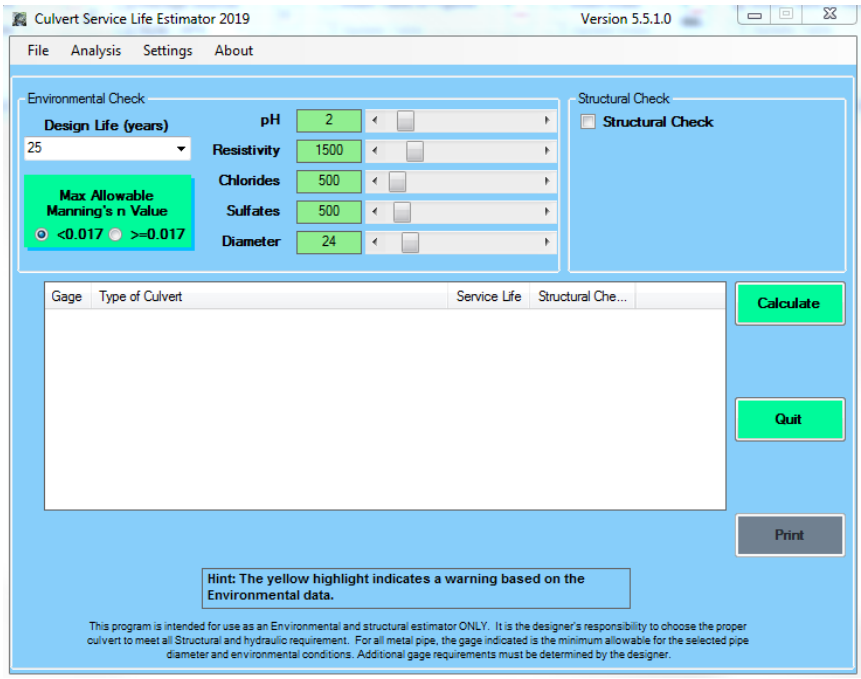

Figure 3. FDOT Culvert Service Life Estimator software [2]

1.2. Conventional Reinforced Concrete Pipes (RCPs)

Most of the concrete pipes are reinforced by conventional steel cages. The steel cages are produced by a cage-welding machine, as shown in Figure 4.

Figure 4. Cage-welding machine

After cage preparation, they are placed inside a pipe mold, then dry cast concrete will be poured into them, and finally, concrete will be compacted by a packerhead machine, as depicted in Figure 5.

Figure 5. Packer head machine

After compaction, since dry cast concrete is being used for RCPs' production and the steel cages can support the integrity of the sections, these pipes are instantly ready to be demolded, (Figure 6).

Figure 6. Removing the RCP molds

After production, the pipes are ready to be installed after seven days of curing, and the installation process includes preparation of the site, excavation, pipe's placement, and backfilling of the pipe sections as shown in Figure 7.

Figure 7. RCP installation

Besides all the advantages of RCPs, the usage of steel in these pipes increases their vulnerability to the oxidizing elements in the environment. Currently, one of the main threats to reinforced concrete pipes is the corrosion of embedded steel. Steel corrosion in RCPs would occur in acidic and high-chloride environments. Figure 8 illustrates a steel corrosion-related failure of a reinforced concrete pipe.

Figure 8. Steel corrosion in an RCP

To avoid these deterioration scenarios, this study is focused on the service life assessment of an alternative concrete pipe composite, which is called Synthetic Fiber Reinforced Concrete Pipe (SYNRCP).

1.3. Literature Review

Reinforced concrete pipes are widely used as sewer and drainage pipes, but concrete and reinforcements deteriorate because of chemical reactions. For example, hydrogen sulfide (H_2S), which is usually derived from sulfur-reducing bacteria, transforms into sulfuric acid (H_2SO_4) and attacks concrete and these reactions result in concrete deterioration and steel corrosion which will cause partial spalling of concrete cover as shown in Figure 9 [3, 4].

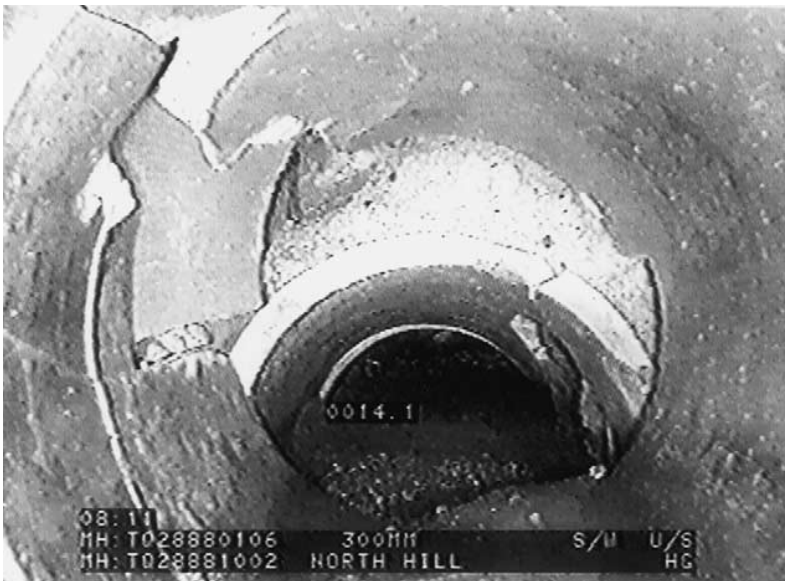

Figure 9. CCTV image of collapsed sewer pipes [3]

Dissolved chloride ions in wastewater can also result in chloride-induced corrosion of reinforcements [5], and chloride-induced corrosion of steel reinforcements shortens the service life of concrete sewer pipes [1,5-7]. In order to mitigate these unwanted reactions and to increase durability, many researchers have studied various composites [8, 9, and 110]. Wilson and Abolmaali eliminated ordinary steel reinforcements and replaced them with polypropylene fibers. They studied the load-bearing performance of synthetic fiber-reinforced concrete pipes (SYN-FRCP) by three-edge bearing tests, Figure 10, and based on the results, which are depicted in Figure 11, they concluded that polypropylene fibers are a good alternative for steel reinforcement [8].

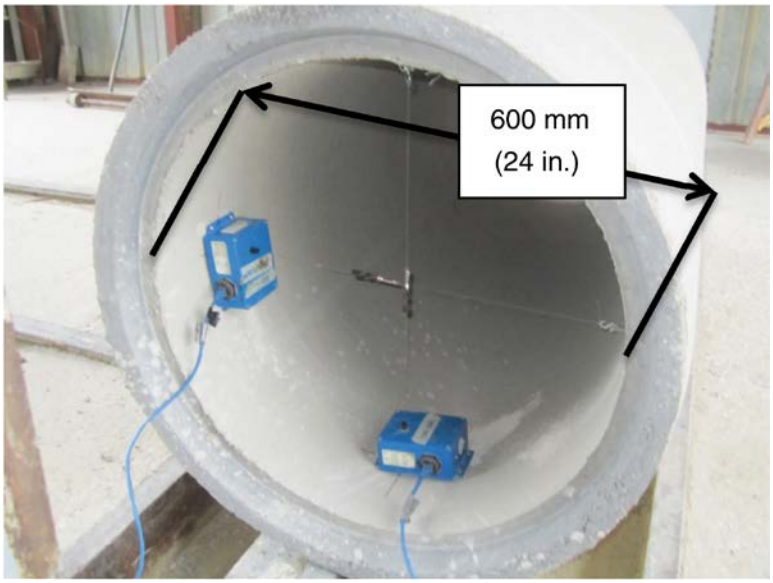

Figure 10. Three edge bearing tests by Wilson and Abolmaali [8]

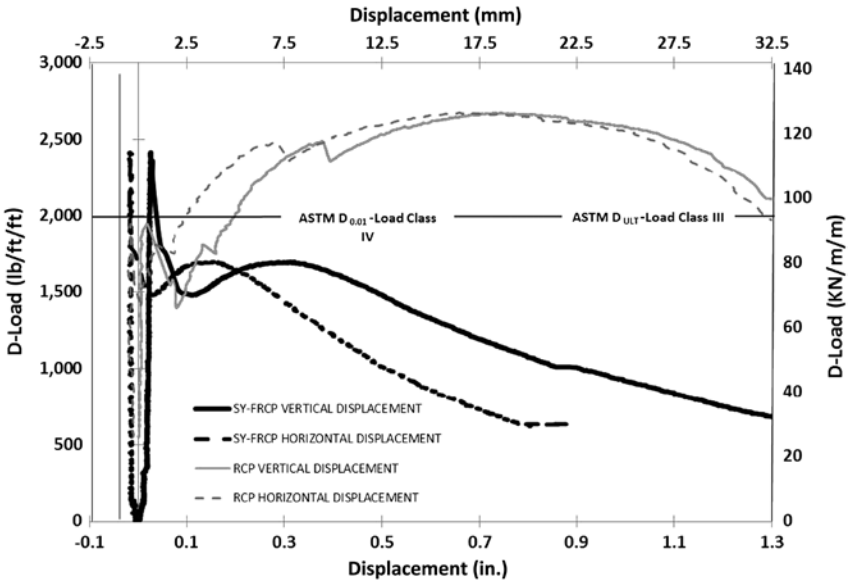

Figure 11. RCP versus SYN-FRCP load-deformation comparison by Wilson and Abolmaali [8]

Park et al. investigated the time-dependent behavior of synthetic fiber-reinforced concrete pipes. In this research, two precracked 24-in. and two precracked 36-in. pipes were buried under 2 ft. of native soil and then backfilled with 14 ft. of gravel to simulate the maximum field load for these pipes based on ASTM C76. The pipes deflection were measured by two displacement sensors

vertically at two sections along the pipes' length. Their tests setup and testing procedures are shown in Figure 12.

Figure 12. The long-term load bearing capacity of SYN-FRCPs test setup by Park et al. [9]

Their findings, which are demonstrated in Figures 13 and 14, showed that the long-term load-carrying capacity of pipes improved with the addition of BASF synthetic fibers and the SYNFRCPs could adequately resist the sustained loads and showed less than 3% change of the inside diameter after almost six months [11].

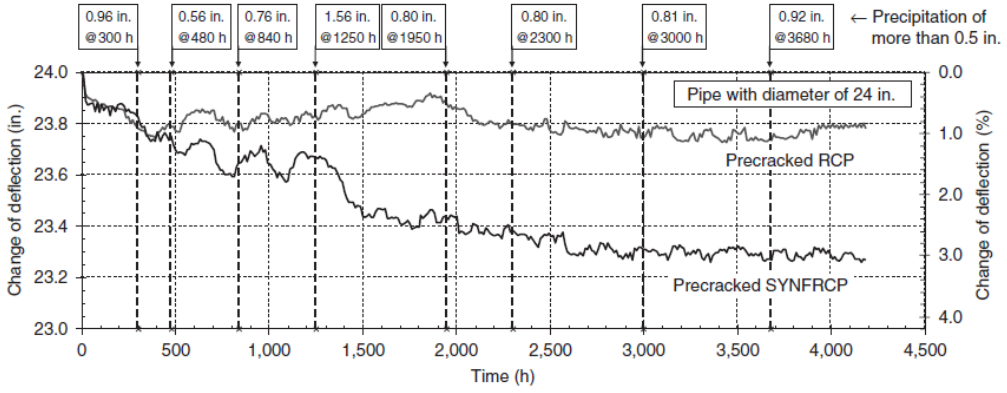

Figure 13. Time-dependent behavior of 24-in. pipes [11]

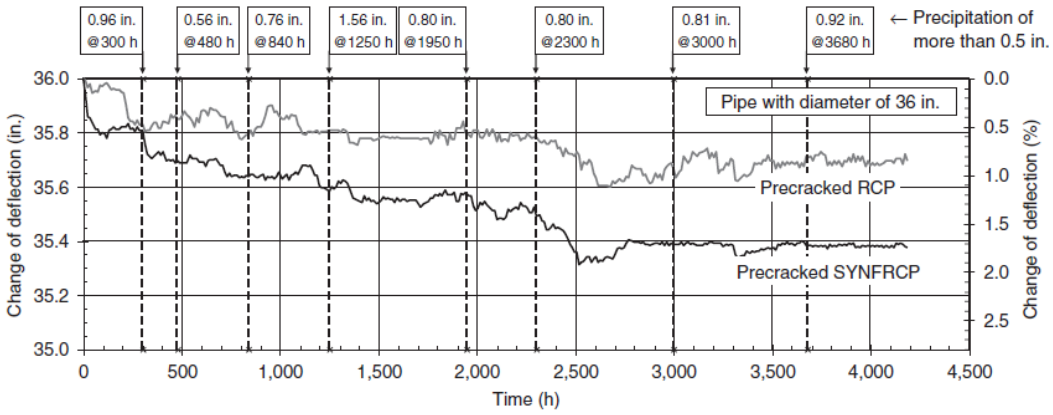

Figure 14. Time-dependent behavior of 36-in. pipes [11]

In another research by Wilson et al. the load bearing capacity of SYN-FRCPs was determined after testing more than 250 pipes, and the fiber dosages were identified for each pipe class strength [13]. Furthermore, concrete cylinder tests were also performed to determine the material properties. Finally, because of the time-dependent behavior of polypropylene fibers, laboratory tests were conducted for 10,000 hours to investigate the long-term load bearing serviceability of these pipes. This study led to the determination of an α factor for ASTM C1818-15 [12] to address the long-term function of the fibers in these pipes, as shown in Figure 15.

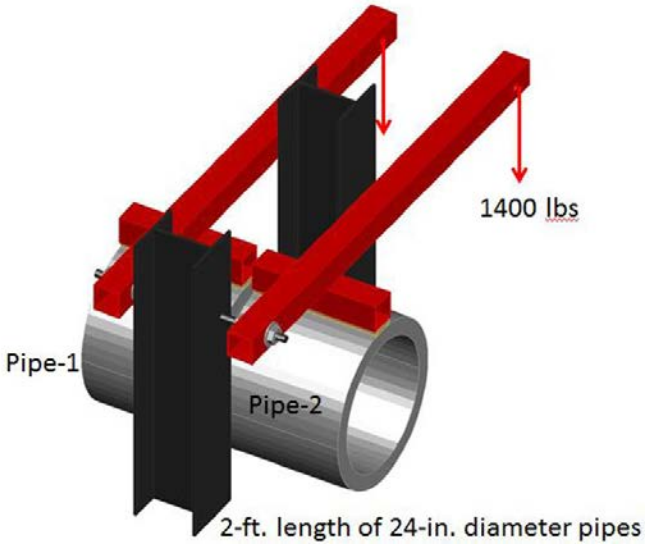

Figure 15. Long-term testing simulation, Wilson et al. [13]

This study resulted in the "ASTM Standard Specification for Synthetic Fiber Reinforced Concrete Culvert, Storm Drain, and Sewer Pipe", ASTM C1818. The loading protocol proposed for this standard can be summarized in Figure 16.

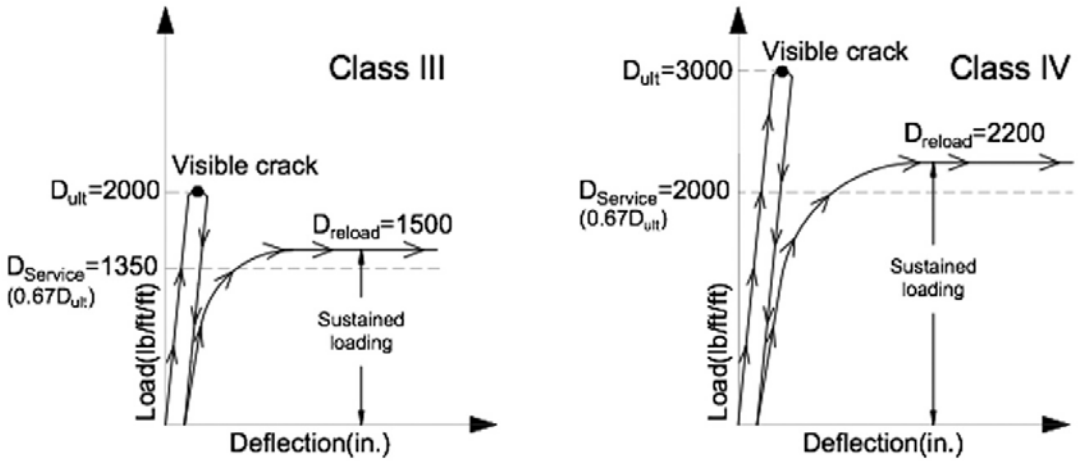

Figure 16. ASTM C1818 loading protocol, developed by Wilson et al. [13]

For further investigation of this composite, Mostafazadeh and Abolmaali studied the shear behavior of concrete reinforced with MasterFiber synthetic fibers, and their results demonstrated that synthetic fibers improve the material properties, shear strength, shear toughness, flexural strength, and flexural toughness, Figures 17 [14].

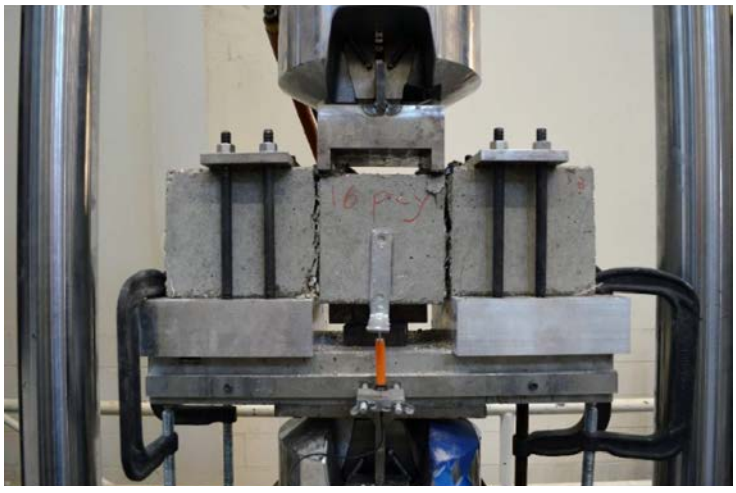

Figure 17. Test setup for direct shear test and fractured specimen, Mostafazadeh et al. [14]

In addition to these, research has been performed by Ghahremannejad et al. to investigate the cracking pattern of SYNFRC beams by digital image correlation method [15]. Based on the results, using 1% of fibers increased the failure load. This volume fraction improved the serviceability by reducing the number of cracks and the crack widths.

In another study, Mahdavi et al. investigated the effect of pH and temperature on SYNFRCP cylinders [16]. The results showed that higher temperatures and lower pH lead to extreme deterioration and specimens immersed in pH 2.5 were deteriorated almost twice as much as pH 4.5 specimens.

Approving this composite for vital and expensive infrastructural applications, however, requires even further investigation of the material durability. Since concrete pipes usually deteriorate because of acids, and plastic fibers are sensitive to temperature increases, many researchers have studied the effects of both on concrete, fibers, and their composition. Alcock et al. studied highly oriented polypropylene (PP) tapes to determine the effects of temperature on the mechanical properties of fibers, and the results showed that the tensile strength of the fibers drops suddenly in a transition temperature, which is 90°C as depicted in Figure 18 [17].

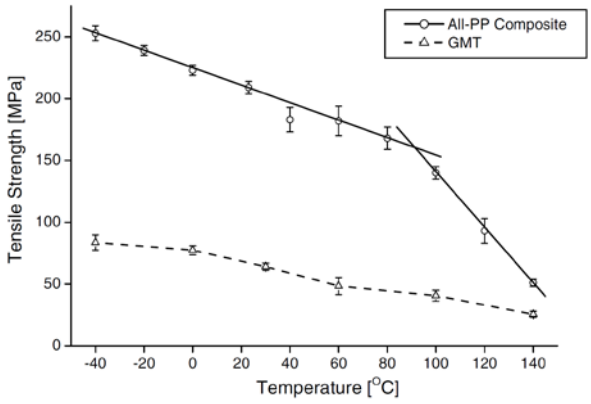

Figure 18. Temperature effect on the tensile stress PP fibers, Alcock et al. [17]

Khajuria et al. studied the long-term durability of synthetic fibers in concrete to investigate the impacts of high-temperature curing and reached the conclusion that the fibers performed well and provided post-crack resistance at a curing temperature of 50°C [18]. Additionally, Xiao and Falkner [19] investigated the residual strength of high-performance concrete, with and without polypropylene fibers, at temperatures ranging from 20 to 900 °C. Their study showed that there is a significant reduction at the temperature of 400 °C, regardless of the presence of PP fibers, and the mass loss is relatively small (below 100 °C), Figure 19.

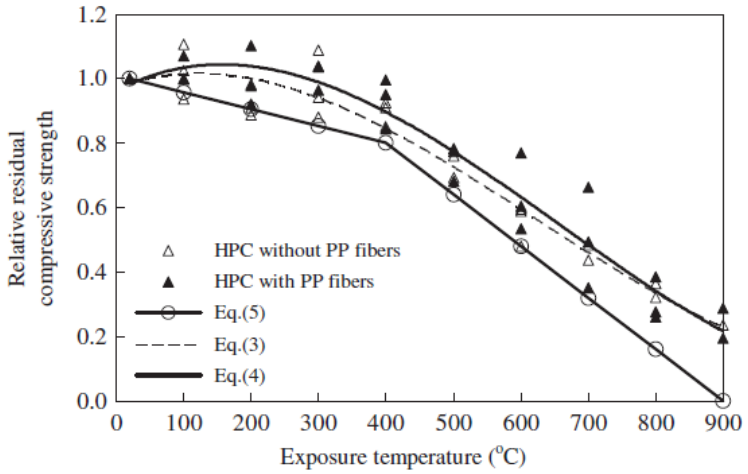

Figure 19. Regression for the residual compressive strength of HPC, Xiao and Falkner [19]

Many studies have been focused on the effects of acids on different types of concrete, and they have determined their influence on the concrete's mechanical properties. Bertron et al. used accelerated tests of hardened cement pastes altered by organic acids to analyze the pH effects. The alteration mechanisms of the cement-based matrix were compared with two solutions of organic acids, one with a pH of 4 and one with a pH of 6. By microscopic investigation, it was determined that the alteration mechanisms of the paste were similar for both solutions, with only minor differences but the pH 4 acid deteriorated the concrete 9-times faster than the pH 6 one [20]. The deteriorating influences of different chemicals, including sulfuric acid, on synthetic fiber-

reinforced shotcrete, was studied by Kaufman [21], and the outcomes indicated that both sulfate and sulfuric acid cause considerable deterioration of shotcrete. An experimental study on the erosion of concrete specimens containing polyethylene terephthalate (PET) particles in a 5% sulfuric acid solution demonstrated that while the amount of PET particles increased, the load-bearing capacity of the specimens decreased less than it did in the specimens containing lower amounts of these particles [22]. In a 27-month research study related to the effects of an acidic environment on fiber-reinforced concrete, Kim et al. determined the effects of Acetic acid with a pH of 4.5 on uncracked and pre-cracked concrete beams. The fibers used in this study were hooked-end steel, polypropylene (PP), and polyvinyl alcohol (PVA). In all of the cases, the low pH solutions significantly reduced the residual strength and toughness, as shown in Figures 20 [23].

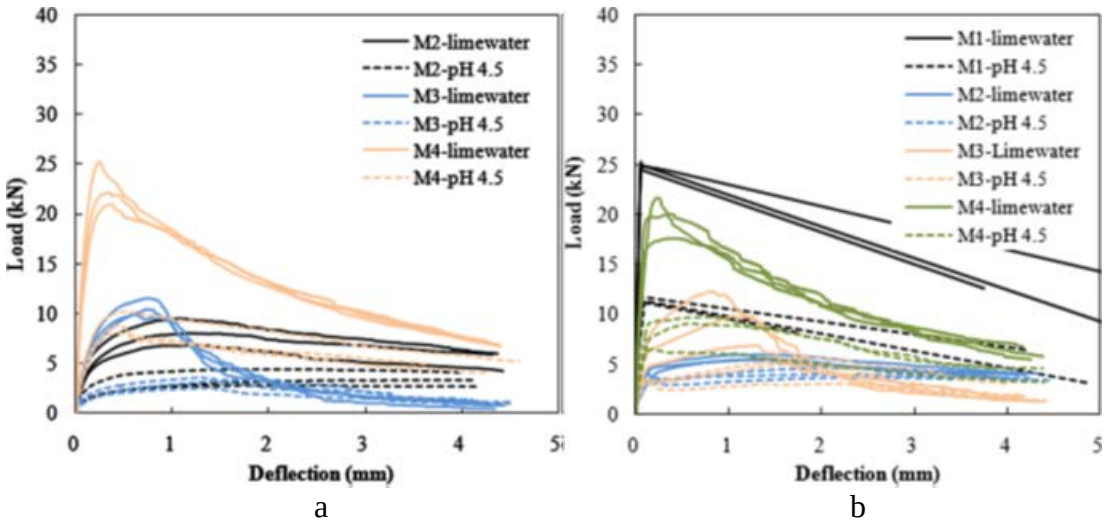

a b

Figure 20. (a) Test results for precracked beam, (b) Test results for uncracked beam (residual strength), Kim et al. [23]

Nematzadeh and Fallah [24] conducted research on the erosion resistance of Forta-Ferro (twisted bundle, non-fibrillated monofilament, and fibrillated polypropylene network) fiber-reinforced concrete in a 5% sulfuric acid solution. Based on this study, it was concluded that increasing the

fiber volume fraction, results in a smaller reduction in weight loss (Figure 21), crushing load, and ultrasonic pulse velocity.

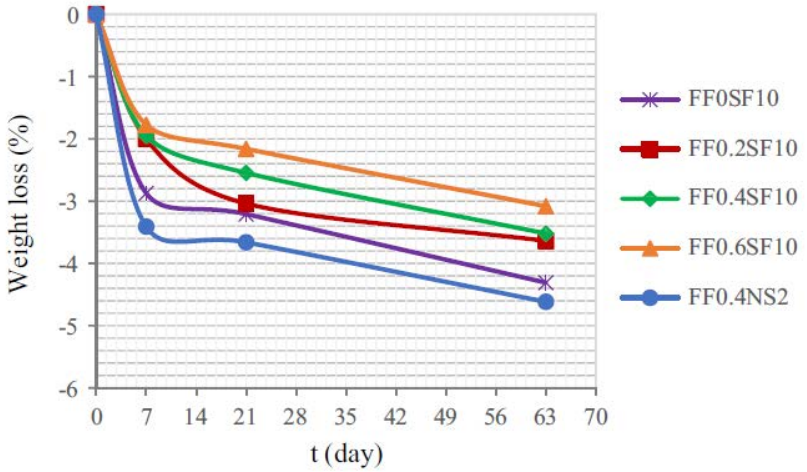

Figure 21. Weight loss of specimens after exposure to 5% sulfuric acid solution, Nematzadeh and Fallah [24]

In this study, Nematzadeh and Fallah also studied the relationship between crushing loads and weight loss of the specimens and found linear relationships to correlate these properties with each other, Figure 22.

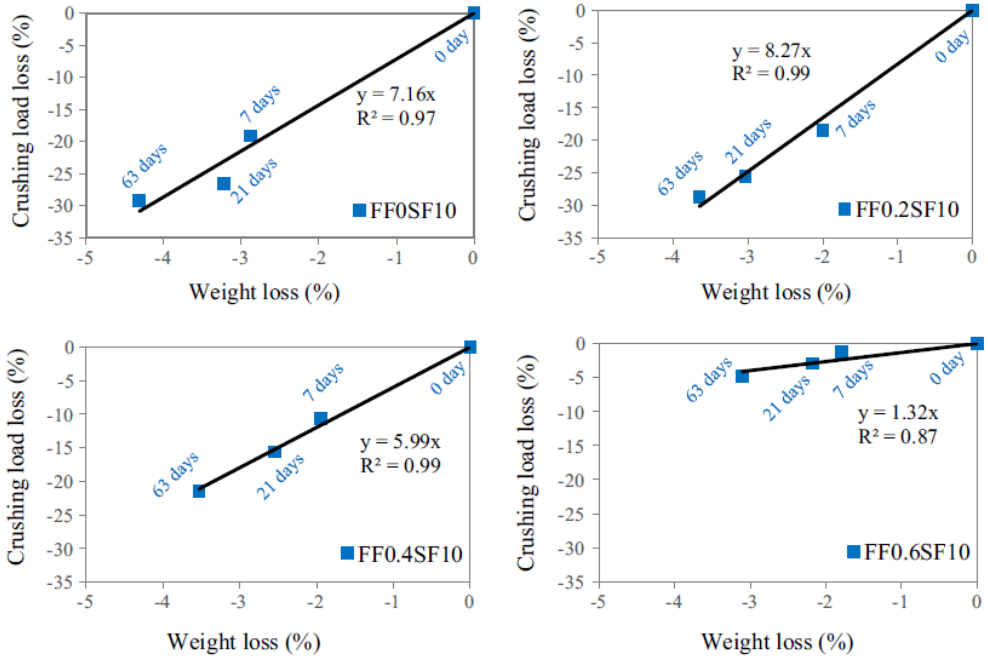

Figure 22. Weight loss-crushing load reduction relationship of concrete specimens during immersion in 5% sulfuric acid solution, Nematzadeh and Fallah [24]

In another study, Rafieizonooz et al. [25] investigated the durability of concrete containing coal ash and determined a linear relationship between compressive strength change and mass loss, as depicted in Figure 23.

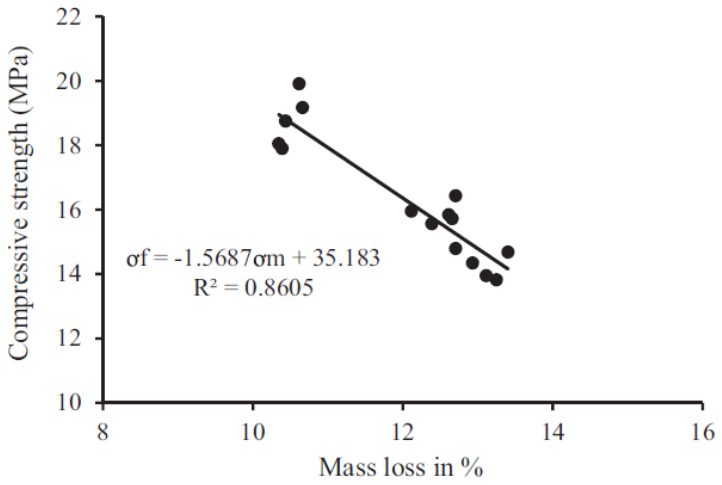

Figure 23. Relationship between reduction in compressive strength and weight loss after 180 days submersion in 5% sulfuric acid solution, Rafieizonooz et al. [25]

1.4. Scopes and objectives

The final goal of this research is to investigate the long-term durability of SYNFRCPs by using accelerated aging methods to determine their 100-year service life in highly corrosive environments. For this purpose, long-term accelerated aging tests were conducted in two phases, and the results were evaluated with different methods.

1. Material testing phase: At this phase, 114 cylinders with two different volume fractions were immersed in six different corrosive solutions for four months. The fiber volume fractions were 0.52% and 1.04%, and the solutions had two different levels of pH (2.5 and 4.5), and three different temperatures (25°C, 37°C, and 50°C). After seven days, three cylinders from each volume fraction were tested, and the results were used as the reference compressive strength values of the mix designs. The rest of the cylinders were tested to

determine their compressive strength at one, two, and four months of immersion. The reduction of compressive strength that was due to acidic environments was determined by comparing the post-immersion results to the reference values.

2. Mechanical tests of pipes: at this phase, 31 two-ft. sections of 24-inch diameter SYNFRCPs with a fiber volume fraction of 0.52% were manufactured and immersed in four different corrosive solutions for 12 months. These solutions had two different pH levels (2 and 4) and two different temperatures (25°C and 50°C). The pH 4 at 25°C was considered as the reference environment, which is expected in the field, and this reference deterioration scenario was accelerated by increasing the temperature and decreasing the pH. Three of the pipes were tested to determine the reference D-load strength of the specimens. The rest of the sections were tested at 2, 5, 8, and 12 months after immersion. The service life of the SYNFRCPs will be determined based on a comparison of the post-immersion D-load capacity of the sections with the reference values.
3. Microscopic analysis of pipes: In addition to the mechanical properties, chemical components and microscopic structures of the specimens were studied by Scanning Electron Microscope and Energy-Dispersive X-ray spectroscopy (EDX) Analysis, before and after immersion. By comparing the material analysis of immersed specimens with the control ones, the extent of deterioration, and the amount of corrosive elements on the surface of deteriorated samples after each immersion period was determined.
4. Service life estimation: Based on the pipe testing results, and by utilizing curve-fitting methods on these values, the best curve to fit the test results were determined. By extrapolating that function to 100-years, the service life of SYNFRCPs in these highly corrosive environments were determined.

CHAPTER 2. ACCELERATED AGING

2.1. Overview

To simulate long-term effects of environmental conditions on any material, accelerated aging methods are being used in material science and engineering. Accelerated aging utilizes aggravated conditions to speed up deterioration processes. By adopting this method, long-term effects can be evaluated in a very short period. One of the main applications of this method is in the pharmaceutical industry to determine useful life of medications. In material science applications, this method is widely used to determine the service life of the products in severe environmental conditions. For example, Reynolds [26] used thermally accelerated aging to investigate semiconductor components. In a study, which was done by Naser for the U.S. Department of Energy [27], an accelerated aging method was used to study the service life of electronic instruments and circuit boards in power plants.

Recently, accelerated aging methods have been widely used for civil engineering applications. These methods were mainly utilized to determine the service life of different materials and structural elements. These methods are focused on increasing the ambient temperature, increasing the concentrations of the corrosive ions or significantly reducing/increasing the pH level of the corrosive fluids.

2.2. Concept and Theory

All materials will be aged over time and according to German Standard DIN 50 035, “aging is the totality of irreversible chemical and physical alterations that may occur within a material in the course of time.” In any aging scenario, two major components are working simultaneously. The first part is the development process, and the second part is the deterioration process. These

processes are both chemically controlled and the deterioration part usually results in physical alterations [28]. This pattern is also applicable to accelerated aging scenarios. In accelerated aging, accelerated deterioration and accelerated development will occur simultaneously. Accelerated aging methods are utilized to simulate long-term effects of development or degradations in a shorter time. Figure 24. shows the schematic definition of the accelerated aging.

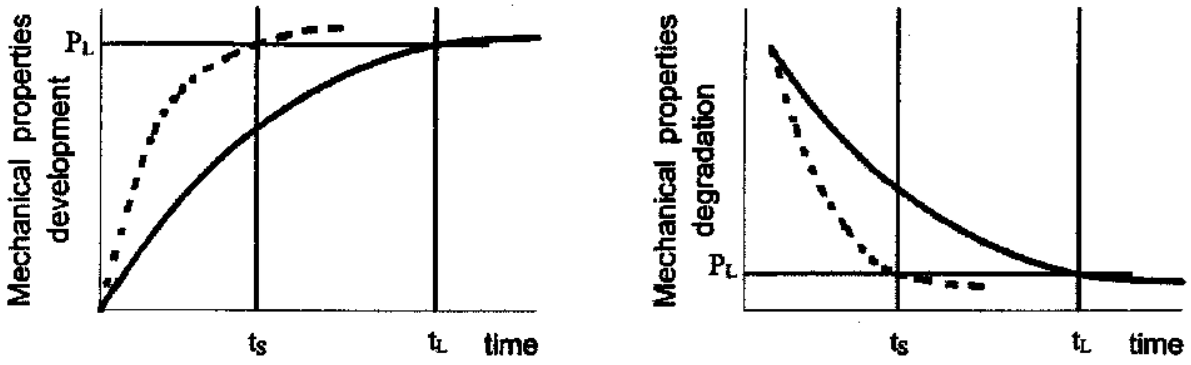

Figure 24. Schematic accelerated development and degradation of mechanical properties over time, Pinto et al. [28]

Generally, various factors can be used to influence the aging scenarios in concrete. Some of them are increasing temperature, increasing pressure, increasing concentrations, and corrosion products removal.

2.3. Concrete deterioration and improvement reactions

Concrete aging, like any other material, includes improvement reactions, which are the hydration reactions, and environmental deterioration reaction, like acid deterioration, sulfate attack, and alkali-silica reactions.

2.3.1. Improvement reactions (Hydration)

When cement is mixed with water, it makes a paste that binds the coarse and fine aggregates. The reaction between cement and water is called hydration of cement, which results in a product that sets and hardens. A microscopic picture of a hydrated cement paste is shown in Figure 25.

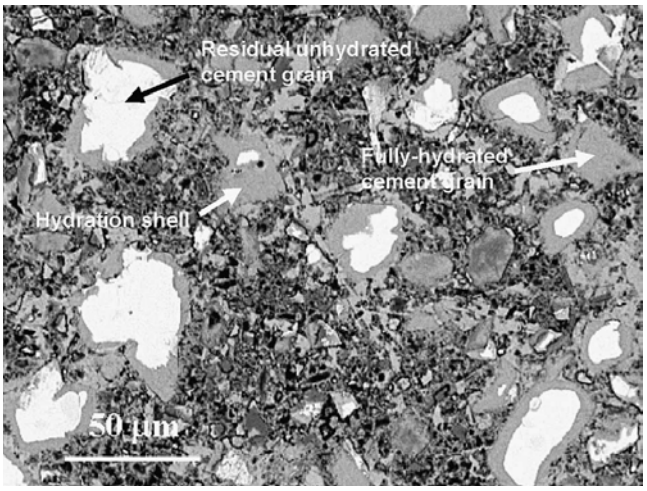

Figure 25. View of the microstructure of a 100-day old w:c 0.30 cement paste, cured at room temperature, Diamond [29]

There are two mechanisms for hydration; the first one is called through-solution hydration that involves dissolution of non-hydrated components to their ions. This will form the hydrates in the solution, and eventually, the hydrates precipitate from the solution. Another mechanism is called solid-state hydration. In this mechanism, reactions occur on the surface of the cement. At early ages, the through-solution hydration is the dominant mechanism. After a few days, the solid-state hydration will be the major hydration mechanism [30].

Aluminate hydration

Aluminate hydration is fast. It quickly results in Crystalline hydrates, and it generates a large amount of heat. To slow down these hydration reactions, gypsum is usually added to the Portland cement mix for practical purposes [30]. Aluminate hydration reactions are listed in Equations 1 and 2.

Ettringite:

$$[AlO4]^{-} + 3[SO4]^{2-} + 6[Ca]^{2+} + aq. \rightarrow C_6AS_3H_{32} \quad \textit{(Eq. 1)}$$

Monosulfate:

$$[AlO4]^{-} + [SO4]^{2-} + 4[Ca]^{2+} + aq. \rightarrow C_4AS_3H_{18} \quad \textit{(Eq. 2)}$$

Silicates hydration

The C_3A and βC_2S hydration produces multiple calcium silicate hydrates that are similar structurally. This material is not crystalized and it was called tobermorite gel [30]. The Silicate hydration reactions are listed in Equations 3 and 4.

$$2C_3S + 6H \rightarrow C_3S_2H_3 + 3CH \quad \textit{(Eq. 3)}$$

$$2C_2S + 4H \rightarrow C_3S_2H_3 + CH \quad \textit{(Eq. 4)}$$

2.3.2. Deterioration of concrete:

Many environmental conditions can deteriorate concrete mix. Other than physical sources of concrete damage, there are chemical reactants that can deteriorate concrete. Most of these corrosive materials react with the cement paste, which will damage the integrity of the mix.

Freezing and thawing

Frost damage to the concrete can be seen in many forms. Spalling and cracking is the most common form of this phenomenon, which is the result of internal expansion of the paste. Frosting can damage both cement paste and aggregates [30]. Figure 26 illustrates the effects of freezing and thawing on concrete specimens.

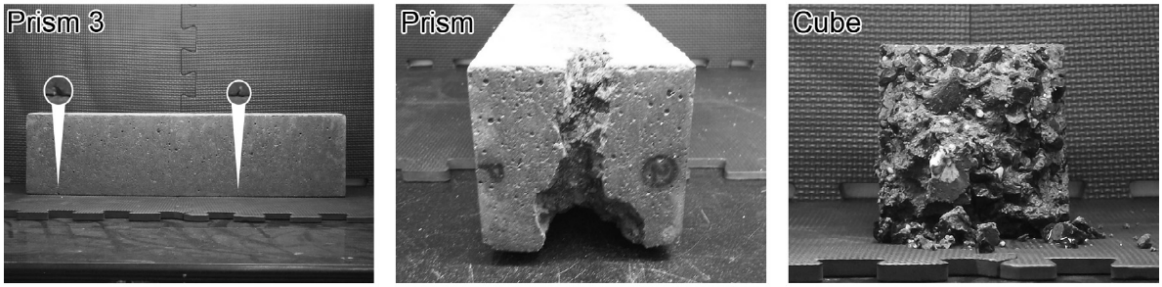

Figure 26. Freeze-thaw damage on concrete material, Quin et al. [31]

Hydrolysis

Hard water containing calcium, sulfate, bicarbonates, and magnesium usually do not attack the cement paste, but pure water can dissolve materials that contain calcium. This process is called hydrolysis, and it will continue until a chemical equilibrium is reached. This process will be continuous in the case of flowing water, and highly soluble calcium hydroxide will be easily dissolved in this process. This process will ultimately dissolve the remaining part of the paste, which is silica and alumina gels, which do not have considerable strength.

Sulfate attack

The reaction between sulfate ions and hydrated cement has two forms. Type of attack depends on the source of ion in water and cement paste composition. The reaction products of sulfate attacks are expansive. The expansion will result in cracking and spalling of the concrete surface, Figure 27. When the concrete surface is cracked, the permeability is increased and consequently, deterioration process will be accelerated. The spalling will result in a material loss, and as a result, strength loss will be observed after sulfate attacks.

Figure 27. Sulfate attack on a concrete cylinder, Hartell and Boyd [32]

Sulfate ions will react with calcium hydroxide and alumina-bearing phase of the hydrated cement and will produce ettringite crystals in cement paste, Figure 28. These reactions are shown in Equations 5 and 6.

$C_3A.CH.H_{18}+2CH+3S+11H \rightarrow C_3A.3CS.H_{32}$ *(Eq. 5)*

$C_3A.CS.H_{18}+2CH+2S+12H \rightarrow C_3A.3CS.H_{32}$ *(Eq. 6)*

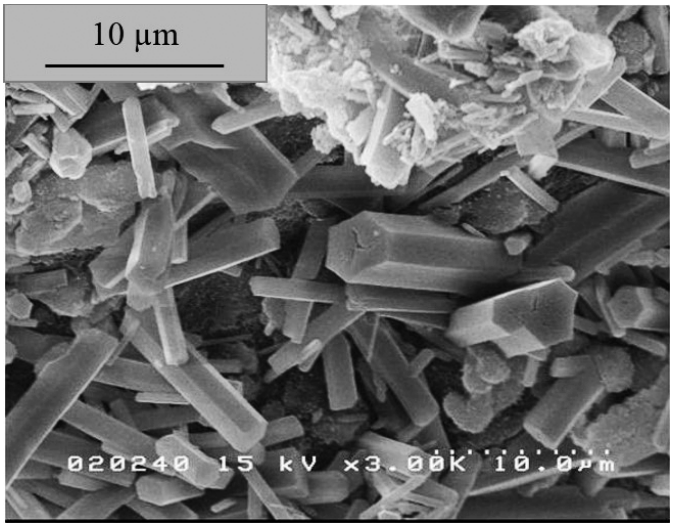

Figure 28. Scanning electron microscope image of ettringite crystals, Jewell et al. [33]

The expansion of cement paste is mostly believed to be a result of ettringite formation, but there are theories, which relate it to cation exchange reactions, which produce gypsum and they are also mentioned as a reason for the sulfate attack related strength loss of concrete elements. Depending on the source of sulfate ion, gypsum formation reactions can be listed, as shown in equations 7, 8, and 9.

$$Na_3SO_4 + Ca(OH)_2 + 2H_2O \rightarrow CaSO_4.2H_2O + 2NaOH \quad \textit{(Eq. 7)}$$

$$Mg_3SO_4 + Ca(OH)_2 + 2H_2O \rightarrow CaSO_4.2H_2O + 2NaOH \quad \textit{(Eq. 8)}$$

$$3Mg_3SO_4 + 3CaO.2SiO_2.3H2O + 8H_2O \rightarrow 3(CaSO_4.2H_2O) + 3Mg(OH)_2 + 2SiO_2.H_2O \quad \textit{(Eq. 9)}$$

Alkali-aggregate reactions

Depending on the alkalinity of the Portland cement, the pH of pore fluid in concrete elements are usually 12.5 to 13.5 and it is a strong alkaline. The reaction of this strong alkaline with aggregates is very expansive and it will cause cracks in concrete.

Acid attack

Being a very alkaline mix, concrete is prone to be damaged by acidic solutions. This process is called an acid attack. An acid attack reaction can be shown in the following equation [30].

$$HX + C(OH)_2 \rightarrow CaX + H_2O \quad \textit{(Eq. 10)}$$

When strong acids like HCl, H_2SO_4, CH_3COOH, and HNO_3 react with hardened Portland cement, the products will be calcium salts that are highly soluble in water. For weaker acids like H_3PO_4, the produced salts are less soluble, and they will block the fluid passage routes and halt the deterioration. Figure 29 shows the effect of a 5% sulfuric acid on concrete cylinders after 8 weeks of immersion.

Figure 29. Visual assessment of degraded concrete samples after 8 weeks of exposure to a 5% sulfuric acid solution, Joorabchian [34]

2.4. Accelerated aging of concrete

Several factors can be used to accelerate the improvement and deterioration scenarios in concrete elements.

2.4.1. Temperature

Based on the Arrhenius equation, temperature increase will result in a higher reaction rate in most of chemical reactions. Arrhenius equation relates the rate constant of a reaction to its activation energy, temperature and gas constant as shown in Equation 1. [35]

$$k = Ae^{\frac{-E_a}{RT}} \qquad (Eq.\ 11)$$

Where:

k is the rate constant

T is the absolute temperature (in kelvins),

A is the pre-exponential factor (a constant for each chemical reaction. According to collision theory)

E_a is the activation energy for the reaction (J / mol.)

R is the universal gas constant (R = 8.314 J / mol. · K)

Temperature increase can simultaneously accelerate the deterioration and improvement reactions. For concrete, the improvement reactions are the reactions that contribute to the hydration process, and the deterioration reactions can be acid-concrete reactions, sulfate attack reactions, and alkali-aggregate reactions.

2.4.2. Concentration

Increasing the reactants' concentration will generally increase the rate of reactions. This relationship is shown in Equation 12. [35]

$$R = k[A]^{\alpha} \qquad \textit{Eq. 12}$$

Where:

R is the reaction rate (mol/s)

k is the rate constant

[A] is the concentration of the reactant A

α is the order of the reaction

For concrete elements, this can be achieved by reducing the pH level of corrosive acidic solution, increasing the sulfate ion concentration, and increasing the pH level of alkaline solutions.

2.5. Accelerated aging of SYNFRC and service life assessment

In this research, to determine the long-term effects of pH 4 acidic environment at room temperature on synthetic fiber reinforced concrete specimens, the concentration of hydrogen ion and immersion temperature were increased to accelerate the aforementioned mildly aggressive field environment.

2.5.1. Material testing

At this phase, concrete cylinders with two different fiber dosages were immersed in sulfuric acid solutions with two different pH levels at three different ambient temperatures. After each period of immersion, the specimens were brought out of the solutions and were tested to determine their compressive strength and compare their results with control specimens. Post immersion tests were performed after 1, 2, and 4 months of immersion. The specimens were also inspected visually before and after each set of tests to assess the visible effects of these solutions on the specimens.

2.5.2. Pipe testing

At this phase, 2-ft. pieces of 24-in. pipes were immersed in sulfuric acid solutions with two different pH levels and at two temperatures. The specimens were taken out of the solutions after immersion, their strength was determined by three-edge bearing tests, and the results were compared with control specimens. After three-edge bearing tests, chemical composition of tested pipes was also assessed by Scanning Electron Microscope (SEM) and Energy-dispersive X-ray spectroscopy (EDX) analysis of small cores extracted from the body of these pipes. This phase of the study was done for 12 months.

The results of these accelerated tests were ultimately used for 100-year service life assessment of SYNFRCPs.

CHAPTER 3. ACCELERATED AGING OF SYNTHETIC FIBER REINFORCED CONCRETE CYLINDERS

3.1. Overview

This research aims to estimate the service life of synthetic fiber reinforced concrete pipes utilizing the accelerated aging method. For this purpose, both the material and the actual pipe elements should be tested to assess their behavior in harsh environments. The material testing phase was focused on compressive strength of the cylinders and visual inspections of the broken specimens to evaluate the physical effects of these harsh environments on polypropylene (PP) fibers. The pipe-testing phase was focused on the specimens' D-load bearing capacity and chemical alterations of concrete utilizing Scanning Electron Microscope (SEM) and Energy-dispersive X-ray spectroscopy (EDX).

To investigate the effects of low pH and high temperatures on synthetic fiber reinforced concrete, a series of materials tests were conducted. At this phase, SNFRC cylinders were immersed in solutions with two different pH levels and three different temperatures. After each period of immersion, the specimens were taken out of the solutions. Then the specimens were air-dried for one day and were tested to determine their compressive strength. The post-immersion compressive strength of specimens was compared with control specimens, and the strength reductions after immersion were ascertained.

3.2. Specimens

The specimens were 4×8 in. synthetic fiber reinforced concrete cylinders. The tests were designed for two fiber dosages, two pH levels, three temperatures, and three immersion periods [15]. The number of specimens for this phase are listed in Table 1.

Table 1. Material test plan

Fiber dosage	8 PCY (Vf=0.52%) 16 PCY (Vf=1.04%)
pH	2.5, 4.5
Temperature F (°C)	77, 95, 122 (25°C, 37°C, 50°C)
Test intervals (Months)	1,2,and 4
Number of cylinders (3 specimens per test)	108 immersed 6 control Total = 114

3.2.1. Material properties

Fibers

The PP fibers used in these cylindrical specimens were produced by BASF with the commercial brand name of MasterFiber MAC Matrix. The properties of these fibers are listed in Table 2.

Table 2. Geometric and material properties of MasterFiber MAC Matrix fiber

Material	100 % virgin polypropylene
Specific Gravity	0.91
Chemical Resistance	Excellent
Alkali Resistance	Excellent
Absorption	Nil
Melting Point	320 ^{0}F (160 ^{0}C)
Ignition Point	1094 ^{0}F (590 ^{0}C)
Type	Embossed
Length	2.1 in (54 mm)
Aspect Ratio	67
Tensile Strength	85 ksi (585 MPa)

These fibers have an embossed surface to ensure the proper bond with concrete. These fibers were manufactured to satisfy the requirements in ASTM C1116. These fibers are shown in Figure 30.

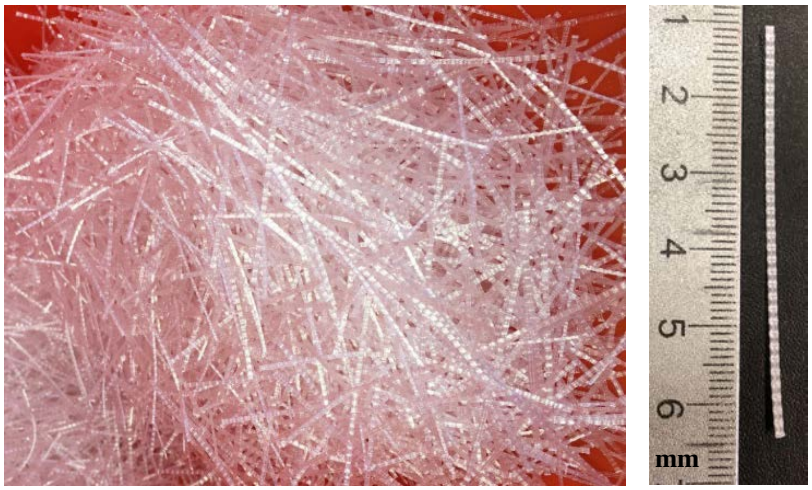

Figure 30. MasterFiber MAC Matrix synthetic fibers

Concrete

The concrete produced in this study was designed based on a dry cast mix that is shown in Table 3.

Table 3. Dry cast concrete mix design

Ingredient	**Quantity**
cement (lb./yd^3)	444
Fly ash (lb./yd^3)	113
water (lb./yd^3)	255
sand (lb./yd^3)	1496
aggregate 3/8" (lb./yd^3)	1774
W/C	0.46
1 lb./yd^3 = 0.59 kg/m^3	

The coarse aggregates' maximum size in this mix was 3/8 in. and the water to cement ratio was 0.46. Cement and fly ash were added to the mix after coarse and fine aggregates mixing, and then

the fibers were gradually added to the mix, and it was ensured that these fibers are mixed properly and uniformly, as shown in Figure 31.

Figure 31. Uniform distribution of fibers and concrete mix

After preparing the concrete, for each fiber dosage, 57 cylinders were produced. The compaction of the specimens was ensured by impacts of a compaction hammer, as shown in Figure 32.

Figure 32. Specimen casting and compaction

After producing the specimens, for each fiber dosage, three control specimens were tested after seven days of curing to determine the reference compressive strength. This test was conducted based on ASTM C39 [36]. After control tests were conducted, the specimens were immersed in acid baths.

Acid

The acid used in this study was highly concentrated sulfuric acid produced by Millipore SiGMA. To make solutions with pH levels of 2.5 and 4.5, a specific amount of this concentrated acid was added to neutral water until the desired pH is reached.

3.3. Test procedure and instrumentation

This phase of the study was conducted by immersing 54 cylindrical specimens in pH 2.5 and 4.5 solutions. The test temperatures in the acid baths were 77 °F, 95 °F, and 122 °F (25°C, 37°C, and 50°C). Before immersion, three cylinders from each fiber dosage were tested to determine the control compressive strength, as shown in Figure 33. These tests were conducted based on ASTM C39, *Standard Method for Compressive Strength of Cylindrical Concrete Specimens* [36].

Then the specimens were capped by sulfur capping method based on ASTM C617, *Standard Practice for Capping Cylindrical Concrete Specimens*. The capped specimens are depicted in Figure 34.

Figure 33. Compressive strength tests for an 8 PCY (0.52% V_f) specimen

Figure 34. Sulfur capped specimens

After the control tests and specimens preparation, cylindered were immersed in solutions, which were prepared by sulfuric acid dilution, as presented in Figure 35.

Figure 35. Cylinders aging in sulfuric acid and elevated temperature

To maintain the solution temperature, an immersion heater and a temperature control system were utilized in this setup. The heater used in this test was an instant electric immersion heater 300 Watts, and the temperature control unit was an Inkbird Itc-308S 1100W pre-wired digital dual stage temperature controller outlet, Figure 36.

Figure 36. Temperature control system

To ensure the stability of the pH level of the solutions, periodic manual pH measurements were conducted with a pen pH meter shown in Figure 37. The pH meter used in this study was Etekcity 0.05pH High Accuracy Pocket Size Digital PH Meter.

Figure 37. Digital pH meter

In order to ensure the accuracy of the pH meter measurements, pH papers (Figure 38) were also used to double check the pH meter readings.

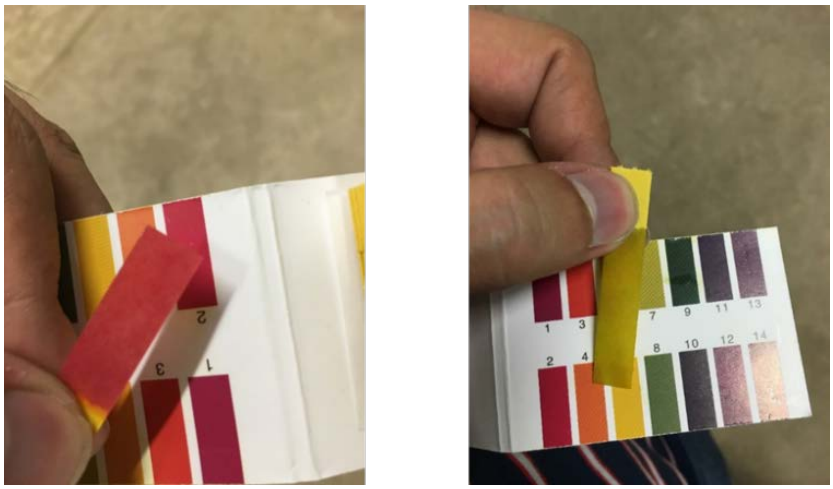

Figure 38. pH papers

The pH meter was calibrated on a weekly basis by using buffer calibration kits with three different pH buffers. The pH levels of these buffers were 4, 7, and 10, as presented in Figure 39.

Figure 39. Innovating Science buffer calibration kit

With all these precautions and instrumentations, the pH could be hardly maintained on the desired level. Initially, the pH of the solutions was rapidly changing because of the high alkalinity of concrete specimens. This trend was slower after a few days of immersion, and after a month of immersion, the pH level in both solutions became almost stable around the target pH level. The pH monitoring results are depicted in Figures 40 and 41.

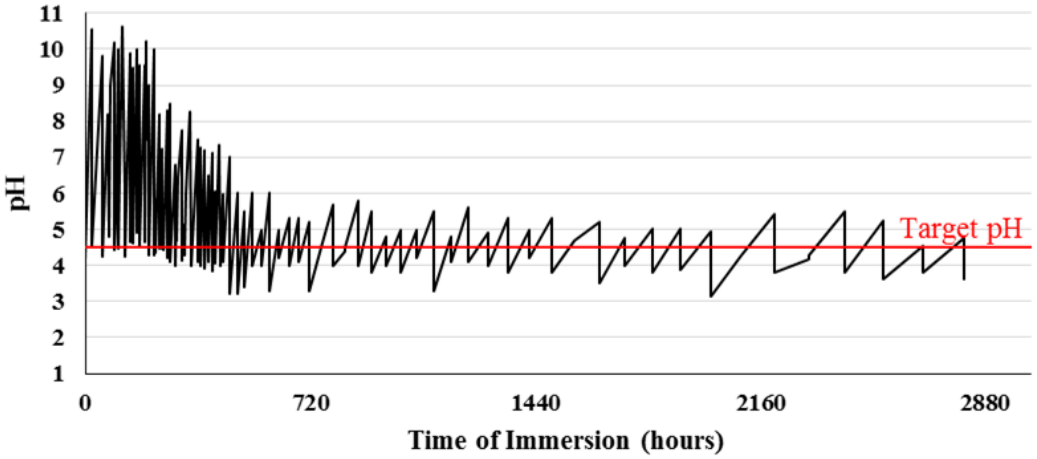

Figure 40. Variation of pH vs. time of immersion for pH4.5 and T=50°C container

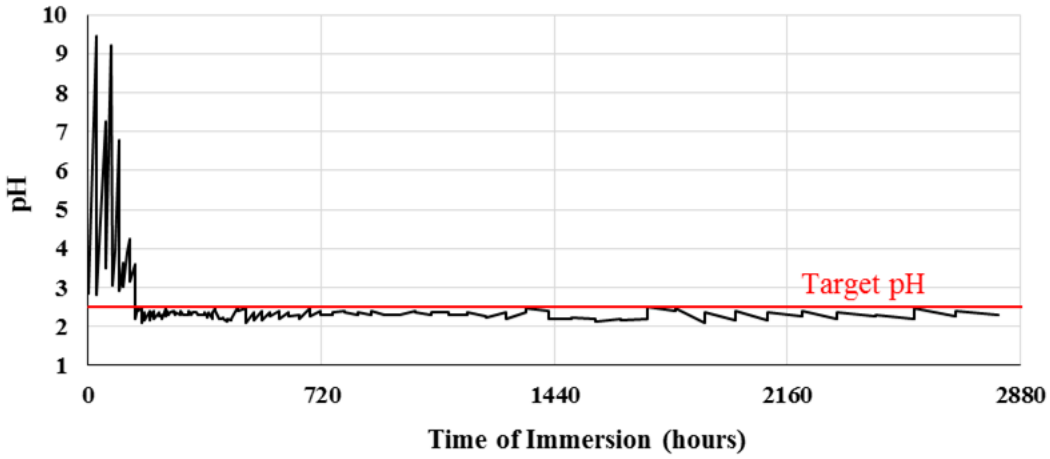

Figure 41. Variation of pH vs. time of immersion for pH2.5 and T=50°C container

The specimens were immersed in these harsh environments and were tested after 1, 2, and 4 months of immersion.

3.4. Results and discussion

Control tests were conducted on three cylinders from each fiber volume fraction after being cured for seven days. The seven-day period was chosen based on the pipe industry standards for dry cast pipe production. In the pipe industry, precast pipes are ready to be installed after seven days of production. The control specimens' results are listed in Table 4.

Table 4. Compressive strength of control specimens.

Volume fraction (V_f)	Average compressive Strength (psi)
0.52%	5264
1.04%	5890

When sulfuric acid reacts with concrete, one of the main reaction products is gypsum, which is also known as Calcium Sulfate or Calcium Sulfate Hydrate. The reactions are shown in Equations 13 and 14.

$$H_2SO_4+Ca(OH)_2 \rightarrow CaSO_4+H_2O \quad \textit{(Eq. 13)}$$

$$3CaO2SiO_2.3H_2O+H_2SO_4 \rightarrow CaSO_4.2H_2O+Si(OH)_4 \quad \textit{(Eq. 14)}$$

The gypsum products can be seen as a white layer on the surface of the reacted specimens, they are very weak mechanically, and they have a very loose structure. The formation and propagation of this material on the test specimens will result in strength loss.

After 1, 2, and 4 months of immersion, 3 specimens from each fiber volume fraction were taken out of these six baths and were air dried for a day. The dried specimens were tested to determine their compressive strength. The immersed specimens' compressive strength were compared with their corresponding control specimens, and the strength reduction percentage was calculated for each set. Table 5 and Figure 42 show a summary of the results.

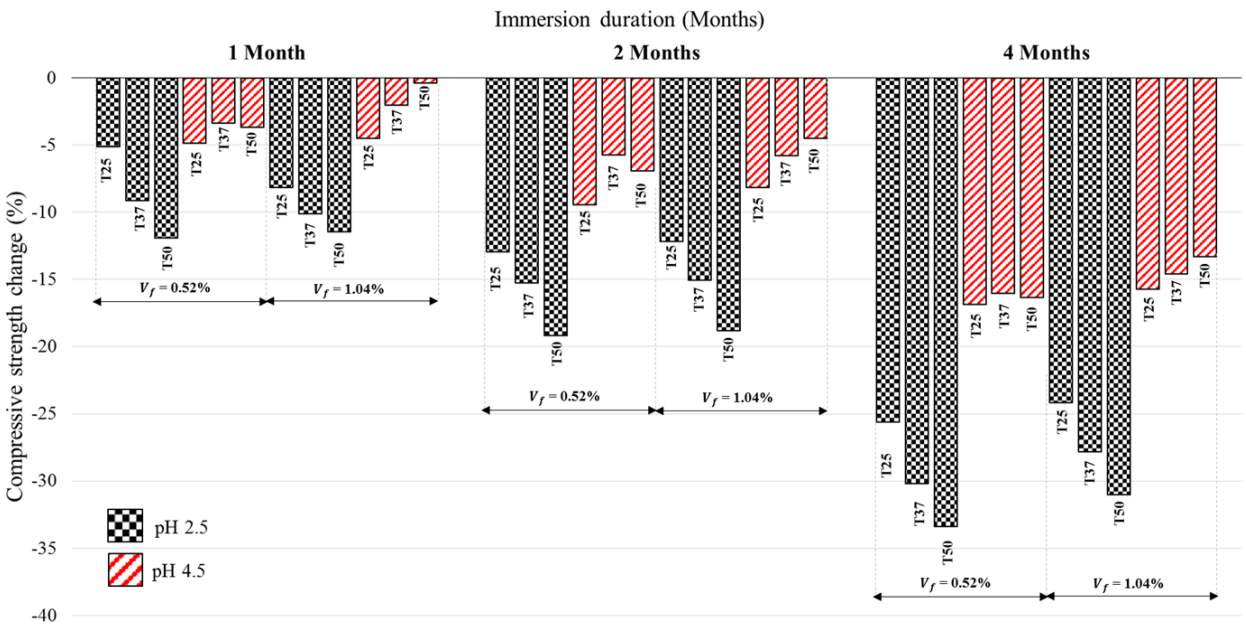

Figure 42. SYNFRC material tests results

Table 5. SYNFRC material tests result summary

Immersion Duration (Months)	0.52% Fiber Volume Fraction Mix Design						
	Environmental Conditions	pH 2.5 T 25	pH 2.5 T 37	pH 2.5 T 50	pH 4.5 T 25	pH 4.5 T 37	pH4.5 T 50
1	Compressive Strength Change (%)	-5.11	-9.15	-11.93	-4.84	-3.37	-3.66
2		-12.93	-15.25	-19.17	-9.45	-5.72	-6.93
4		-25.64	-30.22	-33.37	-16.87	-16.01	-16.35
	1.04% Fiber Volume Fraction Mix Design						
1	Compressive Strength Change (%)	-8.18	-10.13	-11.43	-4.52	-0.81	-0.39
2		-12.16	-15.05	-18.81	-8.13	-3.50	-4.49
4		-24.20	-27.84	-31.00	-16.60	-12.08	-13.33

As shown in Figure 44 and Table 5, the specimens with V_f of 1.04% showed slightly less strength reduction than those with 0.52%. The reason for this difference could be the presence of more fibers in the 1.04% V_f specimens. These polypropylene fibers are highly resistant to acids, and the higher volume of these in the concrete mix would help the acid-resistivity of the composite. The obtained results are conforming to the Araghi and Janfeshan's results [22]. In that paper, it was shown that higher amounts of PET particles in the composite helped the acid resistivity of the specimens. These are also similar to the results obtained by Nematzadeh and Fallah-Valukolaee

[24] who determined the effect of harsh acidic environments of Forta-Ferro fiber reinforced concrete specimens.

Figure 44 also implies that with the temperature increase, the specimens that were immersed in pH 2.5 baths were facing higher strength loss, and this conforms to the Arrhenius equation. Based on the Arrhenius equation, higher temperature results in higher reaction rates, and consequently, for this case, it results in more compressive strength loss.

For pH 4.5, the trend is different from pH 2.5 results. With the temperature increase, the compressive strength increases, and that is related to the comparative reaction rate of hydration reactions and pH 4.5 acid and concrete paste reaction rate. Considering the control tests, which were conducted after 7 days, it can be concluded that the specimens were not mature enough to neglect the effect of improvement reactions (hydration) and pH 4.5 solutions do not have a very aggressive effect on the specimens to overtake the rate of hydration reaction. In this case, by increasing the temperature, hydration reactions took place on a faster rate than the deterioration reactions, and as a result, less compressive strength change was detected in higher temperatures.

The average ratio of compressive strength loss in pH 2.5 and pH 4.5 solutions after 4 months was about 1.87. This value shows that specimens that were immersed in pH 2.5 baths were deteriorated approximately twice as much as those that were put in pH 4.5 Sulfuric acid.

After 4 months of aging, as shown in Figure 44, the specimens' compressive stress was decreased with higher immersion duration.

In addition to load bearing capacity, visual inspection was also conducted after each set of tests. In these inspections, the condition of fibers, depth of penetration, and amount of gypsum on the

surface of the specimens were evaluated qualitatively. Figure 43 presents a summary of the results of 4 months monitoring and inspection of the specimens.

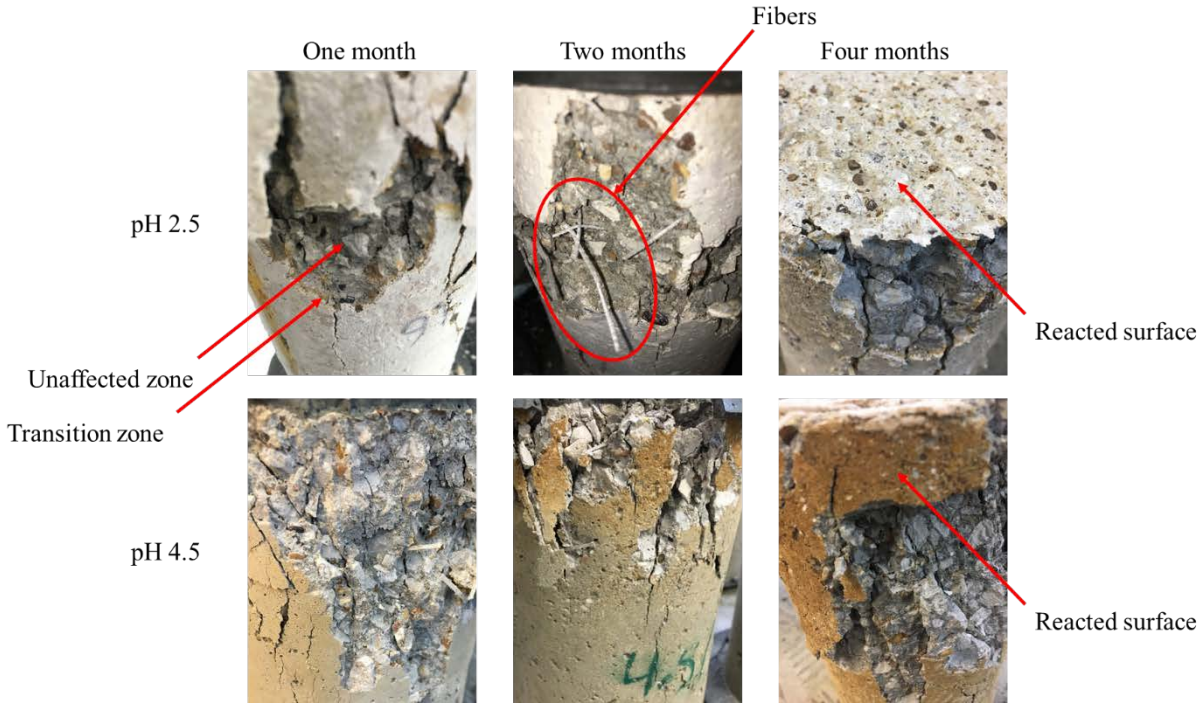

Figure 43. Specimens' deterioration

As depicted in Figure 43, the amount of gypsum on the surface of the specimens that were immersed in pH 4.5 was considerably lower than pH 2.5 ones. The yellowish-brown transition zone indicates the level of deterioration in the depth of the specimens. It was also observed that more deterioration occurs when the immersion duration increases.

In the enlarged part of Figure 45, the fibers near the deteriorated region are magnified, and there was no sign of corrosion on these fibers. Polypropylene is a very acid-resistant material, and it explains their durability in these harsh acidic solutions.

CHAPTER 4. ACCELERATED AGING OF SYNTHETIC FIBER REINFORCED CONCRETE PIPES

4.1. Overview

After the material study phase, the actual synthetic fiber reinforced concrete pipes should be evaluated, and their service life should be estimated based on the accelerated aging test results. In this phase, pipe specimens with one fiber volume fraction (0.52% - 8PCY) will be immersed in solutions with two different pH levels. The tests temperatures were also set on two different temperatures, one set was immersed in room temperature baths, and the other set was soaked in acid solutions with elevated temperatures. The specimens were immersed in the solution for one year, and on certain intervals, some of the pipes were taken out of the solutions and air-dried. Then the sections were tested to determine their D-load capacity after immersion. The D-load of the immersed specimens were compared with the control specimens' load bearing capacity, and the reduction rate graphs were obtained.

4.2. Pipe production and standards

The production, quality control, and test methods used in this phase of study were based on ASTM standards and concrete pipe regulations.

4.2.1. Pipe production and classifications

ASTM C76, *Standard Specification for Reinforced Concrete Culvert, Storm Drain, and Sewer Pipe*, is one of the main manufacturing specifications for pipe producers nationwide and beyond [37]. This standard classifies pipes in five different classes with three different wall thicknesses. Pipe classes are V, IV, III, II, and I. Class I has the minimum strength requirement, and class V has the maximum strength requirement. Pipes wall thickness types are wall A, wall B, and wall C,

where wall A is the thinnest, and wall C is the thickest one for each class. ASTM C76 tables determine the pipes' dimension, strength, and reinforcement requirements, as shown in Figure 44.

NOTE 1—See Section 5 for basis of acceptance specified by the owner. The strength test requirements in pounds-force per linear foot of pipe under the three-edge-bearing method shall be either the D-load (test load expressed in pounds-force per linear foot per foot of diameter) to produce a 0.01-in. crack, or the D-loads to produce the 0.01-in. crack and the ultimate load as specified below, multiplied by the internal diameter of the pipe in feet.

D-load to produce a 0.01-in. crack	1350
D-load to produce the ultimate load	2000

Internal Designated Diameter, in.	Wall A: Concrete Strength, 4000 psi				Wall B: Concrete Strength, 4000 psi				Wall C: Concrete Strength, 4000 psi			
	Wall Thicknesses, in.	Circular Reinforcement[B] Inner Cage	Circular Reinforcement[B] Outer Cage	Elliptical Reinforcement[C]	Wall Thicknesses, in.	Circular Reinforcement[B] Inner Cage	Circular Reinforcement[B] Outer Cage	Elliptical Reinforcement[C]	Wall Thicknesses, in.	Circular Reinforcement[B] Inner Cage	Circular Reinforcement[B] Outer Cage	Elliptical Reinforcement[C]
		Reinforcement, in.[2]/linear ft of pipe wall										
12	1¾	0.07[D]	...	...	2	0.07[D]	...	...	2¾	0.07[D]	...	...
15	1⅞	0.07[D]	...	...	2¼	0.07[D]	...	...	3	0.07[D]	...	...
18	2	0.07[D]	...	0.07[D]	2½	0.07[D]	...	0.07[D]	3¼	0.07[D]	...	0.07[D]
21	2¼	0.14	...	0.11	2¾	0.07[D]	...	0.07[D]	3½	0.07[D]	...	0.07[D]
24	2½	0.17	...	0.14	3	0.07[D]	...	0.07[D]	3¾	0.07	...	0.07[D]
27	2⅝	0.18	...	0.16	3¼	0.16	...	0.14	4	0.08	...	0.07[D]
30	2¾	0.19	...	0.18	3½	0.18	...	0.15	4¼	0.10	...	0.08
33	2⅞	0.21	...	0.20	3¾	0.20	...	0.17	4½	0.12	...	0.10
36	3	0.21	0.12	0.23	4 [E]	0.17	0.10	0.19	4¾ [E]	0.08	0.07	0.09
42	3½	0.24	0.15	0.27	4½	0.21	0.12	0.23	5¼	0.12	0.07	0.12
48	4	0.32	0.19	0.35	5	0.24	0.14	0.27	5¾	0.16	0.10	0.18
54	4½	0.38	0.23	0.42	5½	0.29	0.17	0.32	6¼	0.21	0.12	0.23
60	5	0.44	0.26	0.49	6	0.34	0.20	0.38	6¾	0.24	0.15	0.27
66	5½	0.50	0.30	0.55	6½	0.41	0.24	0.45	7¼	0.31	0.19	0.34
72	6	0.57	0.34	0.63	7	0.49	0.29	0.54	7¾	0.36	0.21	0.40
	Concrete Strength, 5000 psi											
78	6½	0.64	0.38	0.71	7½	0.57	0.34	0.63	8¼	0.42	0.24	0.47
84	7	0.72	0.43	0.80	8	0.64	0.38	0.71	8¾	0.50	0.30	0.56
					Concrete Strength, 5000 psi				Concrete Strength, 5000 psi			
90	7½	0.81	0.49	0.90	8½	0.69	0.41	0.77	9¼	0.59	0.35	0.66
96	8	0.93	0.56	1.03	9	0.76	0.45	0.84	9¾	0.70	0.42	Inner Circular 0.27; Plus Elliptical 0.42
102	8½	1.03	0.62	Inner Circular 0.41; Plus Elliptical 0.62	9½	0.90	0.54	Inner Circular 0.36; Plus Elliptical 0.54	10¼	0.83	0.50	Inner Circular 0.33; Plus Elliptical 0.50
108	9	1.22	0.73	Inner Circular 0.49; Plus Elliptical 0.73	10	1.08	0.65	Inner Circular 0.43; Plus Elliptical 0.65	10¾	0.99	0.59	Inner Circular 0.40; Plus Elliptical 0.59
114	[A]	...	...	... ...	[A]	...	...	... ...	[A]	...	...	... ...
120	[A]	...	...	... ...	[A]	...	...	... ...	[A]	...	...	... ...
126	[A]	...	...	... ...	[A]	...	...	... ...	[A]	...	...	... ...
132	[A]	...	...	... ...	[A]	...	...	... ...	[A]	...	...	... ...
138	[A]	...	...	... ...	[A]	...	...	... ...	[A]	...	...	... ...
144	[A]	...	...	... ...	[A]	...	...	... ...	[A]	...	...	... ...

Figure 44. Class III concrete pipe requirements, ASTM C76 [37]

According to Figure 44, the wall thickness requirements, reinforcement requirements, and dimension requirements for concrete pipes are shown in the tables provided in this standard.

For synthetic fiber reinforced concrete pipes, there is an additional standard to determine the production and quality control requirements of these pipes. ASTM C1818, *Standard Specification for Synthetic Fiber Reinforced Concrete Culvert, Storm Drain, and Sewer Pipe*, is the manual for

synthetic fiber reinforced concrete pipes [12]. This standard determines the strength requirements for these pipes, and they are almost similar to ASTM C76. ASTM C1818 is mainly different from ASTM C76 because of its reload requirement. The reload criteria addresses the long-term serviceability of fibers and fiber-concrete bond testing. D_{Reload} it is related to the service load by the α factor as shown in Equation 15.

$$D_{Reload} = D_{service} / \alpha \qquad \textit{(Eq. 15)}$$

The strength requirements in this standard for SYNFRCPs are shown in Figure 45 extracted from ASTM C1818.

Pipe Class	$D_{Service}$ (lb/linear foot/foot of diameter)	D_{Ult} (lb/linear foot/foot of diameter)	D_{Reload} (lb/linear foot/foot of diameter)
I	800	1200	$D_{Service}/\alpha$
II	1000	1500	where:
III	1350	2025	α = long-term serviceability factor as
IV	2000	3000	determined per Section 9 of this
V	3000	4500	standard

Figure 45. Strength Requirements for SYNFCPs based on ASTM C1818-18 [12]

α in this standard is the long-term serviceability factor for 100-year strength extrapolation. Determination of α is also instructed by this standard via a series of long-term tests.

4.2.2. Pipe testing standards

Concrete pipes quality control and testing protocols are defined in ASTM C497, *Standard Test Methods for Concrete Pipe, Concrete Box Sections, Manhole Sections, or Tile*. This standard defines the three-edge bearing tests machine, setup, and procedure. The results of three-edge bearing tests will be reported in the form of D-load vs. deflection. D-load is defined as the load per length of the pipe per diameter of the pipe (lb./ft./ft.). Three edge bearing tests setup is shown in Figure 46. As shown in Figure 46, there are two bottom edges, and they can be made from wood or hard rubber strips. The lower bearings should be placed 1 in. / ft. of specimen diameter, but not less than 1 inch. The upper bearing should be a rubber strip, and above that, a sound rigid wood

should be attached to the setup beneath the loading apparatus. With a complete setup, the three-edge bearing test can be done with the maximum load rate of 7500 lbf./linear foot of the pipe per minute up to the 75% of the designed strength after that it should be reduced to the maximum uniform rate of 1/3 of design strength.

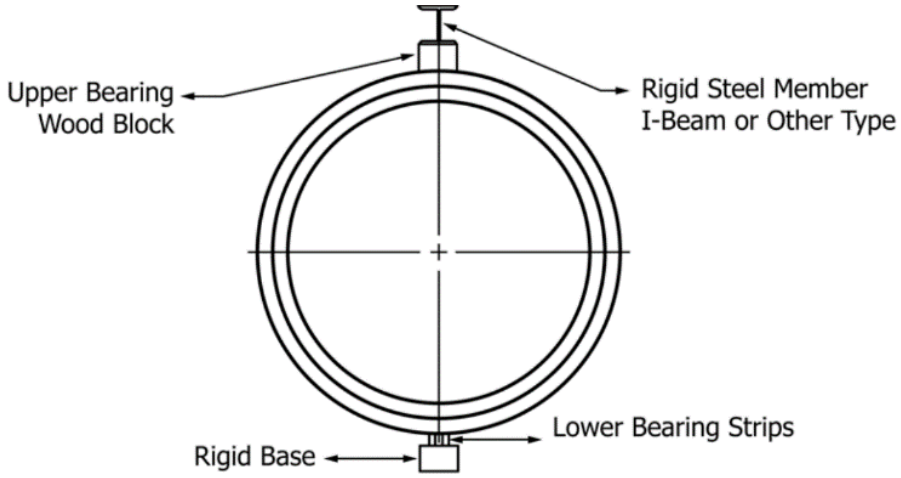

Figure 46. Three edge bearing tests setup, ASTM C497 [38]

For SYNFRCPs, the test method is instructed in ASTM C1818. In this standard, the testing protocol is mostly similar to the ASTM C497 with a difference after the first crack. ASTM C1818 instructs that the pipes should be unloaded after the occurrence of the 0.01” cracks and it should be reloaded up to the D_{Reload} to ensure the bond/ductility/toughness/long-term serviceability.

A sample of the three-edge bearing test is shown in Figure 47.

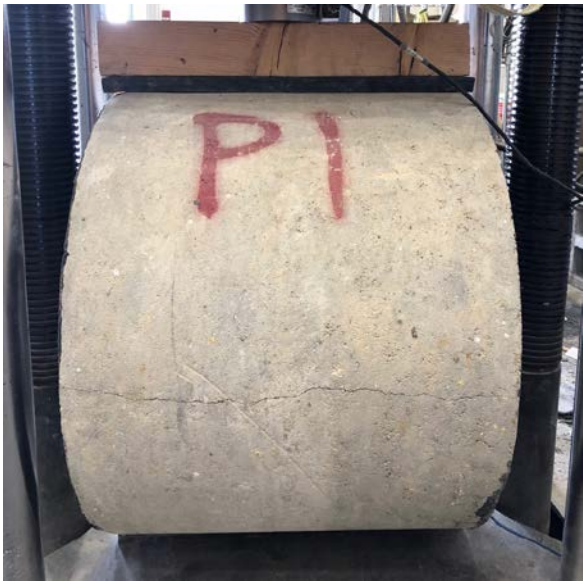

Figure 47. Three-edge bearing test

4.2.3. Proof of design

After testing SYNFRCPs based on ASTM C497 and ASTM C1818, the test results should be compared with the design criteria mentioned in ASTM C1818 to ensure the quality of the tested pipes. ASTM C1818 design limits for the load bearing capacity of SYNFRCPs are listed in Figure 47. The pipes should satisfy the ultimate and reload load-bearing limits to pass the requirements.

For RCPs, the design requirements are specifically mentioned for each pipe class in ASTM C76. A sample of these requirements is shown in Figure 46. The pipes should satisfy the service and ultimate load requirements to be passed.

4.3. Specimen preparation

In this phase of the project, 2-ft. pipe pieces were designed to be immersed in acidic solutions. The pipes were synthetic fiber reinforced concrete pipes, and the fiber volume fraction of these pipes were 0.52% (8PCY). SYNFRCPs were produced by dry cast concrete with packerhead method to fulfill the requirements of ASTM C76 for 24” Class III pipes with wall B. Since the goal of the

project was focused on the demands of the Florida Department of Transportation about the service life assessment of synthetic fiber reinforced concrete pipes, the pipes were produced in Florida and by using the materials available there. The produced pipes are shown in Figure 48, and the materials that were used in these pipes are described in this section.

Figure 48- Twenty four-inch synthetic fiber reinforced concrete pipes

4.3.1. Material properties

Concrete

The concrete pipes, which were used in this phase, was produced by one of the largest concrete pipe producers nationwide. They were manufactured based on the company's mix design. The mix was designed precisely to ensure the satisfaction of ASTM C1818 requirements.

Fibers

The fibers, which were used in the production of SYNFRCPs, were the same fibers used for the material testing phase. The fibers were produced by BASF, the chemical company with the commercial brand name of MasterFiber MAC Matrix. The properties of these fibers are listed in Table 2.

Acid

The acid, which was used in this phase, was also similar to the one used in the material testing phase, Figure 34. It was a highly concentrated sulfuric acid manufactured by Millipore Sigma.

4.4. Test procedure and instrumentation

4.4.1. Test procedure

In this phase, 28 pipe pieces were immersed in an acidic solution with two different pH levels and two different temperatures. The pH levels were pH 2, and pH 4. The temperatures were 77°F and 122°F (25°C and 50°C). Before immersion, three specimens were tested to determine the control specimens' D-load capacity as the reference strength. The summary of the test procedure is presented in Table 6 and the number of specimens for each environment is shown in Figure 49.

Table 6. Pipe testing phase test plan

Environment	Temperature	Duration (Months)
pH: 2.0	25°C	2,5,8
pH: 4.0		2,5,8,12
pH: 2.0	50°C	2,5,8,12
pH: 4.0		2,5,8

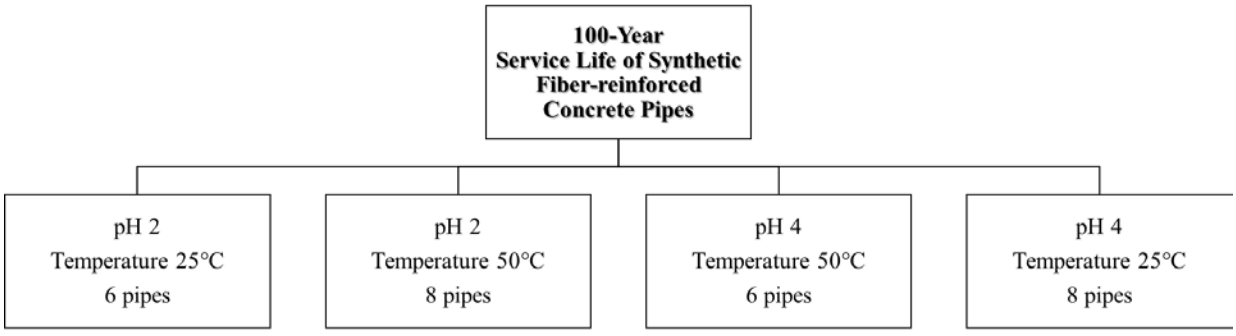

Figure 49. SYNFRCP service life assessment test protocol summary

The tests were conducted based on ASTM C76, ASTM C497, and ASTM C1818. The pipes were produced in 8-ft. pieces and they had to be cut in order to be suitable for immersion in the containers. The pipes were cut into 2-ft pieces, as shown in Figure 50.

Figure 50. Cutting 8-ft. SYNFRCPs into 2-ft. pieces

4.4.2. Instrumentations

To immerse these pipes and control the environmental conditions, many pieces of equipment were utilized to fulfill this purpose. For immersion, 275-gallon totes were used, as shown in Figure 51. The head of these totes was cut to convert them to an immersion pool for the pipes.

Figure 51. 275-gallon totes

In order to make a safe and controlled space for the test setup, a series of shipping containers were used to accommodate the totes and the immersion test set up, Figure 52. These containers were equipped with air conditioners to keep the inside temperature of the containers at the desired level when required.

Figure 52. Shipping containers for the test setup

In order to control the solutions' temperature, industrial immersion heaters and digital temperature control systems were utilized. Since the solutions were acidic, and it was a long-term project, acid resistant heaters were chosen. Figure 53 shows the details of the acid resistant heaters. As

illustrated in Figure 53, the immersion heaters were covered with quartz tubes to protect the metallic parts against acid solutions.

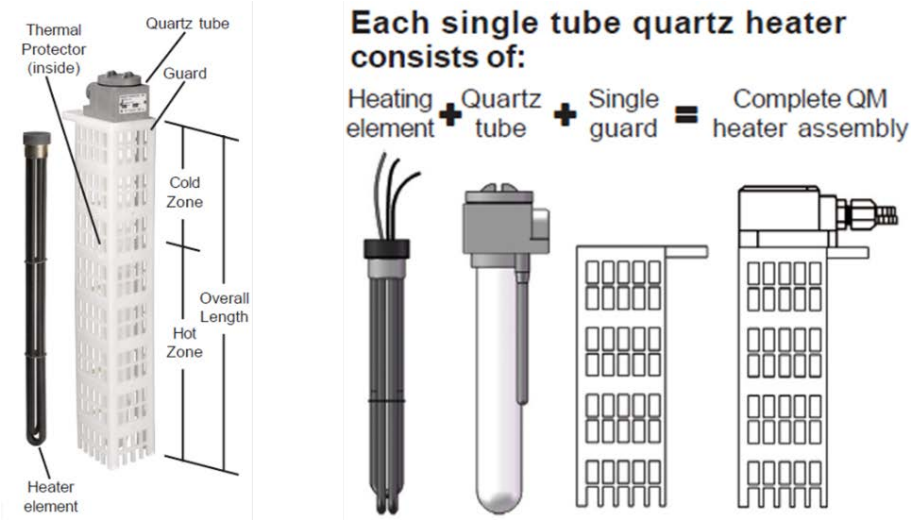

Figure 53. 3500 Watt quartz immersion heater

The QM3.5229E immersion heaters were 29 inches long, with an 18-inch hot zone. The heaters' circuits were guarded with a P1 fuse to cut the current whenever the solution evaporates, and the fluid level goes beneath the tip of the fuse.

In addition to the immersion heaters, to control the solution temperature and keep it at a constant level, digital temperature control systems were utilized. This system, as shown in Figure 54, was a 3-phase temperature control system and were programmed to maintain the temperature at 122°F (50°C).

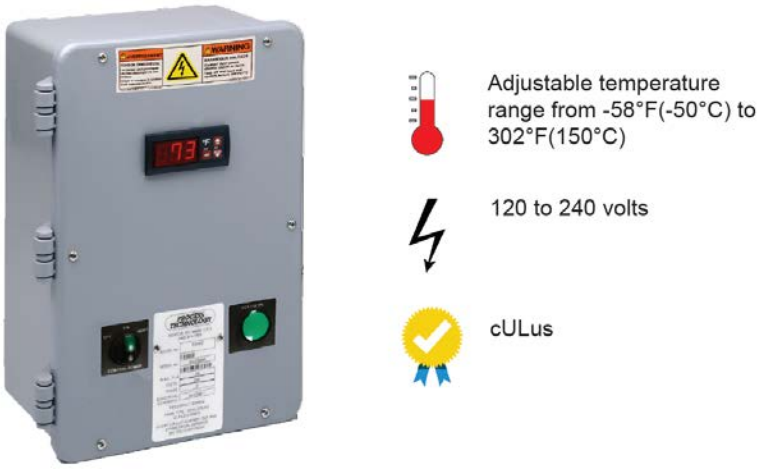

Figure 54. DLC 3-phase temperature control system

Since the immersion heaters required more high capacity 3-phase power, a separate three-phase circuit was designed for them and the three-phase power supply and distribution systems are shown in Figure 55.

Figure 55. Three-phase power supply and distribution

In addition to the immersion setup, three-edge bearing tests after each immersion period were performed at the Civil Engineering Laboratory Building (CELB). The testing machine was a

Tinius Olsen compression and tension machine, Figure 56, with 400 kips capacity. The loading precision of this machine is ± 0.01 from 0.2% to 100% of frame capacity.

Figure 56. Tinius Olsen compression and tension machine

For load measurement, a 200 kips load cell made by Interface Force Measurement Solutions was utilized. The precision of the 200 K Interface load cell was ±0.04.

Figure 57. Interface 200 Kips load cell

For vertical displacement measurement, a Micro-Measurements cable-extension displacement sensor was used, Figure 58. These sensors transmit a voltage proportional to the displacement and with a linear calibration; the actual displacement can be measured in terms of mV.

Figure 58. Micro-Measurements cable-extension displacement sensor

For data acquisition, System 8000 StrainSmart® data acquisition system was utilized. This instrument has eight software-selectable input channels, support a wide range of input transducers and devices like; strain gage, strain gage-based transducers, and thermocouples. System 8000 and its channels are shown in Figure 59.

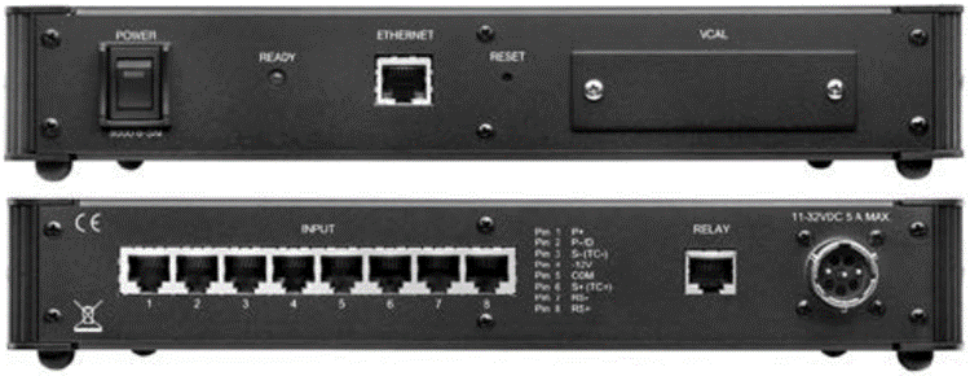

Figure 59. System 8000 StrainSmart® data acquisition system

The software that was used for data acquisition was a StrainSmart 8000 software shown presented in Figure 60.

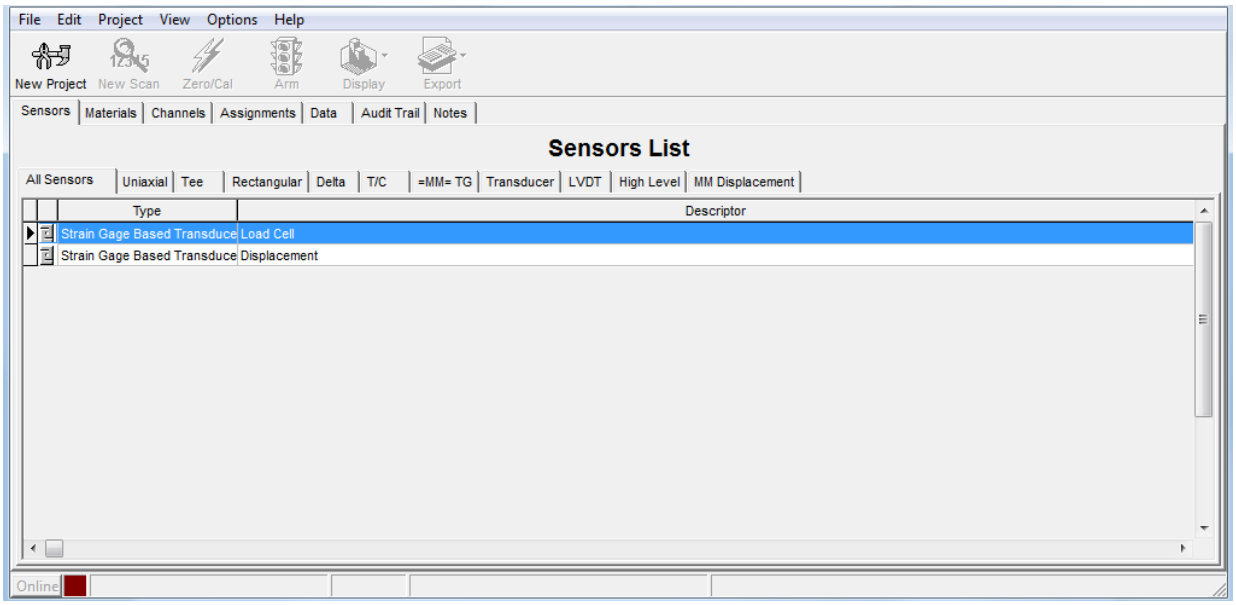

Figure 60. StrainSmart 8000 software

4.5. Immersion test setup

After instruments and materials preparation, the pipes were put inside the totes as depicted in Figure 61.

Figure 61. SYNFRCPs adjustment in 275-gallon totes

After putting the totes inside the shipping containers, they were filled with potable water, Figure 62.

Figure 62. Filling totes with potable water

To make pH 2 and pH 4 solutions, concentrated sulfuric acid was poured into the totes, and the solution was stirred up carefully to make a uniform mix with the desired pH, Figure 63.

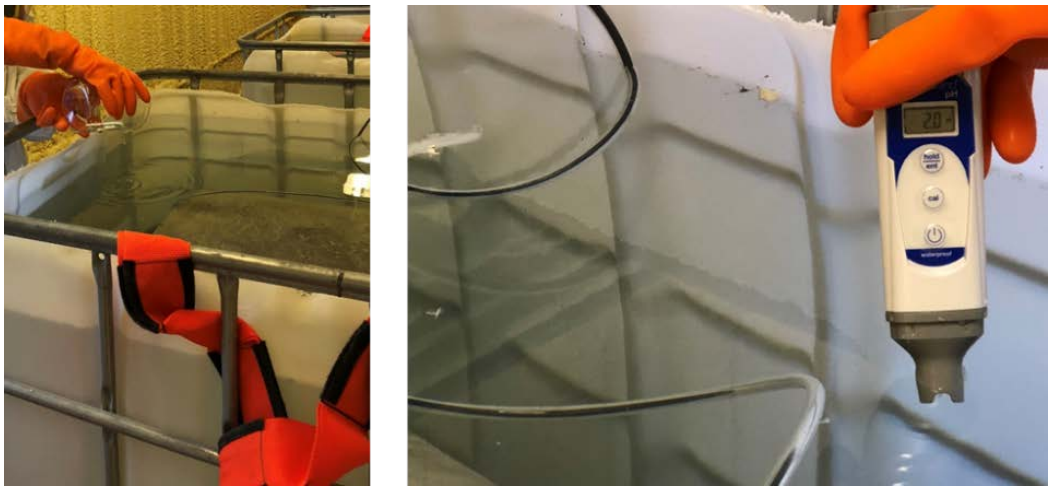

Figure 63. Sulfuric acid solution preparation

After preparing the solutions, the heaters of 122°F (50°C) totes were turned on and the temperature control system was set to maintain the temperature at 122°F (50°C). The temperature of the77°F (25°C) totes were maintained by the air conditioners. The whole immersion setup is shown in Figure 64.

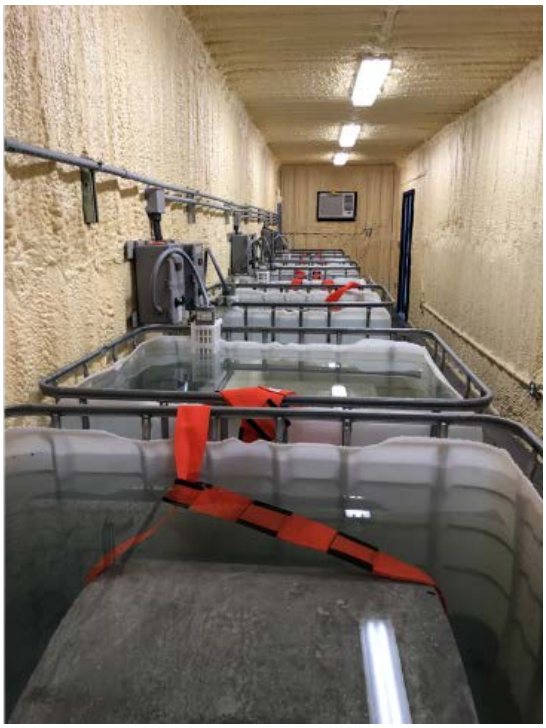

Figure 64. Immersion test set up

4.6. Results and discussion

SYNFRCPs were tested before and after immersion to determine the load bearing capacity loss of the pipes due to acid deterioration in accelerated aging environments. Pre-immersion test results were used as reference and control values, post-immersion results were compared with the control ones, and the load decrease percentage was used as the comparison index.

The D-load tests were conducted at the UTA Civil Engineering Laboratory Building. The tests were performed at the load rate of 500 lb./min. Based on ASTM C1818, after the occurrence of the first crack in the pipes, the specimens were unloaded and reloaded to ensure the long-term serviceability of the fibers. Three edges of the D-Load tests were constructed with two edges in the bottom made from rubber and the top edge was made of high-density rubber strip and a 4×4 wood piece as shown in Figure 65.

Figure 65. Rubber edges of the three-edge bearing tests

The tests were performed to reach to the failure point of the pipes and the results were reported based on the D-load vs. vertical deflection of the specimens. A sample of a SYNFRCP at the point of failure is shown in Figure 66.

Figure 66. SYNFRCP at the ultimate load

4.6.1. Control tests

Six months after production, cut SYNFRCP pieces were tested based on ASTM C1818 to determine their load bearing capacity, as shown in Figure 67.

Figure 67. Control D-load tests

The six months period was chosen to ensure >95% of hydration. As discussed in Chapter 2, specimens that were immersed in pH 4.5 solutions showed less load decrease in higher temperature because of hydration reactions progress. In order to avoid noticeable further hydration progress, 6 months hydration period was set for control specimens tests at this phase. The control tests results are depicted in Figure 68.

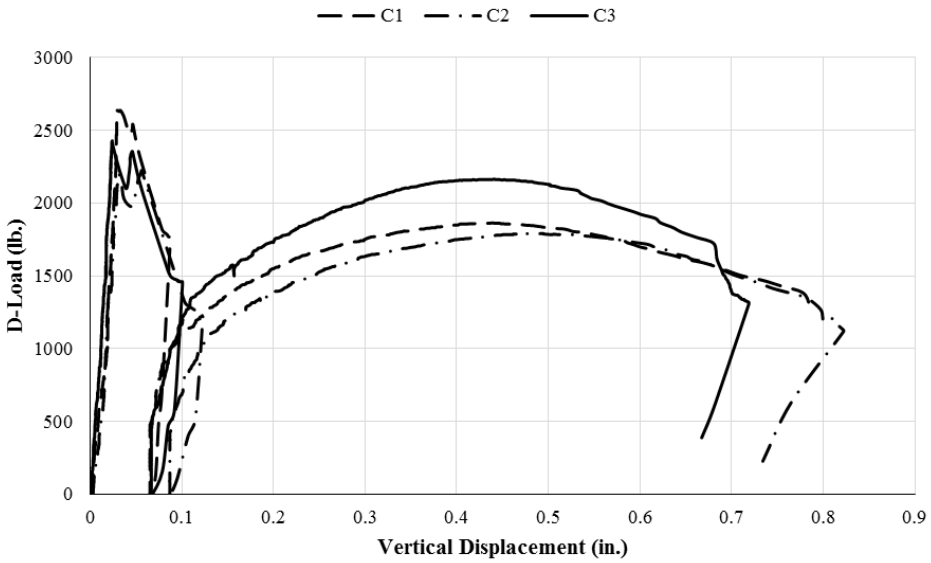

Figure 68. Control specimens tests

4.6.2 Post-immersion tests

After immersing the specimens in corrosive solutions for 2, 5, 8, and 12 months. Two specimens from each environment were taken off, and air dried for at least a day and then were transported to the University of Texas at Arlington Civil Engineering Laboratory (UTA CELB) and were tested to determine their post-immersion load bearing capacity.

Acid - concrete reactions resulted in cement paste deterioration according to the post immersion observations. This deterioration, as depicted in Figure 69, implies that the strength test results of the immersed should be lower than the control ones.

Figure 69. Concrete deterioration sediments

After each immersion period, the solutions should have been neutralized before disposal to avoid adverse environmental impacts. Sodium Hydroxide, which is a strong alkaline, was used for neutralizing the acidic solutions. The process and materials are shown in Figure 70.

Figure 70. Sodium Hydroxide and acidic solution neutralization

Two months tests

After soaking the SYNFRCPs in the solutions for two months. Two specimens from each environment were extracted from the solutions and were tested based on ASTM C1818. Visual inspection of the specimens after the immersion were also carried out to monitor the visual effects of the corrosive environments on the specimens. Figure 71 presents the effect of accelerated aging tests on concrete specimens.

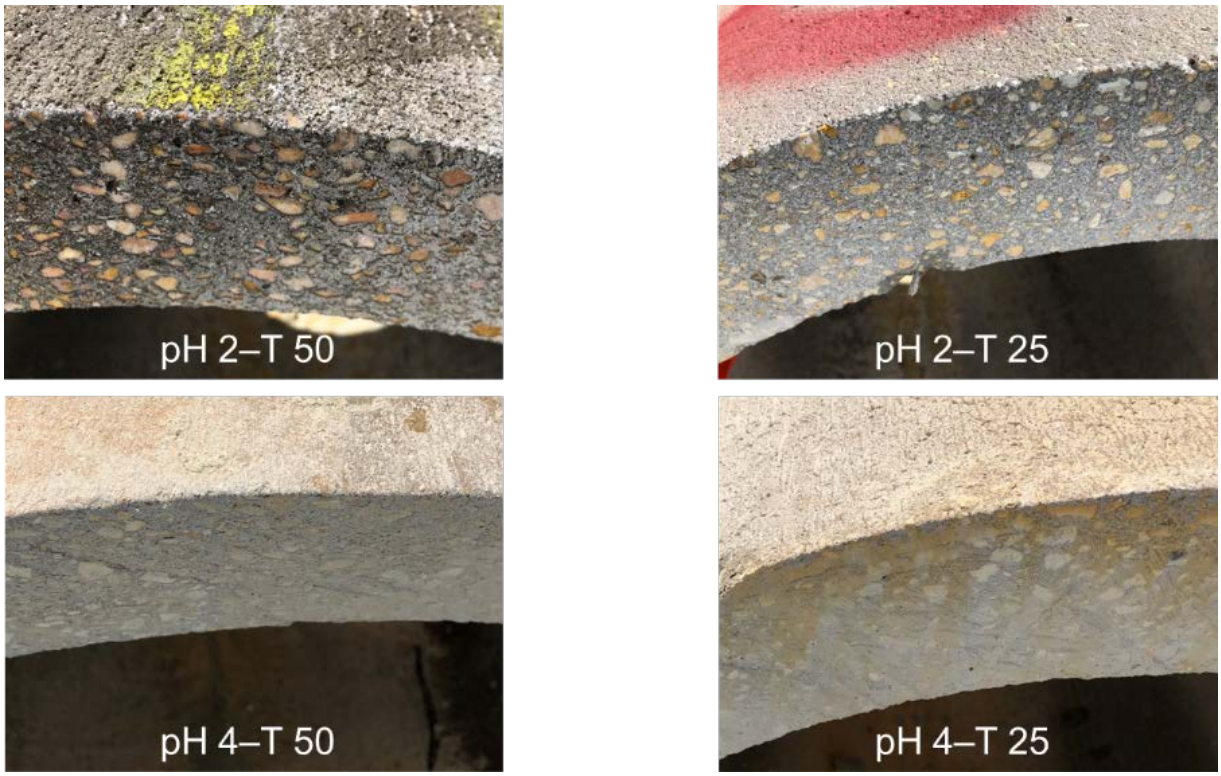

Figure 71. Post-immersion specimens' surface, 2 months tests

The visual inspection of the specimens shows that the highest amount of deterioration occurred on pH2-temperature 50°C ones and the lowest deterioration occurred on pH4-temperature 25°C pipes. pH2-T50 specimens' coarse aggregates are exposed, and a thin layer of the cement paste around them was corroded by the acidic solution. pH4-T25 pipes were almost intact, and a slight discoloration could be observed on their surface.

After putting them outside to air dry for a day, the specimens were transported to the UTA campus for three-edge bearing tests. The tests were conducted with the 400 Kips machine, as shown in Figure 72. The load rate, which was used for these tests was 500 lbs./min. and the load and displacement were recorded every one second by a Vishay data acquisition system and StrainSmart software.

Figure 72. Three-edge bearing tests, two months immersion

The results of the load bearing capacity tests of immersed specimens for two months are shown in Figure 73.

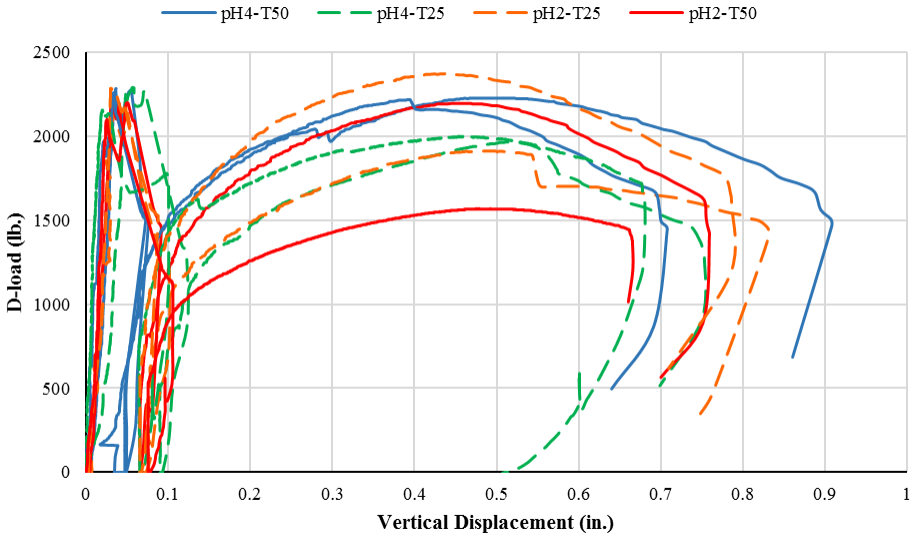

Figure 73. Three-edge bearing tests results after two months immersion

The first peak of the D-load test graphs are the ultimate load capacity of the sections, and these values are listed in Table 7.

Table 7. Two months test results for ultimate load comparison

Specimen	Ultimate load (lb./ft./ft.)	Ultimate load change (%)
Control	2427	N/A
pH2-T50	2245	-7.50
pH2-T25	2241	-7.66
pH4-T50	2259	-6.92
pH4-T25	2272	-6.39

Based on the obtained results, D-load change vs. Time graphs can be generated as presented in Figure 74.

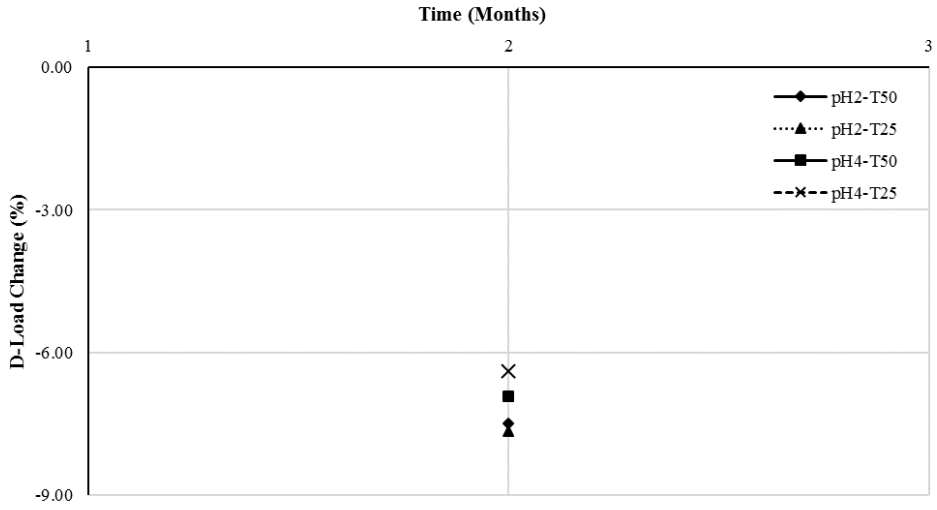

Figure 74. D-load change vs. time after two months immersion

Two months test results showed that strength reduction for all of the specimens was close to each other. Comparing the minor differences also reveals that the highest load reduction occurred in pH 2-T25 specimens and lowest load reduction occurred in pH4-T25 pipes.

Five months tests

After five months, the specimens that were immersed in the solutions were taken out to evaluate the effects of the corrosive environment. The visual inspection of the specimens is shown in Figure 75.

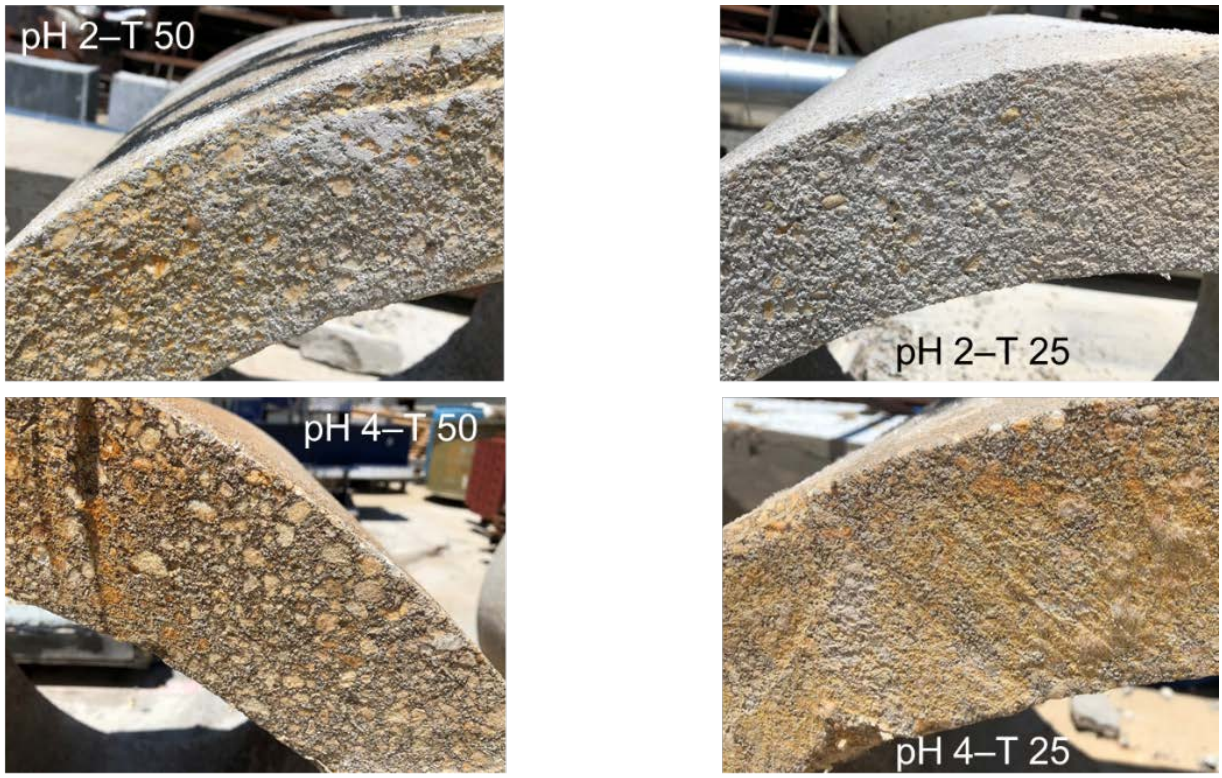

Figure 75. Post-immersion specimens' surface, 5 months tests

As shown in Figure 75, the highest amount of deterioration occurred in pH2-T50 cases, and pH4-T25 specimens did not deteriorate significantly. After five months, specimens that were immersed in pH4-T50 solutions started to show major signs of deterioration, which are significant discoloring and exposed coarse aggregates. Since the solutions are diluted Sulfuric acid and the reaction product of cement paste with this acid is Gypsum, which is a loose white layer on the surface of the pipes, specimens covered with higher amount of this substance on their surface faced more deteriorations. Figure 76 depicts gypsum formation on the surface of a pipe that was immersed in the pH2-T50 solution for five months.

Figure 76. Gypsum formation on the immersed pipe surface, pH2-T50 for five months

Visually comparing the two months and five months specimens reveals that longer immersion period results in higher deterioration and more alterations in the cement paste.

After letting the specimens air dry for two days, they were transported to the UTA campus, as depicted in Figure 77, to test them based on ASTM C1818.

Figure 77. Transportation of the 5-months immersed specimens

All eight specimens were tested with the same load rate (500 lb./ft./ft.) and loading device, as shown in Figure 78.

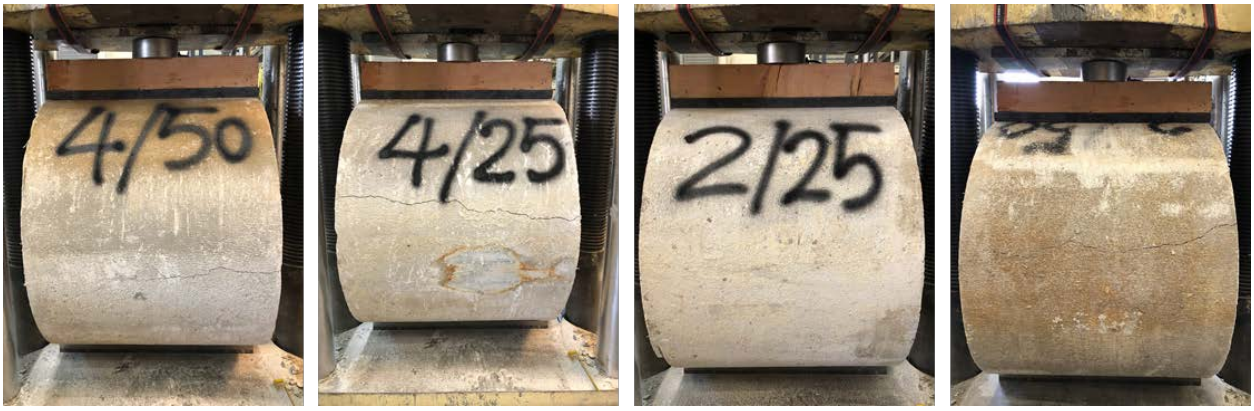

Figure 78. Three-edge bearing tests, five months immersion

The results of the three-edge bearing tests on the immersed specimens for five months are presented in Figure 79.

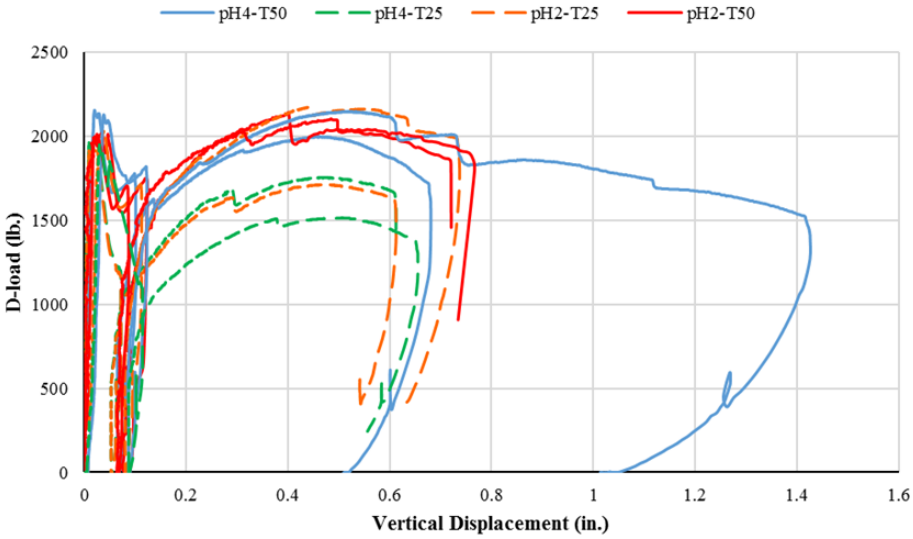

Figure 79. Three-edge bearing tests results after five months immersion

Based on the obtained ultimate loads of the tested specimens as presented in Figure 79, the load change percentage for this set of specimens were determined as shown in Table 8 and the corresponding graphs were generated as depicted in Figure 80.

Table 8. Five months test results for ultimate load comparison

Specimen	Ultimate load (lb./ft./ft.)	Ultimate load change (%)
pH2-T50	1990	-18.01
pH2-T25	2017	-16.89
pH4-T50	2141	-11.78
pH4-T25	2162	-10.92

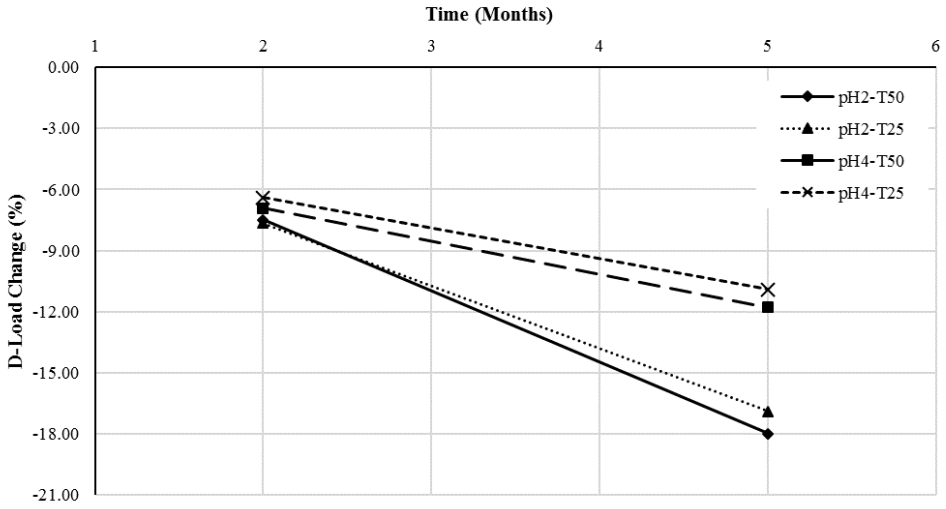

Figure 80. D-load change vs. time after five months of immersion

As shown in Figure 80, pH2 and pH4 specimens load decrease trend deviated from each other after two months tests and pH2 specimens showed approximately 1.5 times more load decrease than pH4 specimens did. The effect of elevated temperature was not significant in these cases; room temperature specimens and 50°C specimens showed marginally different results. The highest load reduction was observed in pH2-T50 specimens, and the lowest load decrease was measured in pH4-T25 pipes.

Eight months tests

For eight months tests, eight specimens, two from each environment, was taken out of the solutions and were visually inspected, (Figure 81).

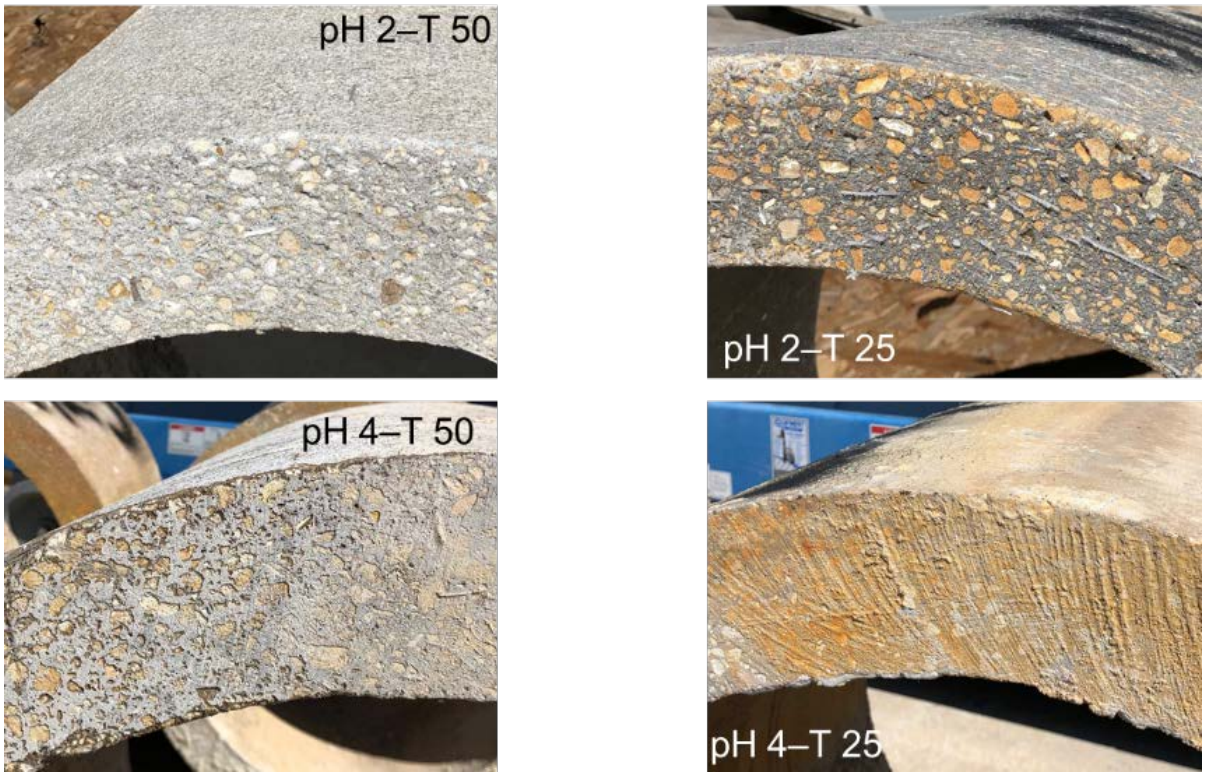

Figure 81. Post-immersion specimens' surface, 8 months tests

As portrayed in Figure 81, pH2-T50 specimens are covered with white gypsum layers, and they show a progressive deterioration. pH2-T25 and pH4-T50 pieces are mildly covered with gypsum while pH2-T25 specimens show more exposed gravels. pH4-T25 pipes were showing the least signs of deterioration among all the specimens, and the pipes' surface is mildly discolored, and there was no vision of exposed aggregates.

After air-drying the pieces for a day, the pipes were taken to the CELB for D-load tests. Similar test procedures were utilized for this set of the tests, as shown in Figure 82.

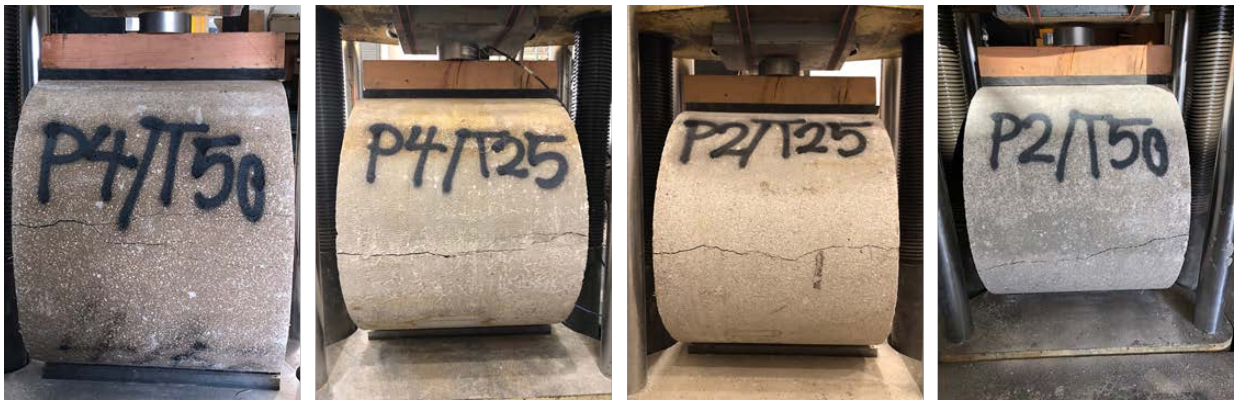

Figure 82. Three-edge bearing tests, five months of immersion

The three edge bearing tests for all of the specimens are shown in Figure 83.

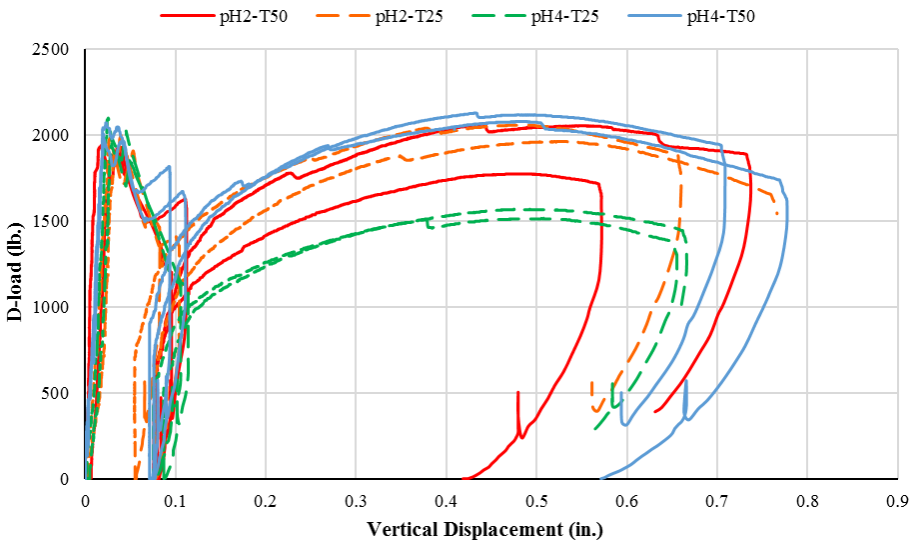

Figure 83. Three-edge bearing tests results after eight months of immersion

Based on the ultimate loads obtained from the graphs in Figure 83, the load decrease percentage of the specimens was determined and listed in Table 9.

Table 9. Eight months test results for ultimate load comparison

Specimen	Ultimate load (lb./ft./ft.)	Ultimate load change (%)
pH2-T50	1941	-20.02
pH2-T25	1954	-19.49
pH4-T50	2023	-16.65
pH4-T25	2036	-16.11

The obtained D-load decrease versus time graphs are shown in Figure 84.

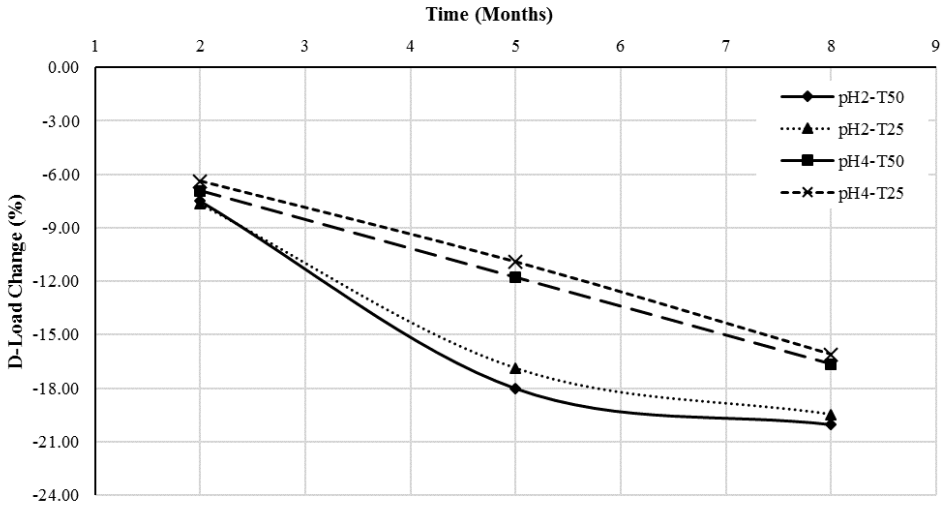

Figure 84. D-load change vs. time after eight months immersion

Eight months tests show that the slope of the load decrease graphs of pH2 solutions became smaller after 5 months. As presented in Figure 81, pH2 specimens' results for both temperatures were converging to a steady state phase. This plateau means that the rate of deterioration reactions became slower after five months, and this is because of the smaller amount of reactants available to continue the reactions. On the other hand, pH4 specimens were still showing a steady decreasing pattern. The effect of temperature in accelerating the reactions in both pH levels was not highly promising.

One year tests

After immersing specimens for eight months, two sets of tests were selected to be continued. These two sets were pH2-T50 specimens, harshest environment, and pH4-T25, reference environment for the Florida Department of Transportation. For one-year tests, two specimens from each of these solutions were taken out and were visually inspected, as shown in Figure 85.

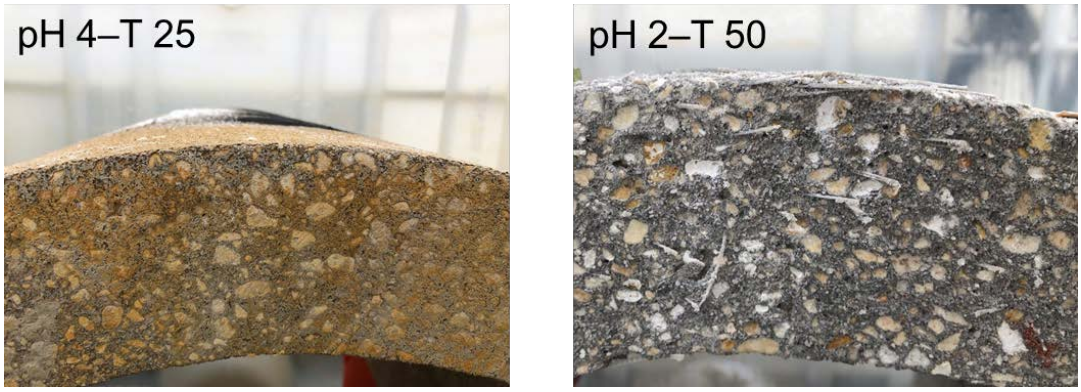

Figure 85. Post-immersion specimens' surface, 8 months tests

Visual inspection of the specimens revealed that pH2-T50 pipes were highly deteriorated and some of the fibers on the surface of these sections were exposed, as presented in Figure 56.

Figure 86. Exposed synthetic fibers in the pH2-T50 pipe after one year

For pH4-T25 specimens, some of the coarse aggregates were exposed, and major discoloration was observed on their surface.

After transporting the pipes to the UTA laboratory, the pipes were tested based on ASTM C1818 with the same machine and loading rate of aforementioned tests as shown in Figure 87, and the results are listed in Table 10.

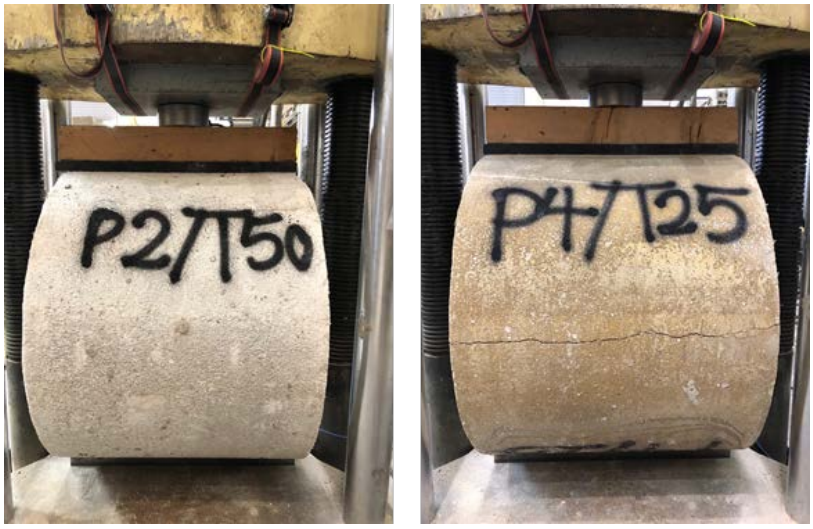

Figure 87. Three-edge bearing tests, one-year immersion

Table 10. One year test results for ultimate load comparison

Specimen	Ultimate load (lb./ft./ft.)	Ultimate load change (%)
pH2-T50	1929	-20.52
pH4-T25	1979	-18.46

Based on the obtained results, the final load decrease versus time graphs were derived as depicted in Figure 88.

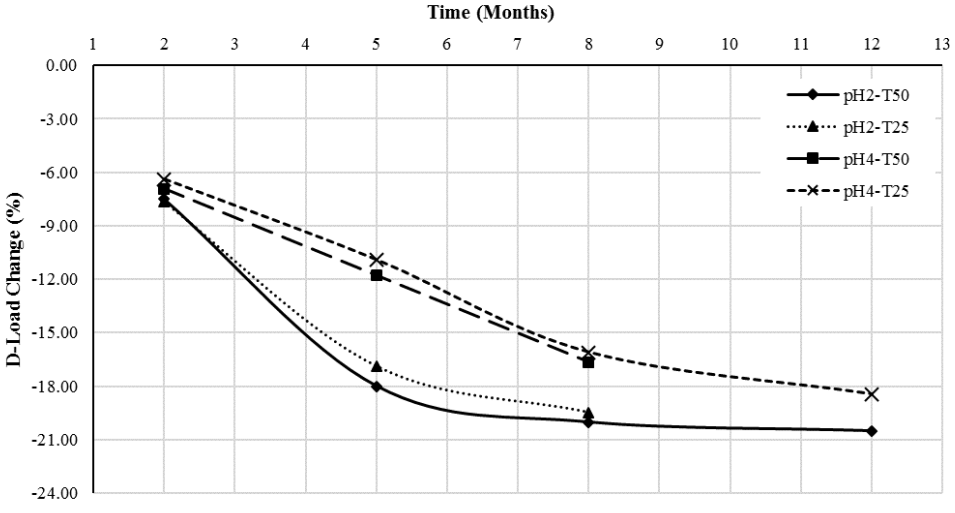

Figure 88. D-load change vs. time after eight months immersion

According to the one-year immersion tests results, it can be concluded that specimens that were soaked in pH2-T50 acids has reached a steady state phase and it is expected that the results are ultimately converging to a specific value close to this plateau, which has to be determined in the service life estimation chapter.

According to the one-year accelerated aging tests performed on 2-ft. pieces of SYNFRCPs, it can be concluded that the effect of temperature was not significant, and this can be a result of lower solubility of the Calcium Hydroxide in higher temperatures. The lower amount of dissolved Calcium Hydroxide would result in lower reaction rates, and this would cancel out the accelerating effect of higher temperature for these cases.

On the other hand, the effect of pH reduction on immersed specimens was significant, and pH 2 solutions showed approximately 25% higher load reduction in average during the yearlong process.

Visual inspection of the specimens showed that deterioration reactions started sooner in pH2 acid. It was also determined that there was no sign of corrosion or deterioration on the polypropylene fibers due to the corrosive environment, and they were intact at the end of the immersion period.

CHAPTER 5. MICROSCOPIC SURFACE ANALYSIS OF THE ACCELERATED AGING TESTS

5.1. Overview

Scanning Electron Microscopy (SEM) and Energy Dispersive X-ray spectroscopy (EDX) are usually used for microscopic analysis of specimens. SEM provides high resolution magnified images of the microstructure and EDX is an analytical technique to investigate the chemical composition and perform a precise element analysis.

5.2. Scanning Electron Microscopy and Energy Dispersive X-ray spectroscopy

SEM is a powerful tool to capture high-resolution and highly magnified microscopic pictures from samples. The images are constructed by surface scanning with a focused beam of electrons. Those electrons interact with the sample's atoms, and it will produce signals that contain information. Recent SEM machines are mainly working with secondary electrons. SEM resolution can be better than 1 nm. Specific preparations are necessary before scanning the specimens by SEM.

5.2.1. SEM settings and operation

To scan a specimen by SEM, initially a proper stage should be picked up, and the specimen should be mounted by a conductive tape. The ordinary tapes for general usage are copper tapes and carbon tapes. In this study, a carbon tape that is shown in Figure 89 was utilized.

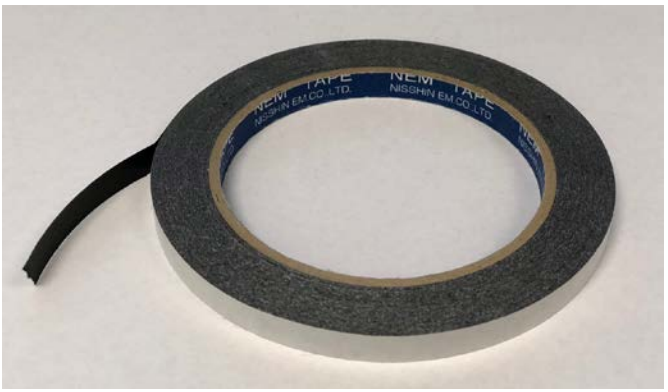

Figure 89. Carbon tape

Mounting the specimens on a proper mount should be properly done, and the sample should stick completely to the tapes to avoid any possible damage to the vaccumed SEM chamber during the test. After putting the mounted specimen inside the chamber, the chamber should be vacuumed, and a proper voltage should be applied. Figure 90 illustrates the components of an SEM test.

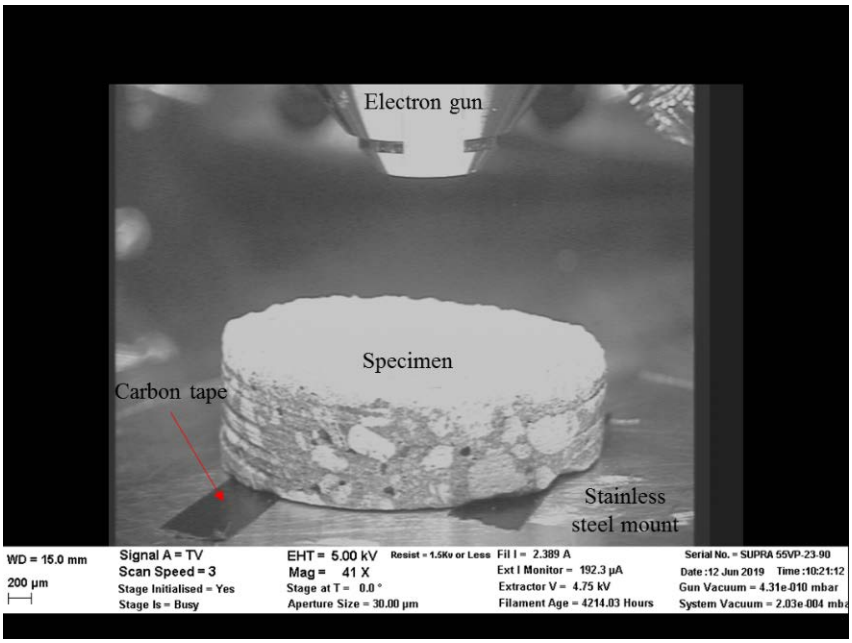

Figure 90. SEM test setup

5.2.2. EDX analysis

For EDX analysis, an additional detector should be inserted into the SEM chamber to detect the materials on the surface of the specimens and to determine their mass and distribution. The

efficiency of this probe will be maximized by a higher voltage. Figure 91 shows the EDX analysis test setup.

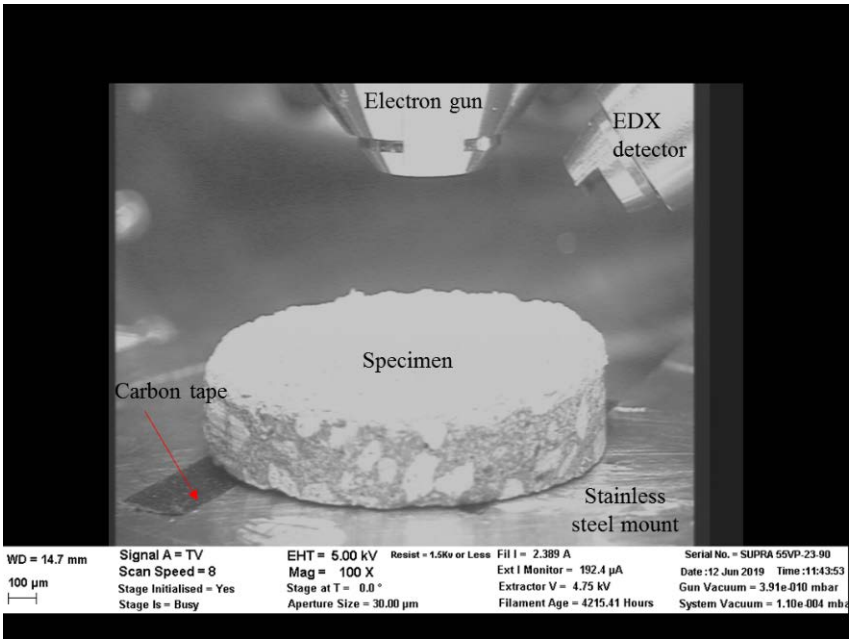

Figure 91. EDX analysis test setup

5.3. Sample preparation and SEM tests

In this study, after each immersion period and three-edge bearing tests, a core was drilled out of the tested pipes and was prepared for SEM and EDX analysis. The coring process and sample preparation are shown in Figure 92.

Figure 92. Coring and SEM sample preparation

After preparing the specimens, they were mounted on a proper mount, Figure 93, and scanned by SEM and their chemical composition and element distribution were analyzed by EDX method.

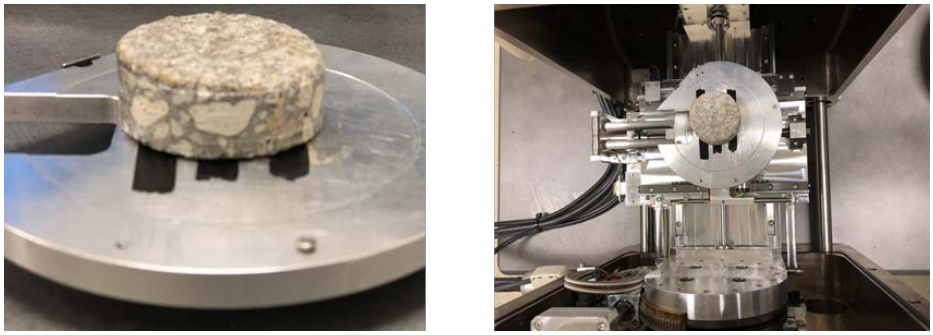

Figure 93. Sample mounting in SEM

After inserting the specimen into the SEM chamber, the chamber was vacuumed, and the voltage was set on 5 kV. The voltage can be set between 1.5 kV to 20 kV. The reason behind this low voltage is the non-conductivity of concrete, and to avoid the charging effect. The working distance, which is the focal distance of the probe, was set approximately around 15 mm, and the scan speed was set on 8. The apparatus size was 30 μm. These settings are based on the available options for the ZEISS GeminiSEM, model SUPRA 55 VP machine, Figure 94.

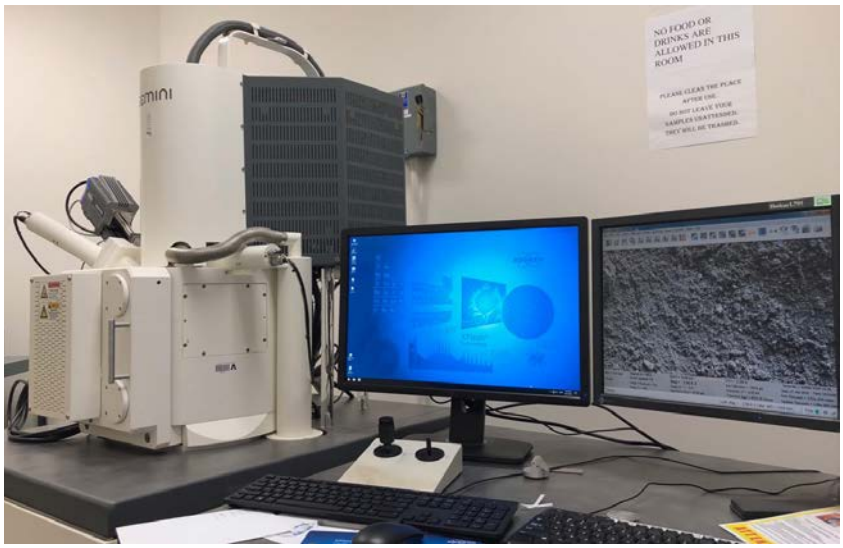

Figure 94. ZEISS GeminiSEM, model SUPRA 55 VP machine

To have a better idea about the microstructure of the specimens, the images were captured with different magnification levels. The magnification levels were 100X, 1000X, 2000X and 5000X.

5.3.1. SEM test

After each immersion period, a sample of the tested specimens was used for microscopic analysis. The test intervals were similar to the load bearing tests and were done after 2, 5, 8, and 12 months of immersion.

Control sample tests

Similar to the load bearing tests, a series of control samples were drilled out of the control pipes and were examined by an SEM machine. The samples' microscopic analysis was conducted with the UTA Shimadzu lab's SEM machine. Figure 95 shows the obtained pictures from the control samples.

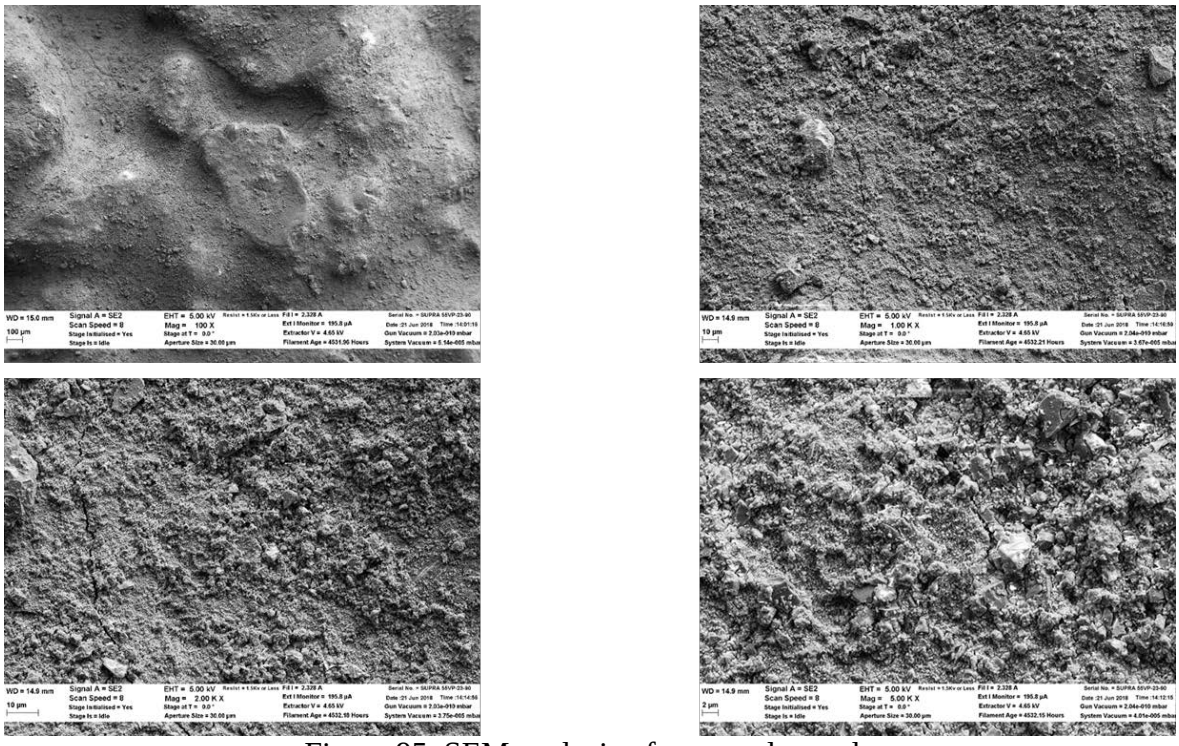

Figure 95. SEM analysis of a control sample

These pictures show the natural structure of concrete and its hydrated products in all of the magnification levels. All of the coarse and fine aggregates in the surface of these specimens were covered with cement paste, and the cement paste seems to be intact and not deteriorated.

Two months tests

After two months immersion period, cores were drilled from all of the specimens, but the samples from those that were immersed in pH2-T50 and pH4-T25 solutions were used for SEM and EDX analysis. These two environments were chosen based on being the harshest and the least harsh environments, respectively. The magnified pictures from these pipes' samples are shown in Figure 96 and 97.

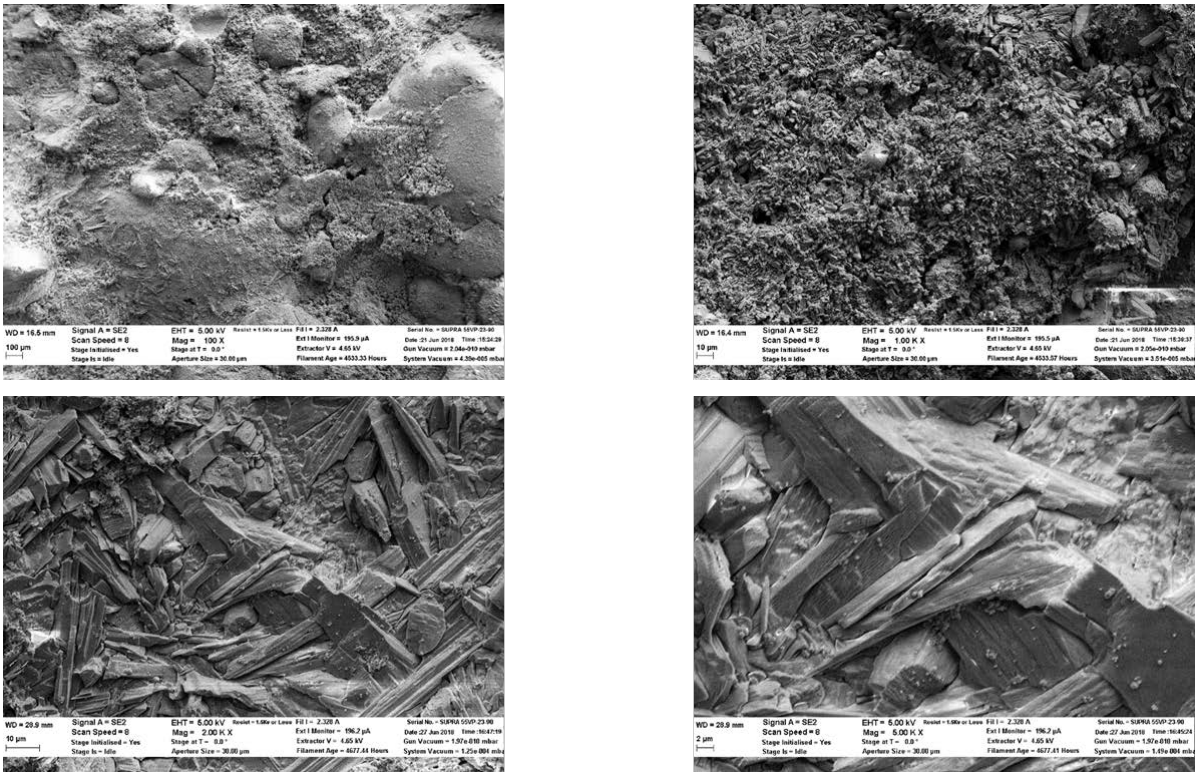

Figure 96. SEM analysis of a pH2-T50 sample, 2 Months

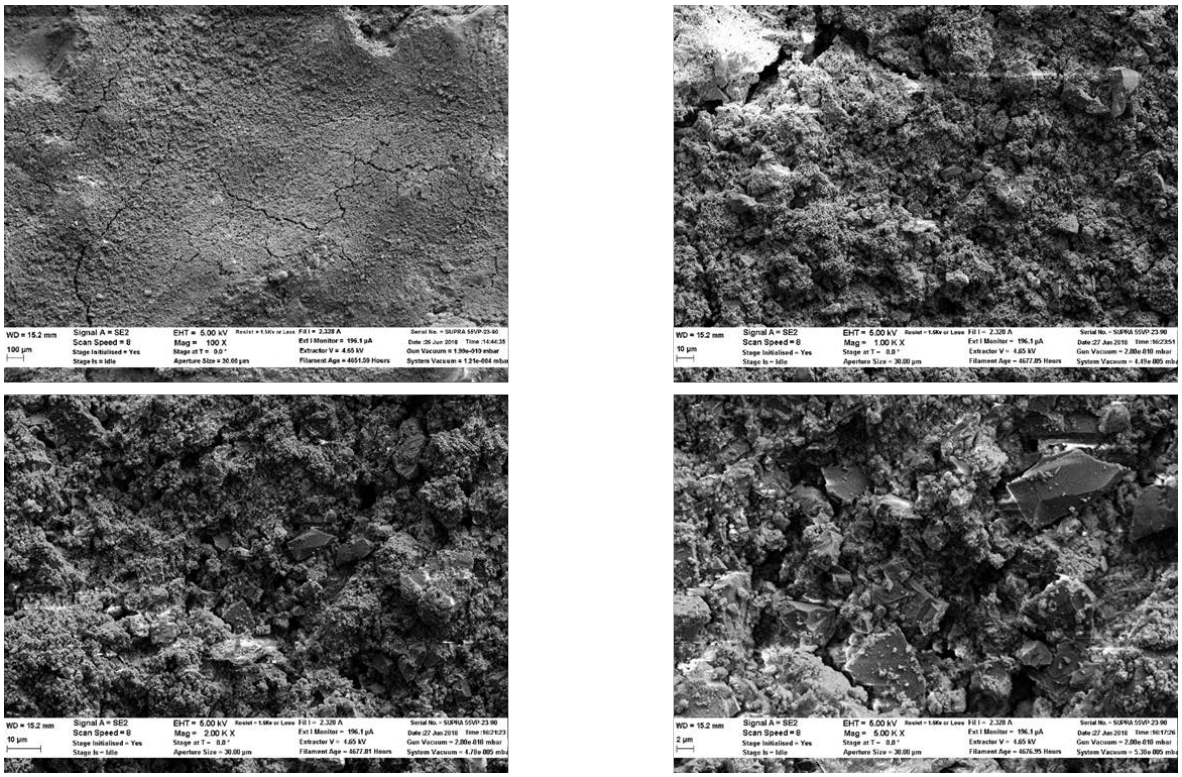

Figure 97. SEM analysis of a ph4-T25 sample, 2 Months

Figure 96 implies that the coarse aggregates are partially exposed and a layer of cement paste is washed out due to the harsh environment deterioration. Higher magnifications show gypsum crystals formation and their concentration on the surface of these specimens. These indicate that the corrosion reactions are initiated and led to strength loss.

Figure 97 shows a very small amount of deterioration, and most of the aggregates are fully covered with the cement paste. In magnified images, there are few gypsum crystals, and this means that the specimens were slightly deteriorated.

Five months tests

After immersing the specimens in corrosive sulfuric acid solutions for five months in four different environments, eight specimens were taken out of the solutions and were tested to determine their load bearing capacity, and a small sample of them was used to perform a microscopic analysis on

them. In this case, similar to the two months tests the harshest and least corrosive environments were analyzed. Figure 98 and 99 present the SEM analysis results.

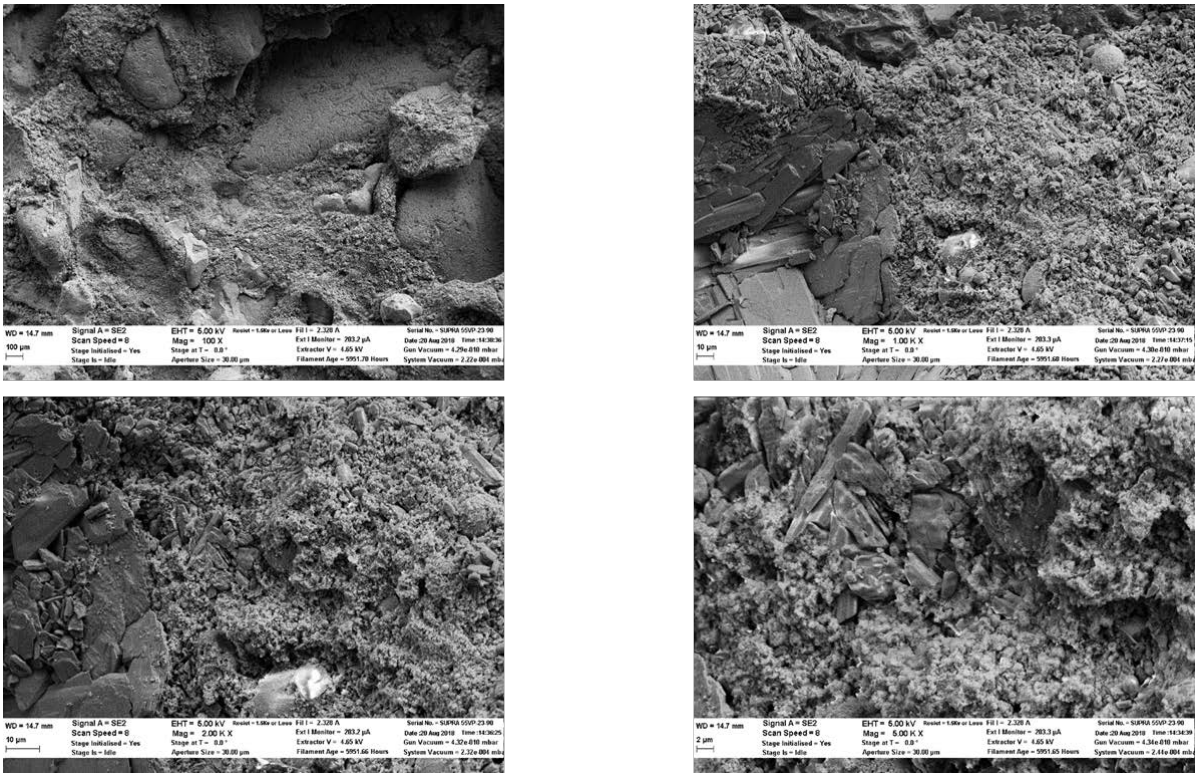

Figure 98. SEM analysis of a pH2-T50 sample, 5 Months

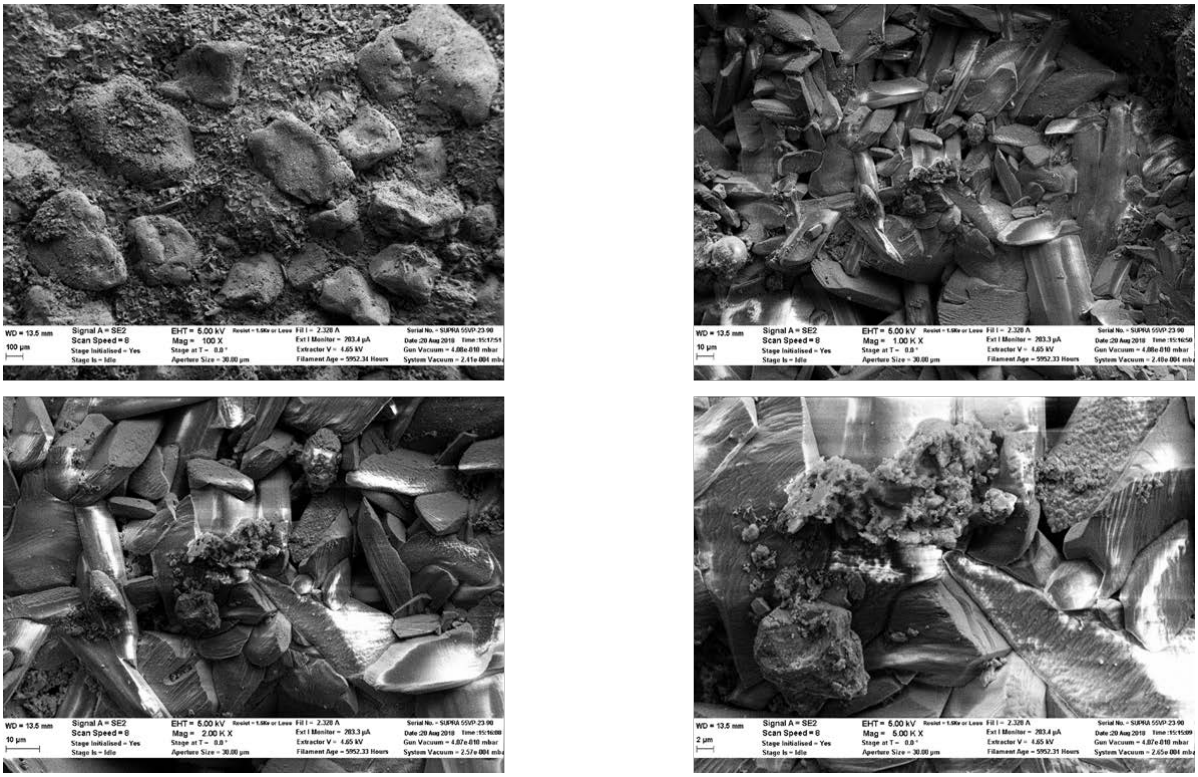

Figure 99. SEM analysis of a pH4-T25 sample, 5 Months

Figures 98 and 99 indicate that deterioration reactions are developing in both cases. For pH2-T50 samples, a layer of cement paste and a layer of coarse aggregates were washed off from the surface of the samples. Consequently, the lower layer of gravels became partially exposed. In the magnified pictures, gypsum crystals can be seen among the hydrated cement products, and it shows it is another layer of deteriorated cement.

For pH4-T25 samples, it can be seen that the cement paste is deteriorated and some of the coarse aggregates were exposed. In magnified pictures, gypsum crystals were detected, and their frequency on the sample's surface indicates that cement paste deterioration is developing.

Eight months tests

After eight months of immersion in sulfuric acid solutions and performing destructive strength tests on the pipes, samples from pH2-T50 and pH4-T25 pools were analyzed by SEM. The acquired images are depicted in Figure 100 and 101.

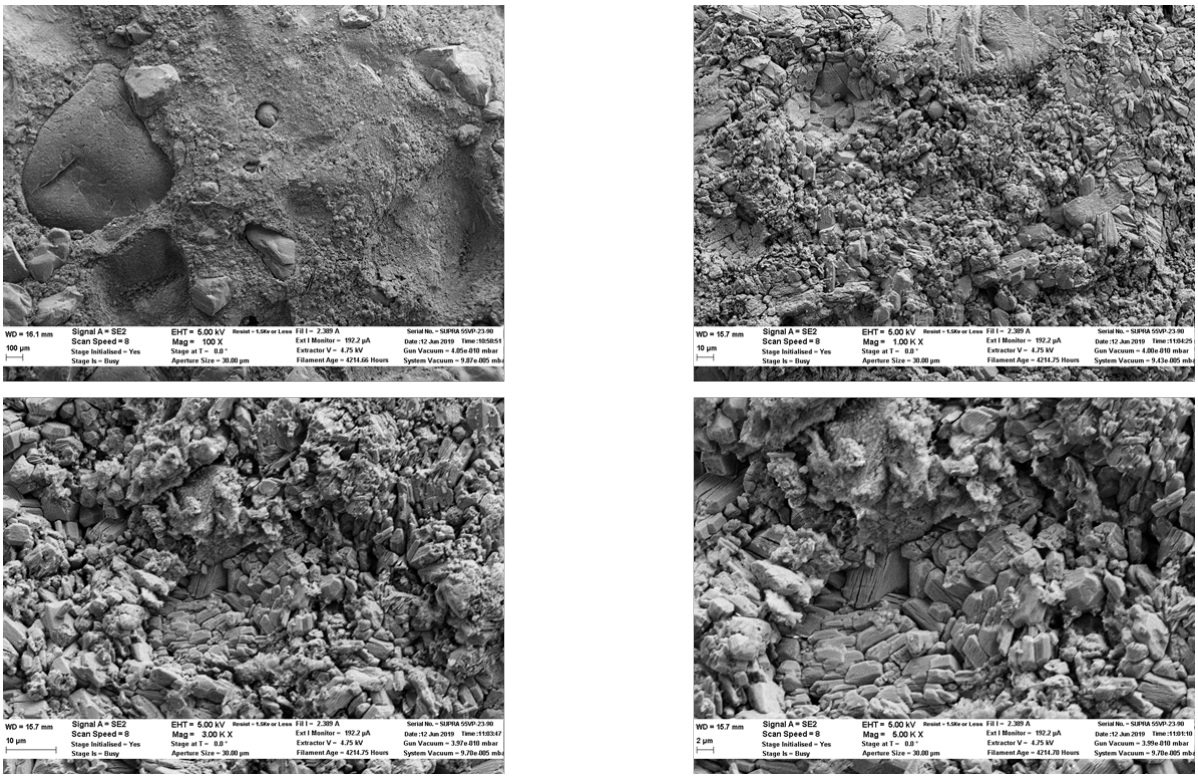

Figure 100. SEM analysis of a pH2-T50 sample, 8 Months

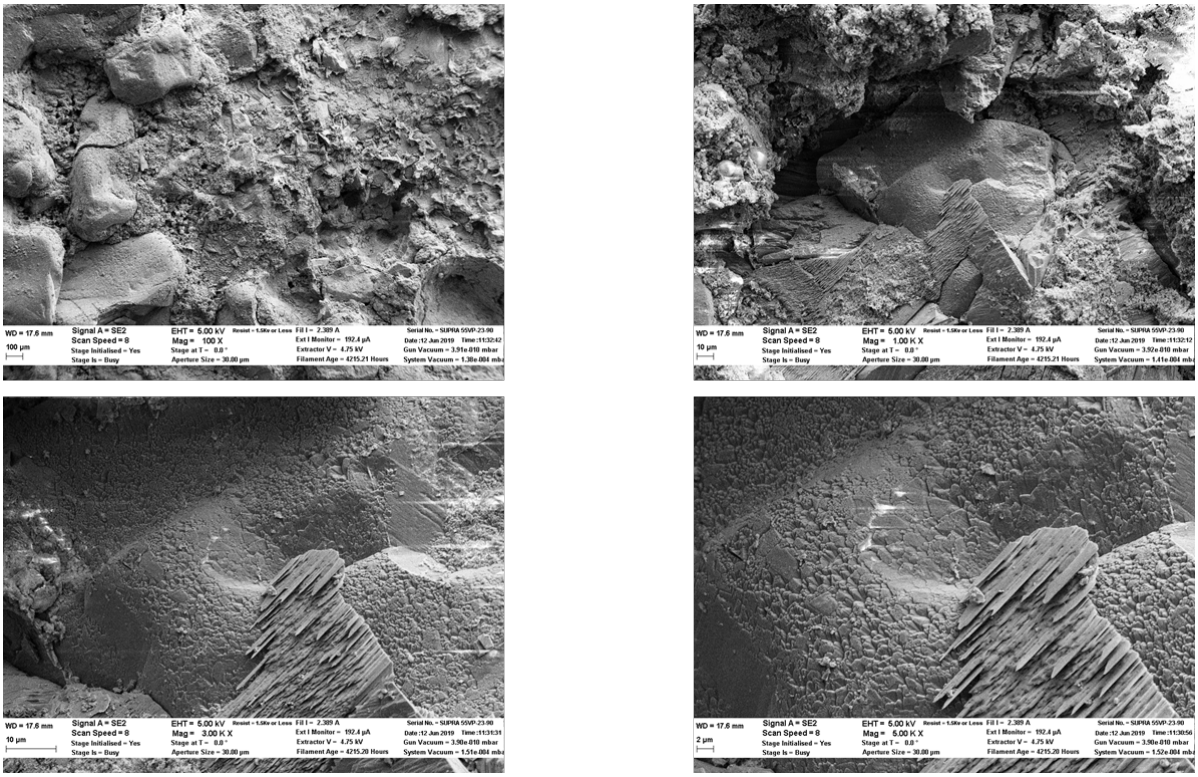

Figure 101. SEM analysis of a pH4-T25 sample, 8 Months

According to Figure 100, samples from the pipes that were immersed in pH2-T50 solutions showed a very high level of deterioration and a very dense layer of gypsum crystals were covering the sample's surface. Some gravels were spalled from the cement paste, and layers of cement paste were washed off from the specimen's surface.

Figure 101 shows the effect of pH4 solution at 25°C on the SYNFRCPs after 8 months of immersion. The pictures illustrate that these specimens are going through similar processes, and some of the coarse aggregates were washed off from the cement paste and moderate to large gypsum crystals were detected on the surface of these specimens.

One year tests

After one year of immersion in acidic solutions, two specimens from pH2-T50 and pH4-T25 solutions were taken out of the solutions and were scanned by SEM. The results of these scans are illustrated in Figures 102 and 103.

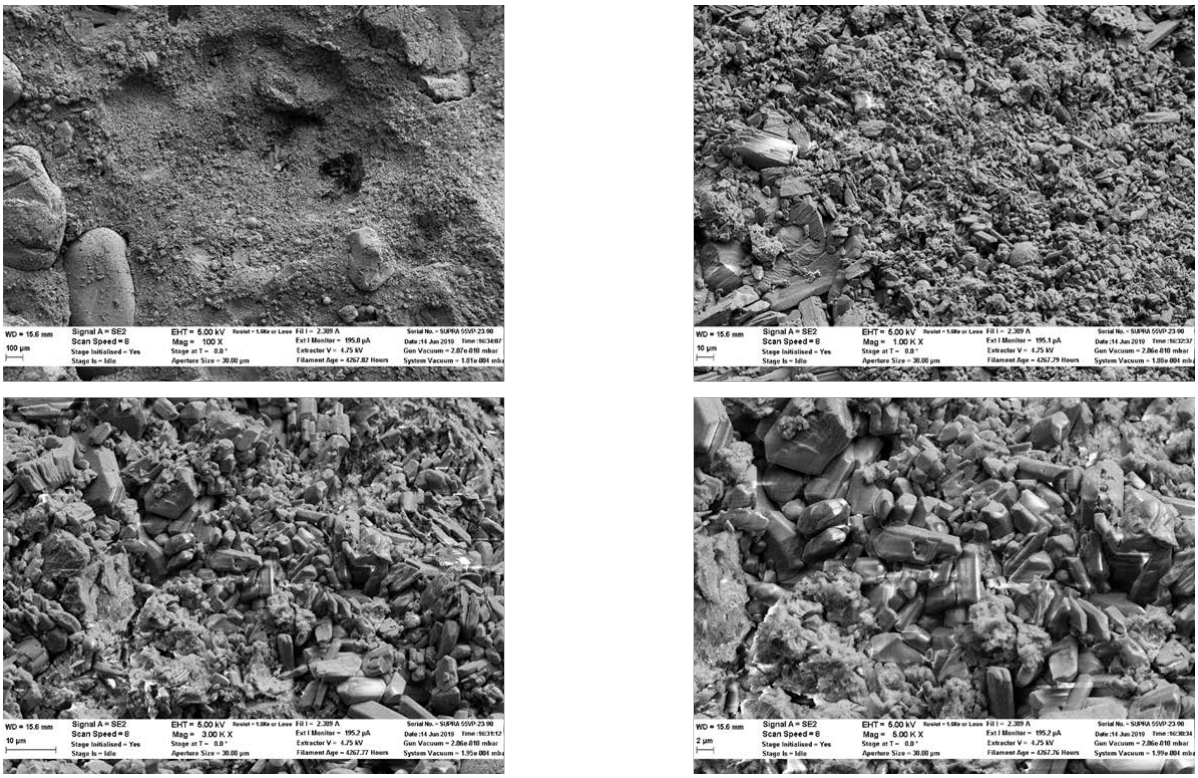

Figure 102. SEM analysis of a pH2-T50 sample, 12 Months

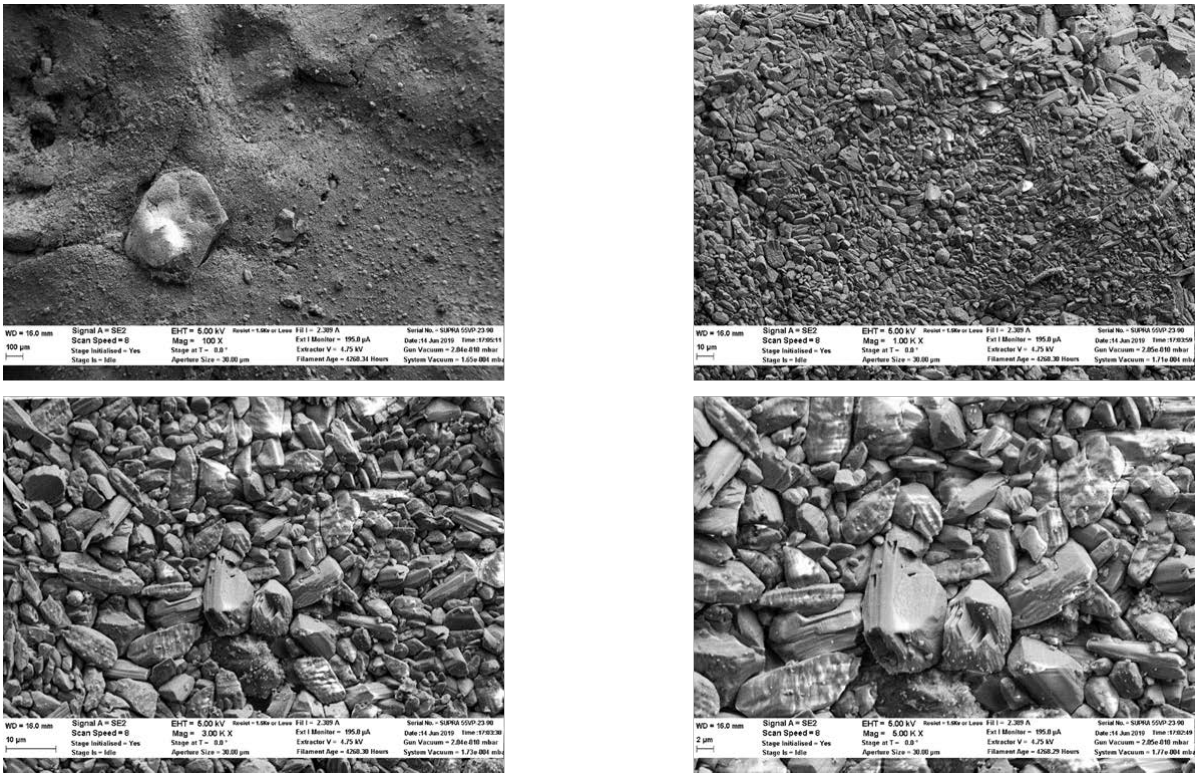

Figure 103. SEM analysis of a pH4-T25 sample, 12 Months

Both Figures show that the surface of the specimens are covered with gypsum crystals, and they seem to be saturated with gypsum. This would be a reason for the steady state of load decrease pattern, this reduces the amount of available concrete reactants, and consequently, it reduces the reaction rate that would decrease the load drop rate.

The overall trend that was observed in the SEM scan images show that pH4-T25 pipes went through the deterioration process slower than pH2-T50 specimens did. The rates were different, but the one-year products showed that although the deterioration scenarios occurred at different rates, and the products of both environments were similar to each other. In other word, it can be concluded that there were the same reactions taking place just at different rates.

5.3.2. EDX element analysis

In this project for elemental analysis, the EDX method has been utilized. The EDX detector that was used in this study was a BRUKER XFlash 6|60 probe, Figure 104.

Figure 104. Bruker EDX detector

This instrument is a detector that uses X-ray fluorescence excitation to determine the chemical characterization of a sample. This detector can do both qualitative and quantitative element analysis.

In this research, after each immersion period and performing three-edge bearing tests, a core sample was extracted from the pipes and was studied by SEM analysis. After all these steps, EDX analysis was used to determine the chemical composition and quantitative measurements of each element on these samples.

Control specimens

After performing D-load and SEM tests on the pre-immersion specimens, a sample of these pipes was studied by EDX elemental analysis method, too. Initially, the chemical composition of these samples was evaluated by their EDX spectrum, Figure 105.

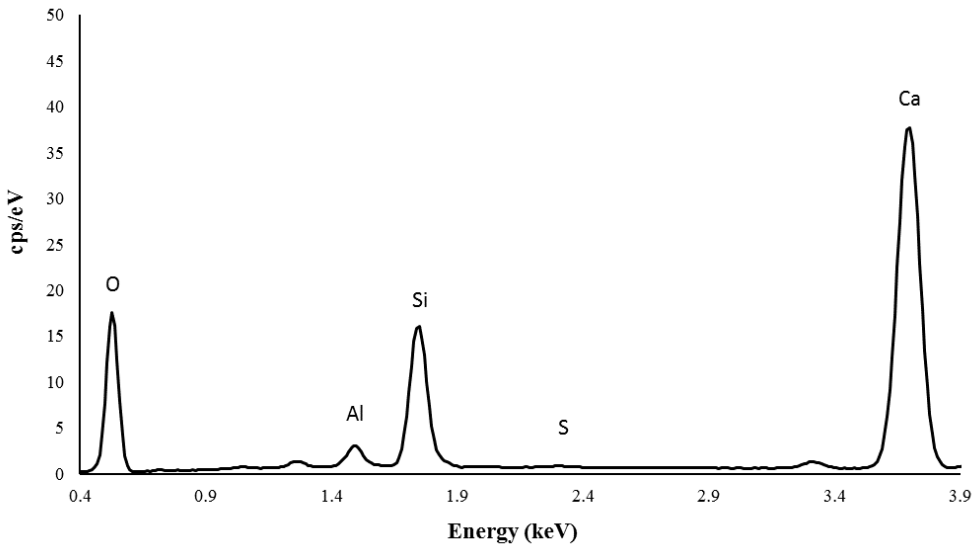

Figure 105. EDX spectrum of the control sample

As depicted in this figure, the major components of this sample are calcium, Silica, Aluminum, and Oxygen. These are the ordinary and major elements of a Portland cement concrete. The analysis does not show any sign of anomaly or contamination. In addition to the qualitative analysis of the samples, quantitative study of the sample's elements were also carried out, and the results are shown in Table 11.

Table 11. Element analysis of control specimen

Element	Mass [%]	Mass Norm. [%]	Atom [%]
Oxygen	55.9	50.03	61.56
Calcium	34.74	31.09	15.27
Carbon	12.22	10.93	17.92
Silicon	6.57	5.88	4.12
Aluminum	1.17	1.05	0.77
Iron	1.15	1.03	0.36
Sum	111.75	100	100

Two months tests

After performing SEM analysis on samples from those pipes that were immersed in solutions for two months, they were examined and analyzed by EDX method. The spectrums from this analysis for pH2-T50 and pH4-T25 specimens and their comparison with the control specimen are shown in Figure 106.

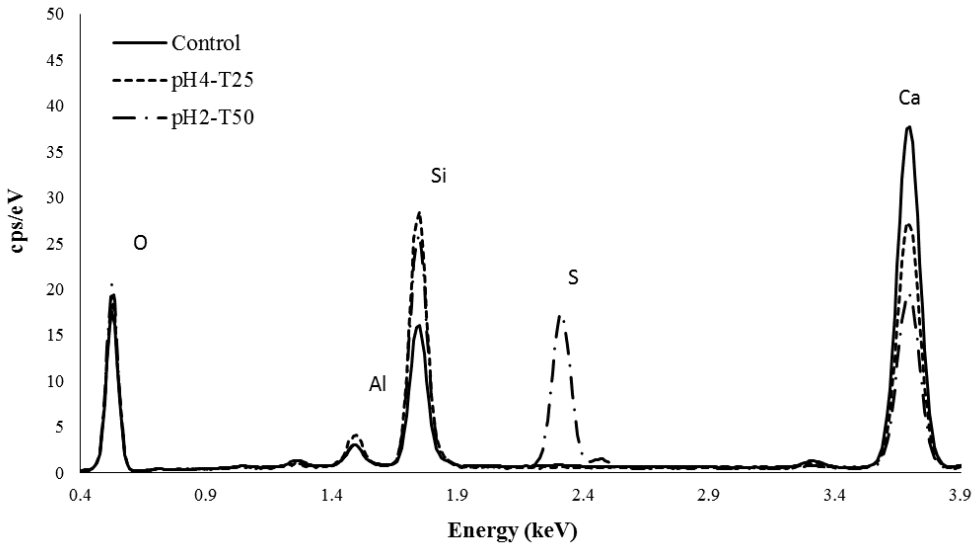

Figure 103. Element analysis of pH2-T50 and pH4-T25 samples (two months)

The graphs indicate that pH2-T50 sample showed a considerable amount of sulfur in its composition, which indicates that deterioration reactions had already started and gypsum crystals were observed as the result of this. For pH4-T25 sample, the amount of sulfur was almost negligible, and a very small amount of that was detected by EDX.

The increase in Si content of the samples can be a result of cement paste deterioration and exposure of aggregates, which are mainly made from Silica. Consequently, some parts of the cement paste were washed off from the surface of the sample, and that results in a lower amount of Calcium in the mixture.

The quantitative analysis of the elements in these specimens is shown in Figure 107, Table 12, and 14.

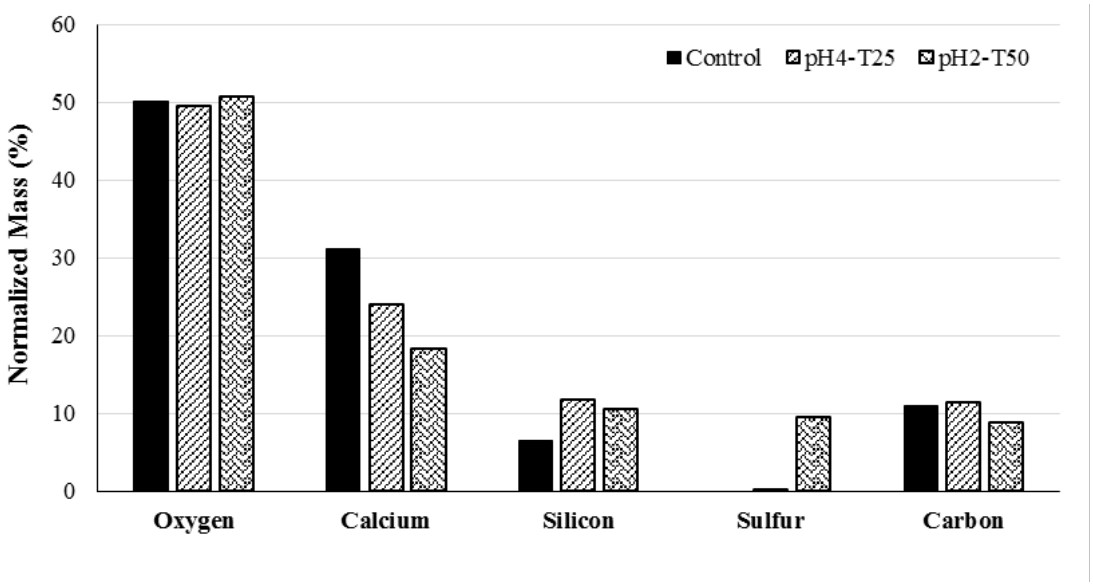

Figure 107. Normalized mass distribution in pH4-T25 and pH2-T50 (two months)

Table 12. Element analysis of pH2-T50 specimen (2 months)

Element	At. No.	Mass [%]	Mass Norm. [%]	Atom [%]
Oxygen	8	56.28	50.71	62.24
Calcium	20	20.34	18.32	8.98
Silicon	14	11.64	10.49	7.34
Sulfur	16	10.51	9.47	5.8
Carbon	6	9.79	8.83	14.43
Aluminium	13	1.34	1.21	0.88
Iron	26	1.09	0.98	0.34
	Sum	110.98	100	100

Table 13. Element analysis of pH4-T25 specimen (2 months)

Element	At. No.	Mass [%]	Mass Norm. [%]	Atom [%]
Oxygen	8	55.74	49.46	59.99
Calcium	20	27.13	24.08	11.66
Silicon	14	13.18	11.7	8.08
Carbon	6	12.86	11.41	18.43
Aluminium	13	2	1.78	1.28
Iron	26	1.73	1.53	0.53
Sulfur	16	0.06	0.05	0.03
		112.69	100	100

As illustrated in the tables and figures, a very little amount of sulfur was observed on pH4-T25 specimens, and the small amount of gypsum that was observed on the surface of these specimens support this measurement.

In addition to these measurements, the area covered by each of these elements were analyzed, and the results are shown in Figure 108.

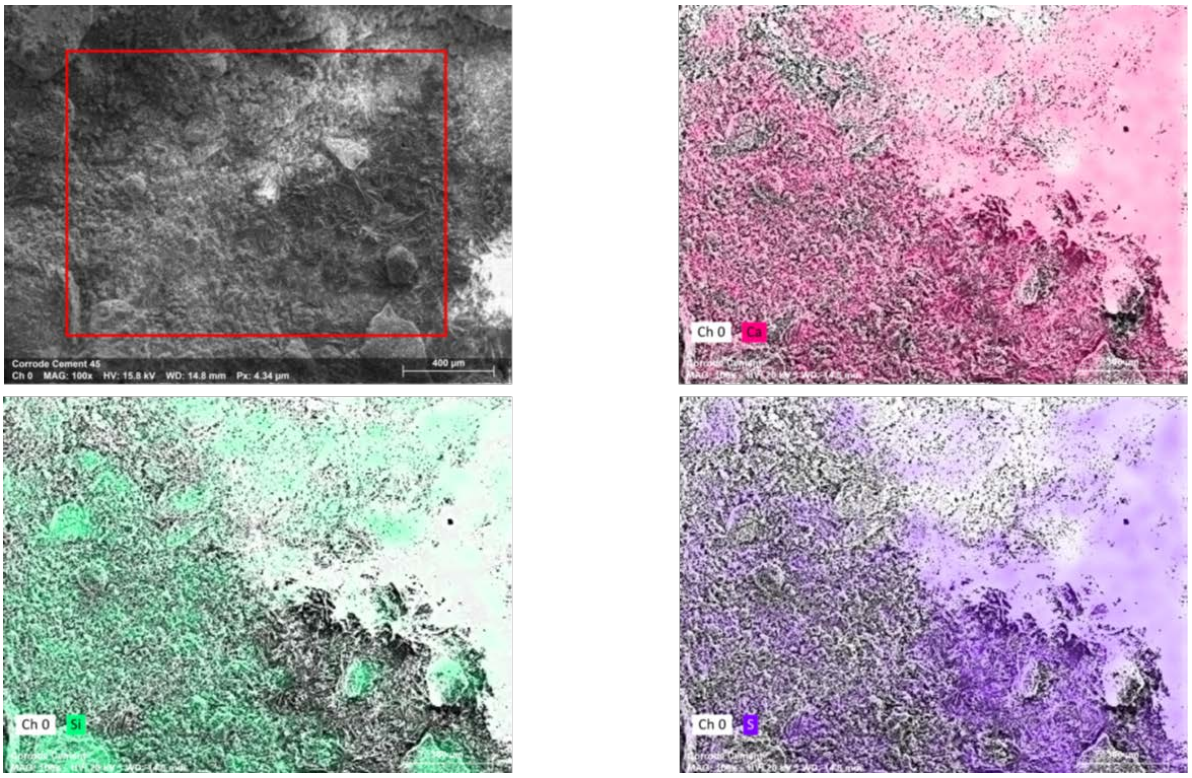

Figure 108. Element analysis of pH2-T50 specimens (2 months)

As shown in the pictures, the majority of coarse aggregates were made from, and some parts of cement paste were covered by calcium and sulfur, which make gypsum crystals together with the combination of oxygen.

Five months tests

After five months of immersion, another set of pipes were evaluated by D-load testing and then analyzed by SEM imaging and finally, as the last step; they were analyzed by EDX method for elemental analysis. The element analysis was carried out for pH2-T50 and pH4-T25 samples. The element spectrums of these samples are depicted in Figure 109.

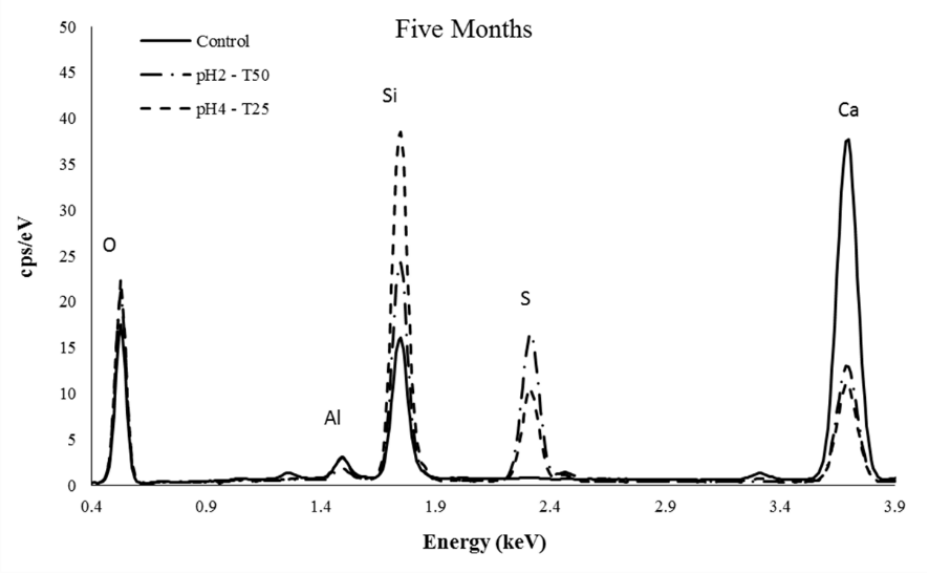

Figure 109. Element analysis of pH2-T50 and pH4-T25 samples (five months)

The spectrums of EDX analysis show that a considerable amount of Sulfur was observed on the pH4-T25 sample, as well as pH2-T50 one. This indicates that a high volume of deterioration products should be observed in both cases. The amount of calcium was decreased after 5 months of immersion. The calcium level decrease is because of concrete layers spalling and exposure of dense, coarse silica-made aggregates, which results in a higher mass of silica.

Additionally, the quantitative results of EDX analysis for these two samples are shown in Figure 110 and Tables 14 and 16.

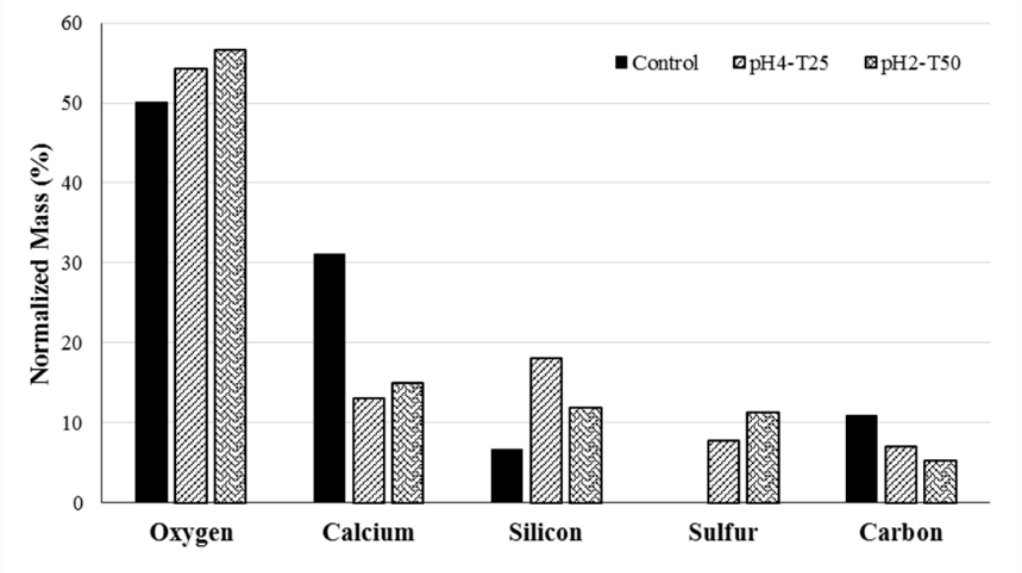

Figure 110. Normalized mass distribution in pH4-T25 and pH2-T50 (five months)

Table 14. Element analysis of pH2-T50 specimen (5 months)

Element	At. No.	Mass[%]	Mass Norm.[%]	Atom[%]
Oxygen	8	63.84	56.63	69.05
Calcium	20	16.83	14.92	7.27
Silicon	14	13.46	11.94	8.29
Sulfur	16	12.69	11.25	6.85
Carbon	6	5.93	5.26	8.54
	Sum	112.73	100	100

Table 15. Element analysis of pH4-T25 specimen (5 months)

Element	At. No.	Mass [%]	Mass Norm. [%]	Atom [%]
Oxygen	8	54.31	54.24	65.41
Silicon	14	18.01	17.99	12.36
Calcium	20	13	12.99	6.25
Sulfur	16	7.75	7.74	4.65
Carbon	6	7.06	7.05	11.33
		100.14	100	100

The results show that sulfuric acid reaction with concrete was progressed for both cases and for pH2-T50, the amount of sulfur in the analyzed samples reached to 11.25% of the whole mass of elements on the surface. For pH4-T25, the amount of sulfur was less than this, and it reached 7.74 and combining these results with SEM findings reveals that the rate of reactions in pH4-T25 was lower than pH2-T50 pipes and this was anticipated because of the higher concentration in pH2 solutions and higher temperature that accelerates the reactions.

In addition, element analysis continued by identifying the regions covered by each element. Figure 111 and 112 show this part of the analysis for both sets of samples.

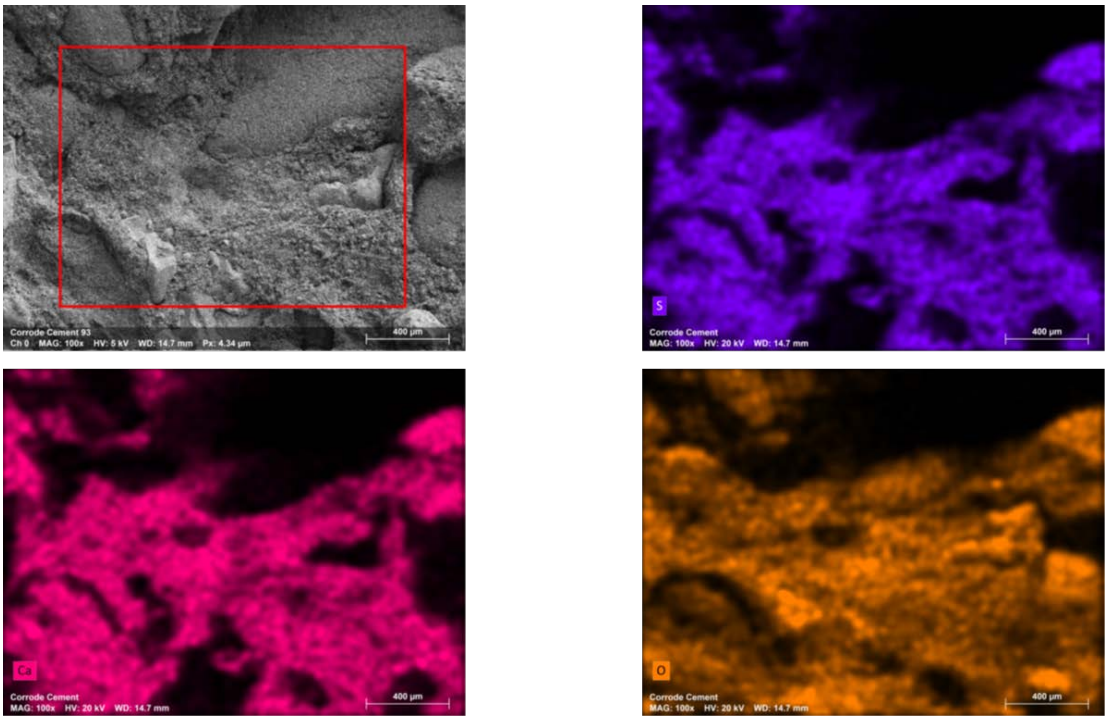

Figure 111. Element analysis of pH2-T50 specimens (5 months)

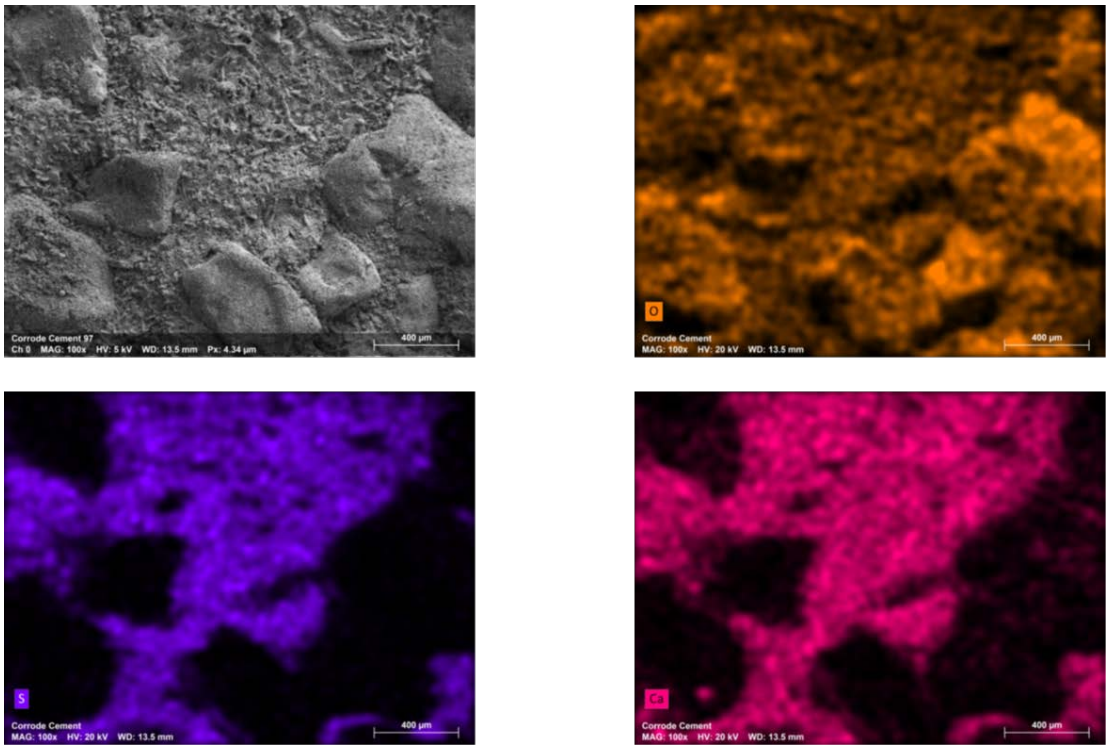

Figure 112. Element analysis of pH4-T25 specimens (5 months)

Based on the figures, it was shown that the regions covered by Sulfur, Calcium, and Oxygen are mostly covered by gypsum crystals. The only regions that are not covered by gypsum are the coarse aggregates. These aggregates as analyzed before, and they are made of Silica, and they don't react with sulfuric acid vigorously.

Eight months tests

After analyzing samples of pipes by three-edge bearing tests and SEM scans, material analysis of the samples was conducted by the EDX method. Specimens that were tested in this part were extracted from pH2-T50 and pH4-T25 pools. The spectrum analysis results are presented in Figure 113.

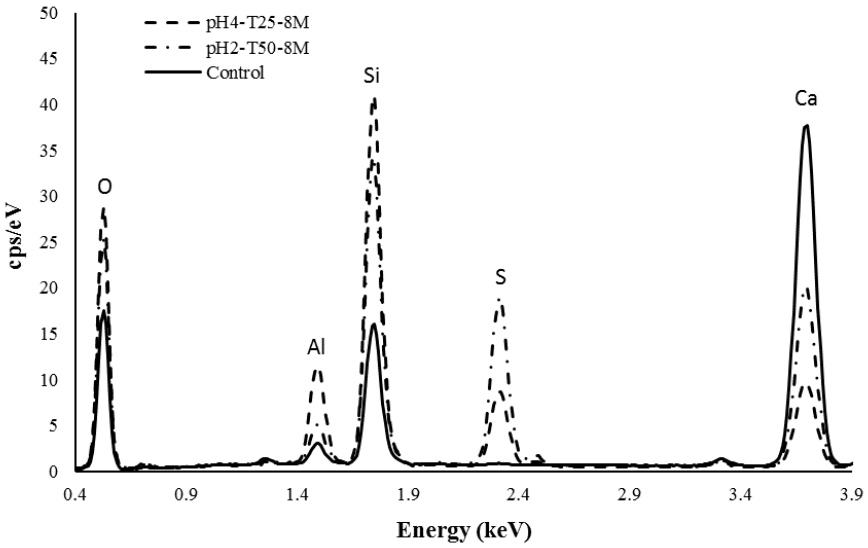

Figure 113. Element analysis of pH2-T50 and pH4-T25 samples (eight months)

As shown in the graphs, the level of Sulfur in pH2-T50 samples was higher than pH4-T25 ones. In addition, the level of Silica was mildly higher in pH4-T25 samples, and Calcium was lower than control specimens for both sets were. These results show that the reactions took place at faster rates, and pH 4 specimens still need more reaction to take place to be saturated with gypsum crystals.

Quantitative elemental study of the specimens was also conducted, and the results are shown in Figure 114 and Tables 16 and 17.

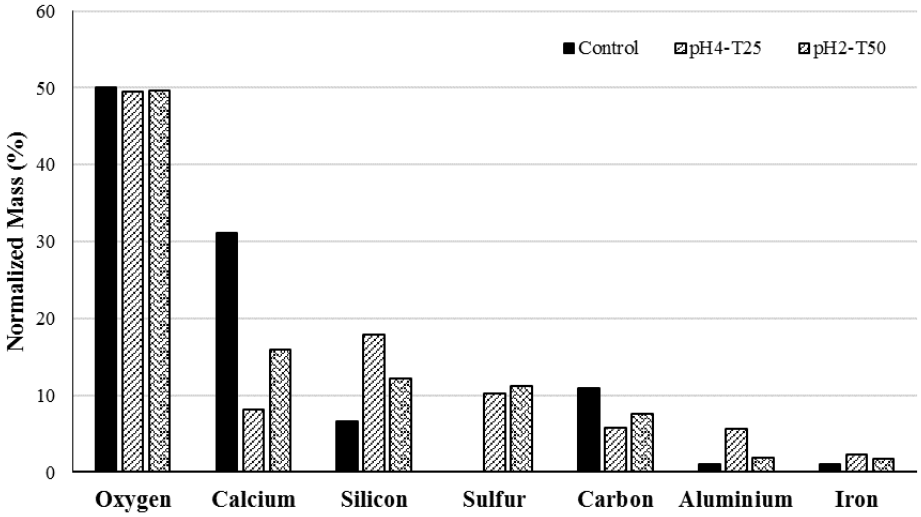

Figure 114. Normalized mass distribution in pH4-T25 and pH2-T50 (eight months)

Table 16. Element analysis of pH2-T50 specimen (8 months)

Element	At. No.	Mass [%]	Mass Norm. [%]	Atom [%]
Oxygen	8	57.43	49.58	63.58
Calcium	20	17.72	15.91	7.83
Silicon	14	13.6	12.22	8.58
Sulfur	16	10.24	11.2	5.66
Carbon	6	8.42	7.56	12.41
Aluminium	13	2.06	1.85	1.35
Iron	26	1.88	1.69	0.6
		111.33	100	100

Table 17. Element analysis of pH4-T25 specimen (8 months)

Element	At. No.	Mass [%]	Mass Norm. [%]	Atom [%]
Oxygen	8	58.13	49.52	65.32
Silicon	14	19.4	17.86	12.42
Calcium	20	9.92	8.17	4.45
Carbon	6	6.35	5.84	9.5
Aluminium	13	6.12	5.63	4.08
Sulfur	16	5.62	10.17	3.15
Iron	26	2.44	2.25	0.79
Potassium	19	0.63	0.58	0.29
		108.61	100	100

Based on the results, it can be seen that still the level of sulfur is higher in pH2-T50 samples, and it implies that these samples are corroded more than pH4-T25 samples did. This trend can be backed up with the load bearing tests, and after 8 months, the level of load decrease in pH4 specimens was less than pH2 pipes.

Additionally, the elemental analysis continued by determining the composition of the scanned area based on the elements region identification on the surface of the samples. Figures 115 and 116 depict the results of this investigation.

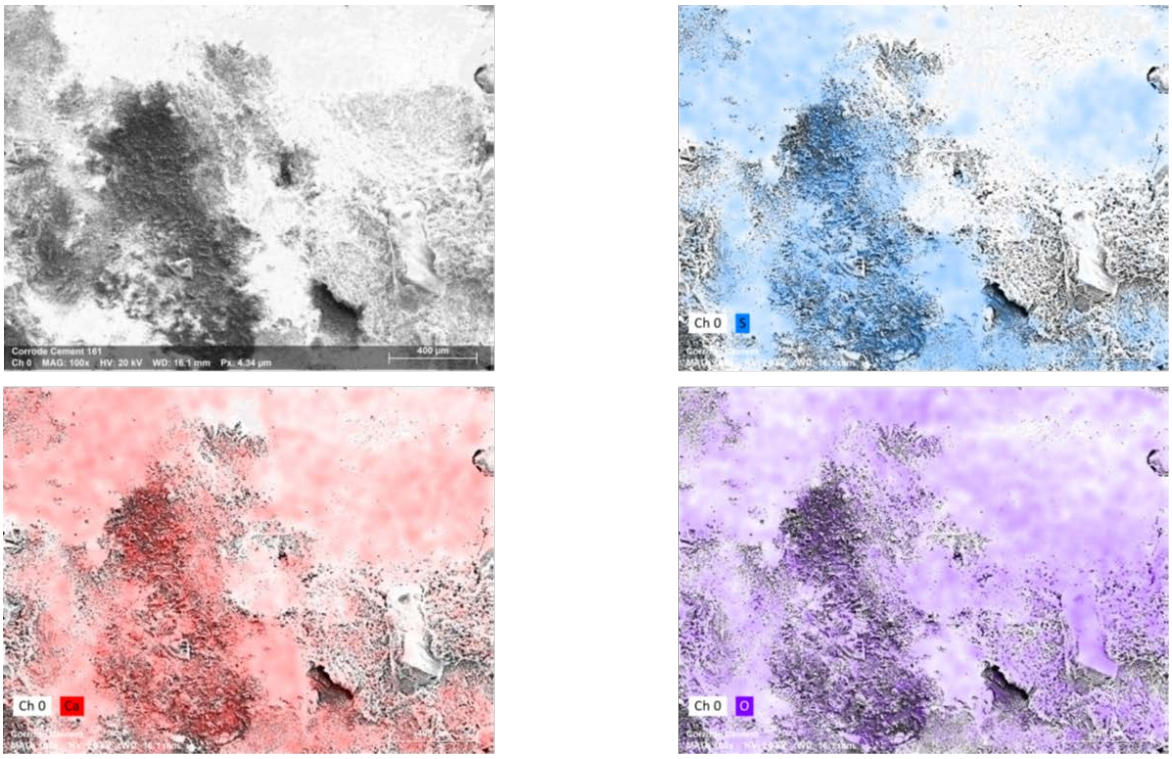

Figure 115. Element analysis of pH2-T50 specimens (8 months)

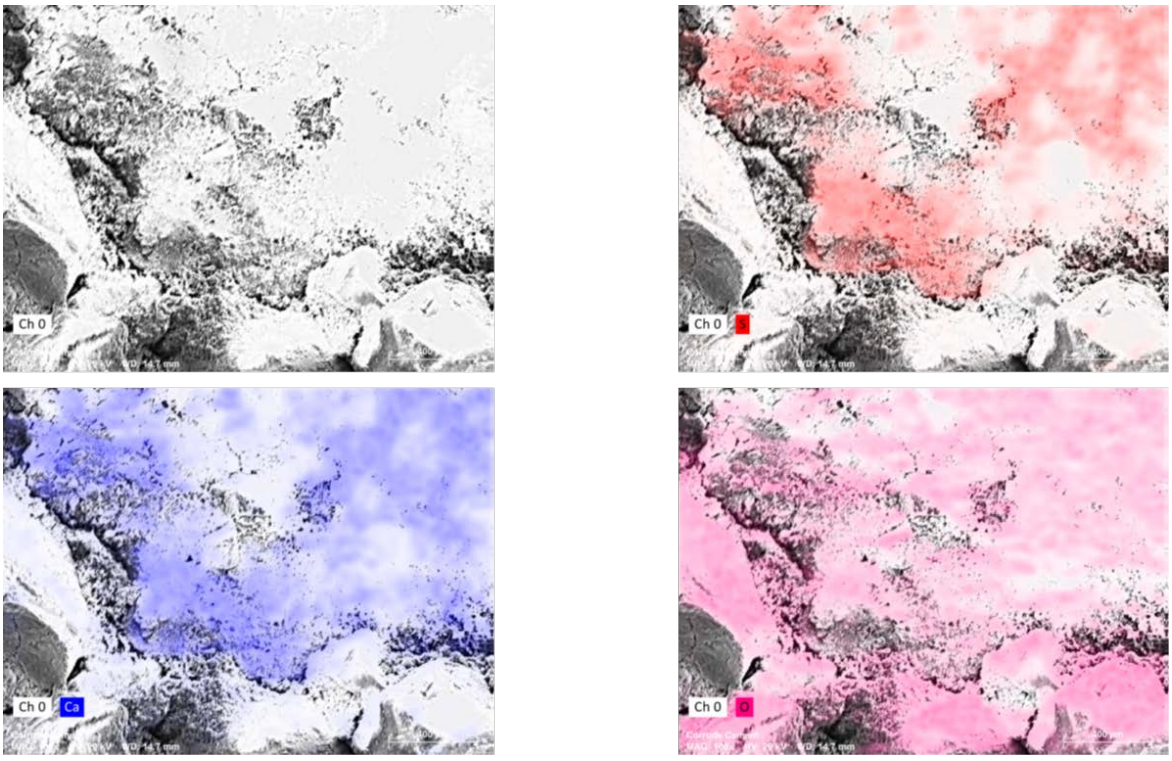

Figure 116. Element analysis of pH4-T25 specimens (5 months)

The pictures show that most of the concrete covered surface in pH2-T50 samples were transformed into the gypsum-covered surface. For pH4-T25 samples, bigger non-reacted regions are still obvious in the pictures. It can be concluded that pH2-T50 specimens are highly deteriorated and their surface is almost saturated with gypsum crystals and deteriorations in pH4-T25 specimens are moving toward the same point of pH2-T50 samples.

One year tests

After one year of immersion, two samples from each of the pH2-T50 and pH4-T25 baths were taken out and tested for their D-load capacity and microstructural formations. As the last step, the chemical composition of the samples was determined qualitatively and quantitatively. The results of the spectrum analysis of the specimens are shown in Figure 117.

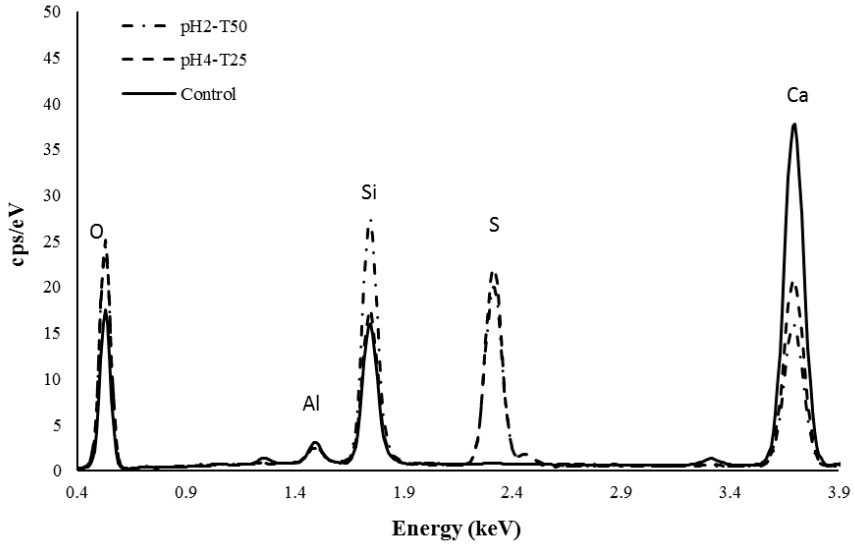

Figure 117. Element analysis of pH2-T50 and pH4-T25 samples (twelve months)

By analyzing the elemental analysis spectrum, it can be concluded that the level of sulfur in both samples was almost similar to each other and this means that the level of the deterioration should be almost similar to each other. This conclusion can be supported by the load decrease results. In

those tests load bearing capacity loss in pH2-T50, and pH4-T25 samples were similar to each other.

Furthermore, the quantitative element analyses were conducted, and normalized mass distribution of elements was determined. The results are listed in Figure 118 and Tables 18 and 19.

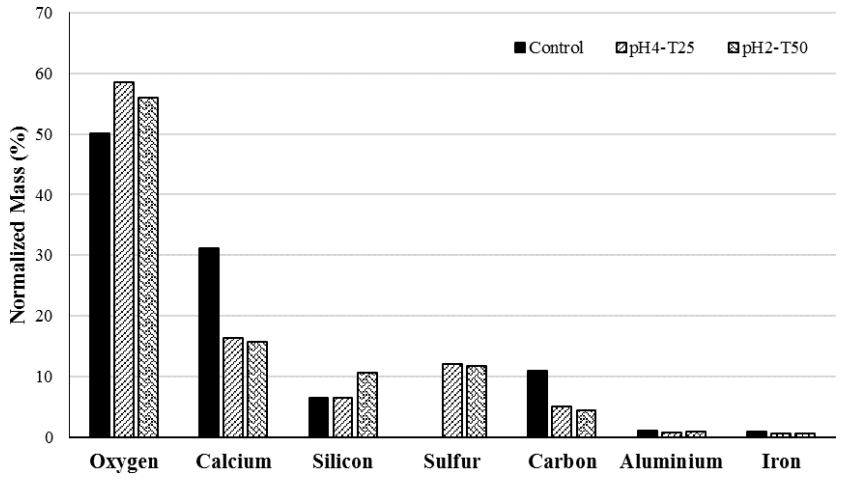

Figure 118. Normalized mass distribution in pH4-T25 and pH2-T50 (twelve months)

Table 18. Element analysis of pH2-T50 specimen (8 months)

Element	At. No.	Mass [%]	Mass Norm. [%]	Atom [%]
Oxygen	8	59.09	56.02	69.26
Calcium	20	16.61	15.81	7.77
Sulfur	16	12.1	11.71	7.08
Silicon	14	11.12	10.58	7.43
Carbon	6	4.61	4.39	7.2
Aluminium	13	0.96	0.92	0.67
Fluorine	9	0.6	0.57	0.59
		105.1	100	100

Table 19. Element analysis of pH4-T25 specimen (8 months)

Element	At. No.	Mass [%]	Mass Norm. [%]	Atom [%]
Oxygen	8	63.29	58.46	71.48
Calcium	20	20.75	16.43	9.36
Sulfur	16	13.84	12.01	7.8
Carbon	6	5.44	5.03	8.19
Silicon	14	7.03	6.56	3.18
	13	0.93	0.85	0.55
	9	0.74	0.66	0.47
		112.02	100	100

The results of the quantitative analysis show that the level of sulfur in both elements reached the same level, and this finding is supported by SEM analysis results and spectrum analysis outcomes. This also shows its effects on the load bearing capacity of the pipes after one-year immersion, and as shown in Figure 85, there was approximately 2% load decrease difference between these two environments.

In addition to these analyses, the regions covered by each element was also studied, and the results are shown in Figures 119 and 120.

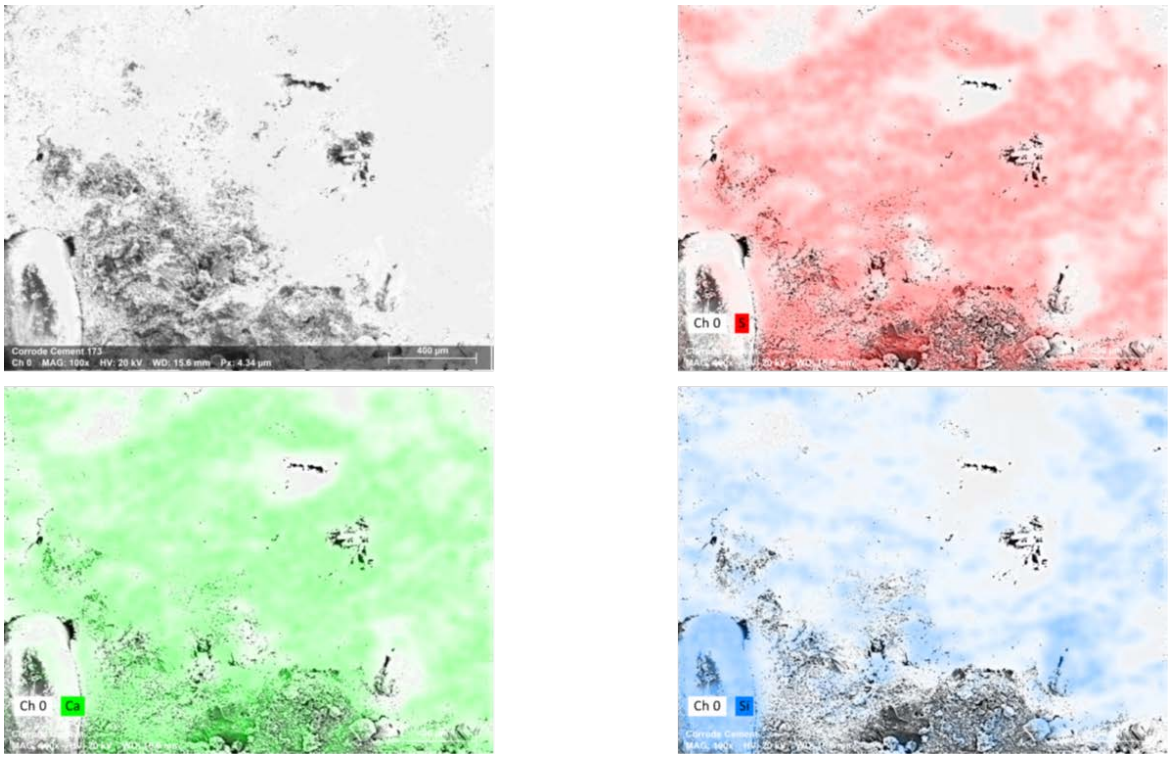

Figure 119. Element analysis of pH2-T50 specimens (12 months)

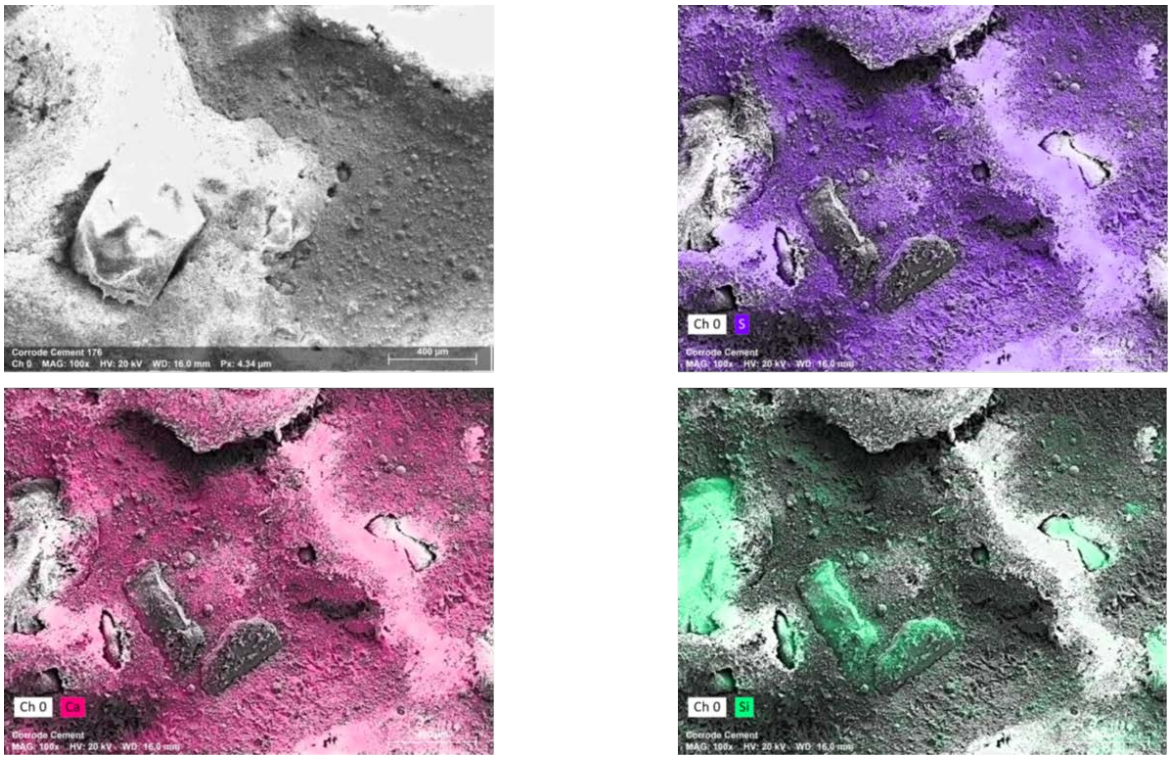

Figure 120. Element analysis of pH4-T25 specimens (12 months)

Based on the obtained pictures from Figure 119 and 120, it can be concluded that in both cases, the majority of samples' surfaces were covered with gypsum. Saturated surfaces with this material were obtained, and this will retard the deterioration progress.

After obtaining all the information based on one-year immersion of SYNFRCPs in harsh solutions and determining their chemical composition based on SEM and EDX analysis, the trend of the chemical composition of this composite for major existing elements are shown in Figure 121- 123.

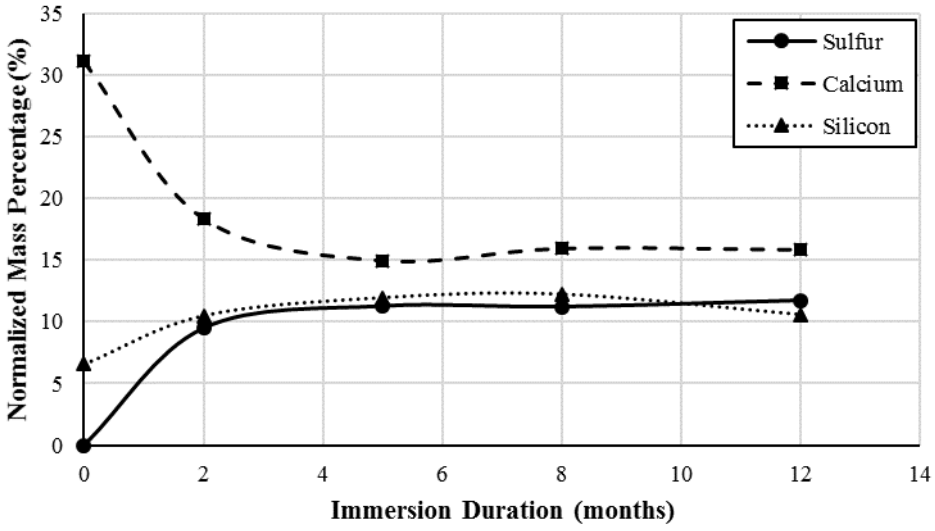

Figure 121. Element analysis summary (pH2-T50)

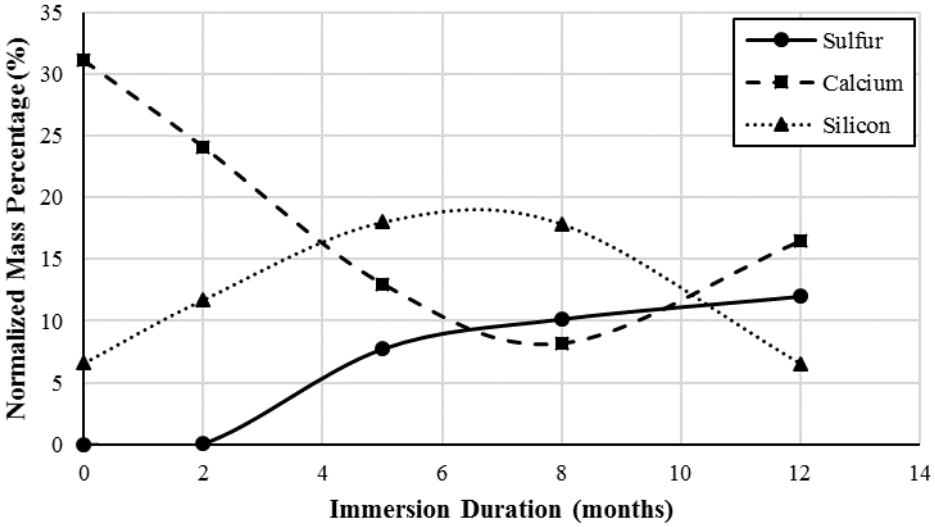

Figure 122. Element analysis summary (pH4-T25)

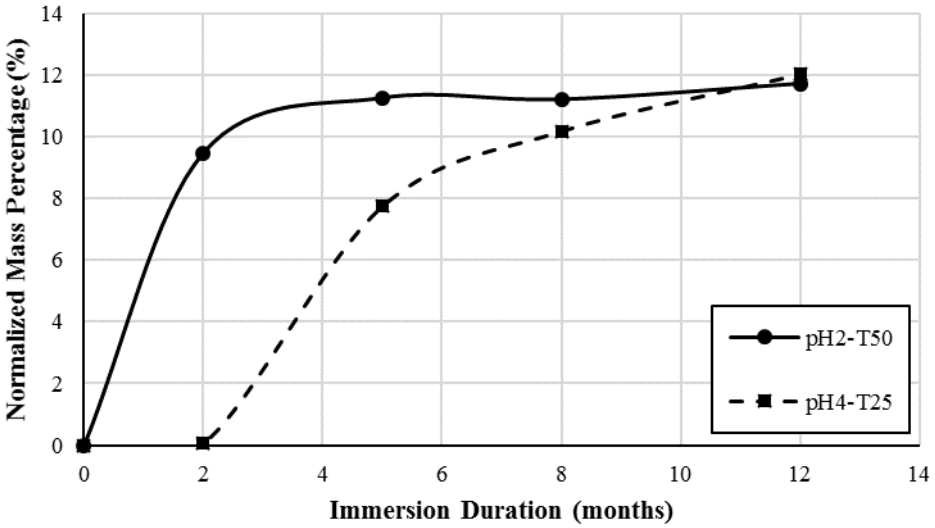

Figure 123. Sulfur normalized mass analysis summary

Based on the summary of the elemental analysis results, it can be concluded that the level of sulfur on the surface of these specimens was limited to a value of around 12% for both solutions. This indicates that on a surface of an SYNFRCP specimen, which is already saturated with gypsum and its load bearing capacity is limited to a certain value; the amount of sulfur would be around 12%.

On the other hand, Calcium and Silica mass percentage was not limited to a certain value for pH4-T25 solutions. This might be because of aggregates being spalled from the surface, which would change the mass distribution dramatically.

For pH2-T50, the normalized mass of Calcium and Silica were almost limited to a certain value, and this difference may be because of spalling the coarse aggregates from the surface of the pipes in early stages of deterioration, and this led to a more consistent pattern.

Generally, SEM scans and EDX analysis of the specimens provided a comprehensive insight into the details of this type of deterioration. The results could be correlated to the mechanical properties of the pipe specimens. The elemental analysis provided supplemental information for service life analysis and estimation of these immersed specimens.

CHAPTER 6. SERVICE LIFE ESTIMATION

6.1. Overview

Service life assessment of infrastructures is one of the important aspects of infrastructures' research. Infrastructural systems that have longer service lives are desired because of their expensive and costly production, installation, and maintenance. Among infrastructure systems, sewer and drainage pipes are one of the most important ones, and service life estimation and improvements are currently critical in this field of research. This chapter is about service life estimation of SYNFRCPs based on accelerated aging methods.

6.2. Service life estimation methods background

There are different models for service life estimation of concrete pipes. Florida Department of Transportation, Ohio Department of Transportation, Hadipriono, and Hurd model are the most famous methods that are currently being used in concrete pipe research and applications [40].

6.2.1. Hurd model

Hurd model [40] development was based on pH levels less than 7 and is based on the following Equation 16:

$$EMSL = \left(\frac{123.5 \times pH^{5.55}}{Slope^{0.42} \times Rise^{1.94}}\right)\left(\frac{1 - Sediment}{Rise}\right)^{-2.64} \quad \textit{(Eq. 16)}$$

Where:

EMSL = estimated material service life (years),

pH = pH of the water,

Slope = pipe invert slope (%),

Sediment = sediment depth in pipe invert (inches), and

Rise = vertical pipe diameter (inches).

In this model, it was assumed that degradation mechanisms would not occur when the pH level is more than seven.

6.2.2. Hadipriono model

This model [41] is based on pH values between 2.5 and 9, shown in Equation 17.

$$EMSL = -33.23 + 160.92 \times \log pH - 4.16 \times Slope^{0.5} - 0.28 \times Rise \quad \textit{(Eq. 17)}$$

Where:

EMSL = estimated material service life (years),

pH = pH of the water,

Slope = pipe invert slope (%), and

Rise = vertical pipe diameter (inches).

6.2.3. Ohio DOT model

Ohio DOT has two different equations for different pH ranges.

For 2.5 < pH < 7

$$EMSL = \left(\frac{\left[0.349 \times pH^{1.204}\right]^{7.758}}{Slope^{0.834}}\right)\left(\frac{1-Sediment}{Rise}\right)^{-5.912} \quad \textit{(Eq. 18)}$$

For pH>7

$$EMSL = \left(\frac{3.5}{K}\right)^{5.9}\left(\frac{Flow^{0.52}}{Slope^{0.31}}\right) \quad \textit{(Eq. 19)}$$

where:

EMSL = estimated material service life (years),

pH = pH of the water,

Slope = pipe invert slope (%),

Sediment = sediment depth in pipe invert (inches),

Rise = vertical pipe diameter (inches),

Flow = velocity rating number (1 – rapid, 2 – moderate, 3 – slow, 4 – negligible, 5 – none), and

K = abrasive constant (0.9 – without abrasive flow, 1.19 – with the abrasive flow).

6.2.3. Florida DOT model

FDOT model includes more parameters as given in Equation 20.

$$EMSL = 1000(1.107^{C} C^{0.717} D^{1.22} K^{-0.37} W^{-0.631}) - 4.22 \times 10^{10}(pH^{-14.1}) - 2.94 \times 10^{-3}(S) + 4.41 \quad \textit{(Eq. 20)}$$

Where:

EMSL = estimated material service life (years),

C = sacks of cement per cubic yard,

D = depth of concrete cover over reinforcing steel (inches),

K = chloride concentration (ppm),

W = total water percentage in the concrete mix (%), and

S = sulfate content (ppm).

Based on this equation, FDOT developed software to estimate the service life of pipes and the commercial name of this software is Culvert Service Life Estimator, Figure 124.

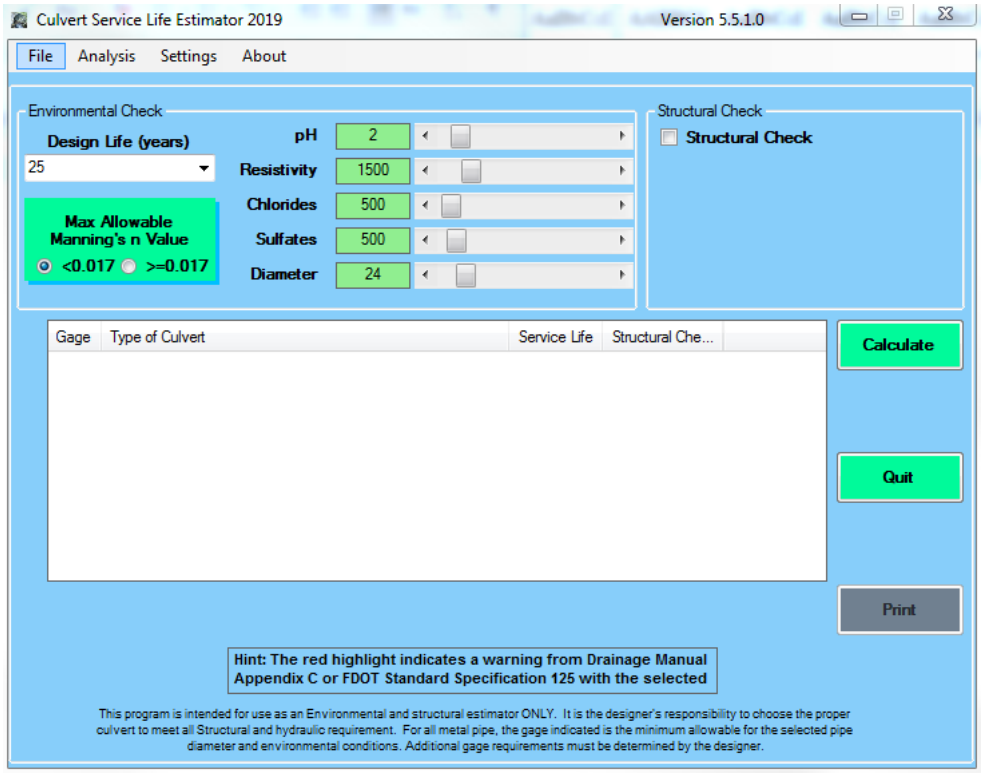

Figure 124. Culvert service life estimator software [2]

The reference environment for service life estimation of SYNFRCPs in this research was applied to this software to determine the service life of reinforced and non-reinforced concrete pipes. Based on DFOT requirements, the reference was set to be pH4 acidic environment. The results of Culvert service life estimator software for this solution are depicted in Figure 125.

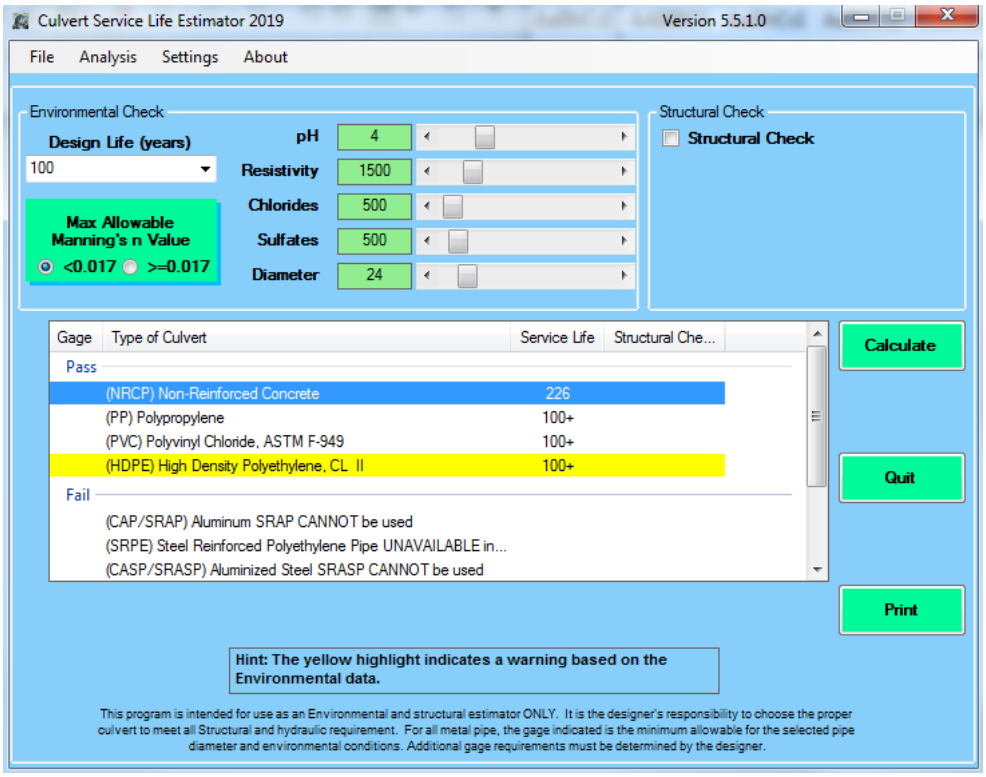

Figure 125. Service life analysis of pipes in pH4 [2]

The results illustrate that non-reinforced concrete pipes will last 226 years in pH 4 environment and reinforced concrete pipe can't be used in this environment at all.

6.3. Service life estimation of SYNFRCPs by accelerated aging tests

To determine the service life of SYNFRCPs, end life criteria should be proposed, and the test results should be compared with that criterion. Since the maximum design service life in pipelines is 100 years, the goal of this study is to determine whether SYNFRCPs can last longer than 100 years in these corrosive environments or not.

6.3.1. End life criteria

Based on ASTM C1818 [12], service load limits of SYNFRCPs are 0.67 of their ultimate load limit, as depicted in Figure 126.

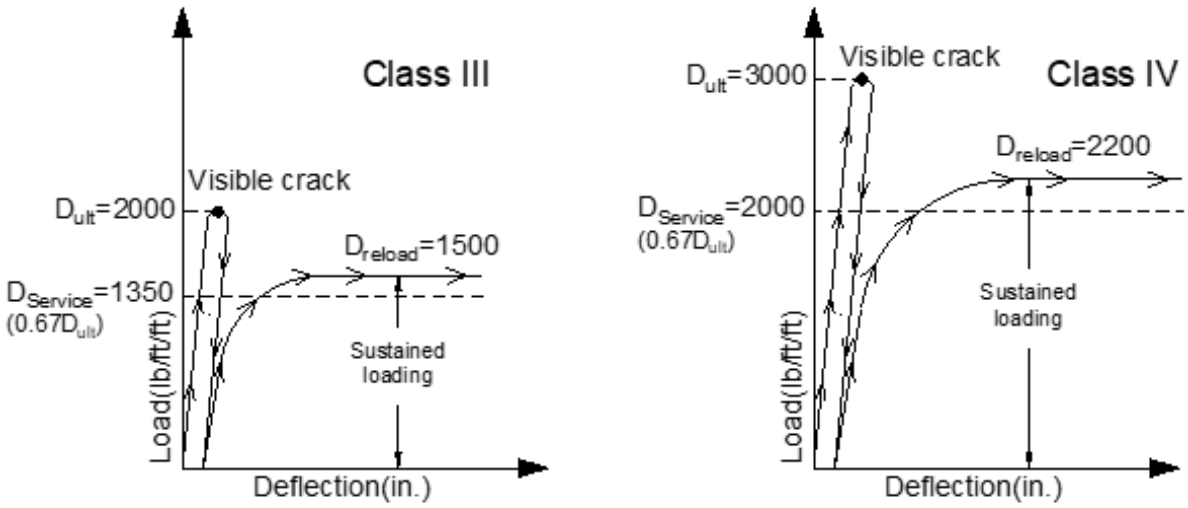

Figure 126. Ultimate and service load relationship, ASTM C1818 [12]

Based on this relationship, the end life criteria can be defined as the moment the ultimate D-load capacity of a pipe drops below the service load limit, which is 0.67 of the ultimate load. In this research, 0.33 ultimate load drop will be considered as the end life criteria.

6.3.2. Service life calculation

The results of load bearing capacity decrease because of accelerated aging are presented in Figure 127.

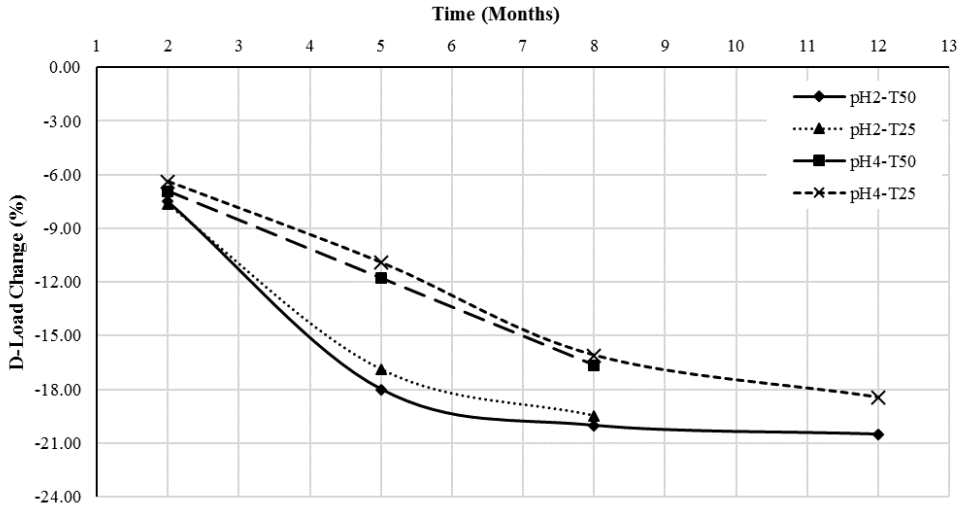

Figure 127. Load decrease vs. time

As depicted in this Figure, pH2-T50 results converged to a plateau, and that means a steady state has been reached in this case. For pH4-T25, which is the goal condition, the results were going through the same way based on the microscopic and load bearing capacity analysis. To achieve the 100-year load bearing capacity of SYNFCPs, an appropriate function should be fitted to the test data, and for 100-year assessment, the obtained regressed function will be extrapolated.

Function selection

Test results' curves can be presented in many different formats, but since the end life criterion is percentage-based, it was better to plot them based on percentage decrease. To choose proper fitting functions on obtained data, functions with similar shapes to the graphs were chosen. By investigating the different combination of these functions, the best fits were used for 100-year load estimation. These constantly decreasing functions with steady-state phase that limits to zero inherently at large x values were chosen to be $f(x) = Ln\ (1+1/x)$ and $f(x) = e^{-x}$. To find the best fits, the curve fitting was performed by Curve Fit Professional 2.6 [42].

The curve fitting results are listed as follows:

Equation: $a \times Ln\left(\frac{1}{x}\right) + b$

Coeff. of Determination (r^2) = 0.98

a = 41.6077 and b = -24.6844

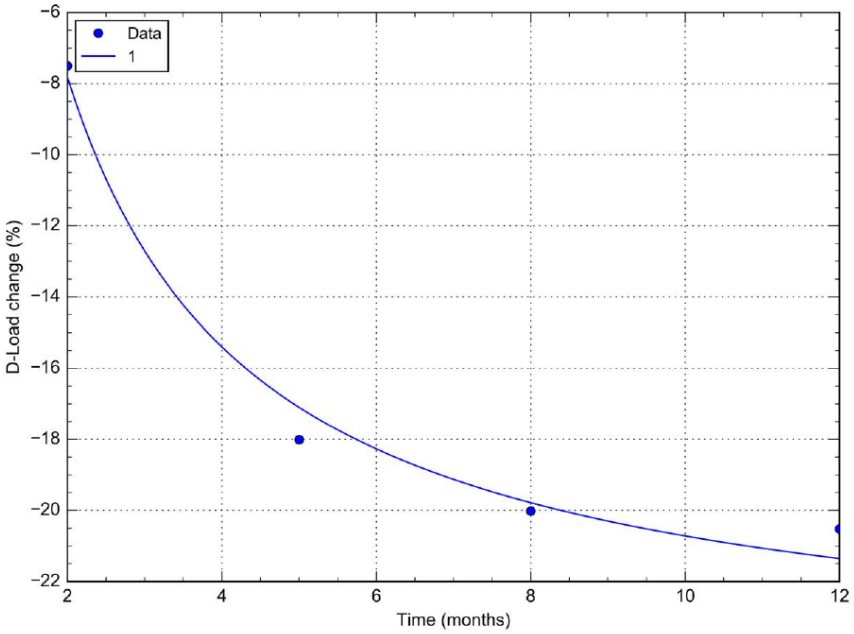

Figure 128. Curve fitting with $a \times Ln\left(1 + \frac{1}{x}\right) + b$ function

Equation: $a \times e^{-x} + b$

Coefficient of Determination (r^2): 0.98

a = 90.9223, b = -19.7497

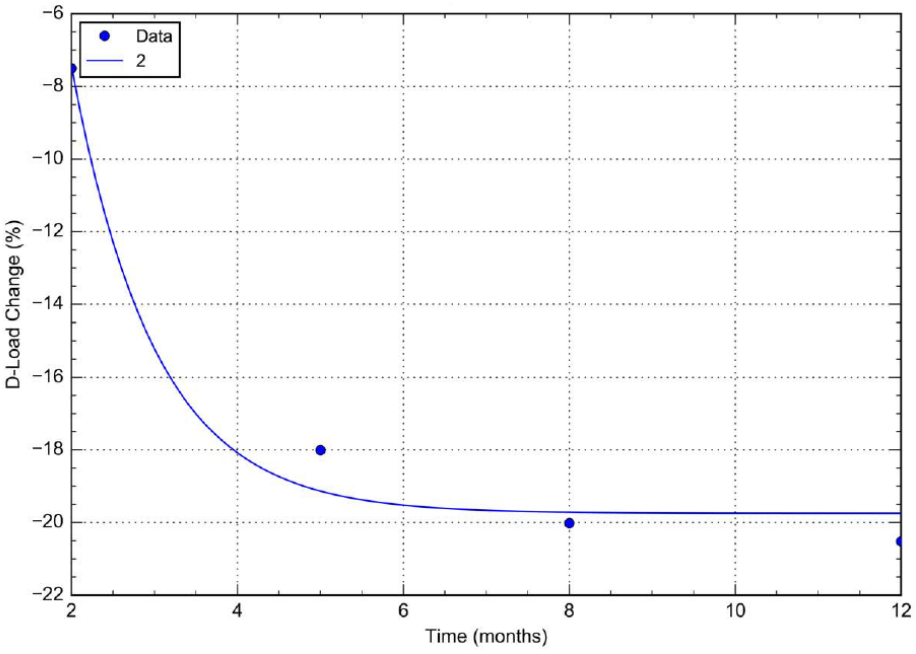

Figure 129. Curve fitting with $a \times e^{-x} + b$ function

Equation: $a \times e^{-x} + b \times \ln\left(1 + \frac{1}{x}\right) + c$

Coeff. of Determination (r^2) = 0.999

a = 44.3771, b = 21.9590, c = -22.4053

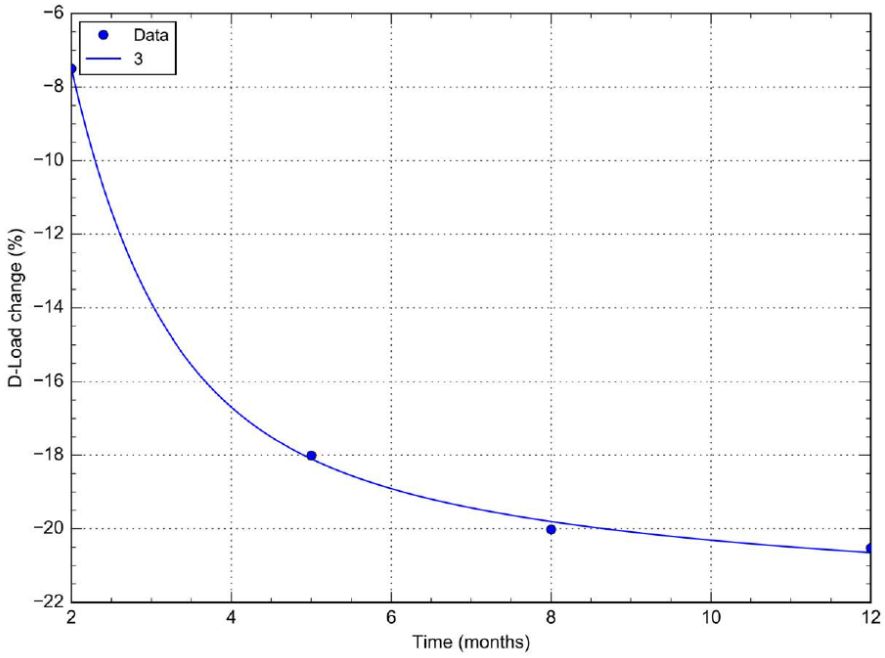

Figure 130. Curve fitting with $a \times e^{-x} + b \times \ln\left(1 + \frac{1}{x}\right) + c$ function

All of these regression results show an $R^2 > 0.98$, and they can be used for further investigations. Since it was observed that pH2-T50 and pH4-T25 specimens are going through the same deterioration scenarios, it is assumed that similar functions can be fit to the pH4-T25 data, but the steady-state constant should be imported from pH2-T50 regression results. This is based on the assumption that pH4-T25 graph ultimately converges to the pH2-T50 results.

Finally, the D-Load change after 100 years can be assessed by extrapolation on the appropriate function.

Curve fitting on pH4-T25

To fit curves on the results of tested pH4-T25 specimens, same functions that were used for the pH2-T50 solution will be used for this set of specimens, but the constant steady state value would be directly adopted from pH2-T50 regression results. This constant value adoption is based on the assumption that these two sets will be ultimately converged to each other after a while.

Equation: $a \times Ln\left(1+\frac{1}{x}\right) - 24.6844$

Coeff. of Determination (r^2) = 0.58

a = 52.4783

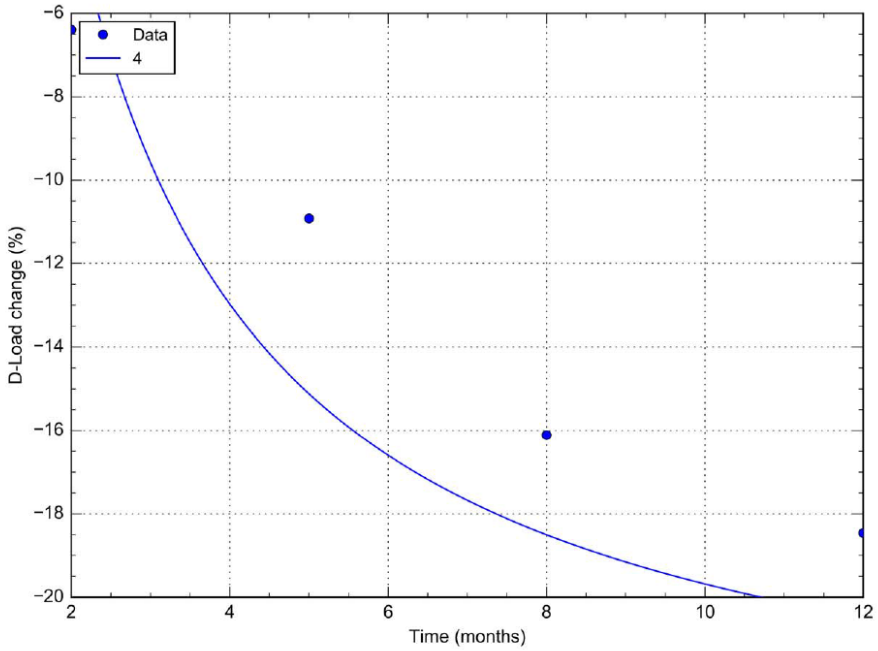

Figure 131. Curve fitting on pH4-T25 with $a \times Ln\left(1+\frac{1}{x}\right) - 24.6844$ function

Equation: $a \times e^{-x} - 19.7497$

Correlation Coeff. (r^2) = 0.07

a = 101.7780

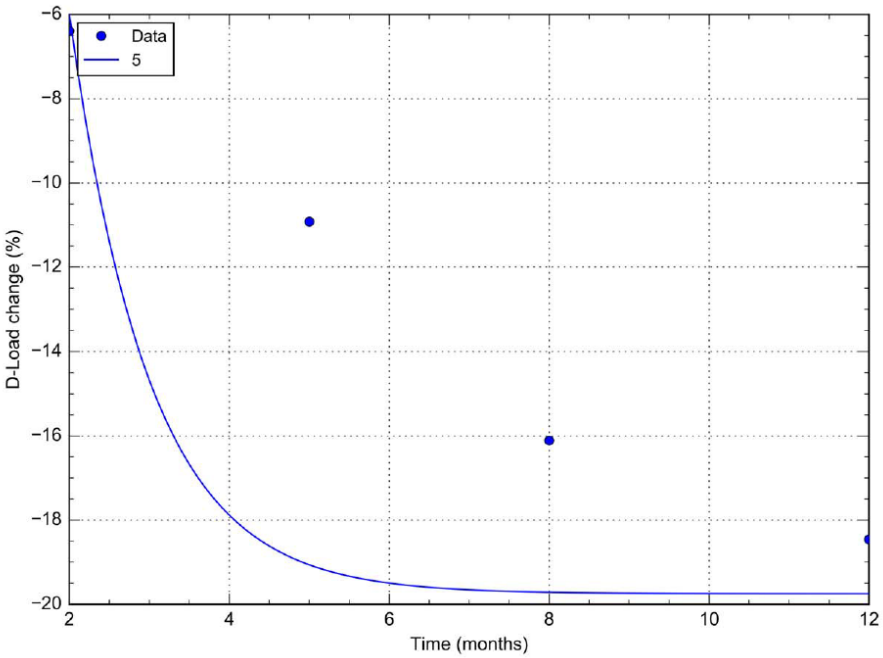

Figure 132. Curve fitting on pH4-T25 with $a \times e^{-x} - 19.7497$ function

Equation: $a \times e^{-x} + b \times \ln\left(1 + \frac{1}{x}\right) - 22.4053$

Coeff. of Determination (r^2) = 0.97, a = -61.0156 , b = 59.9776

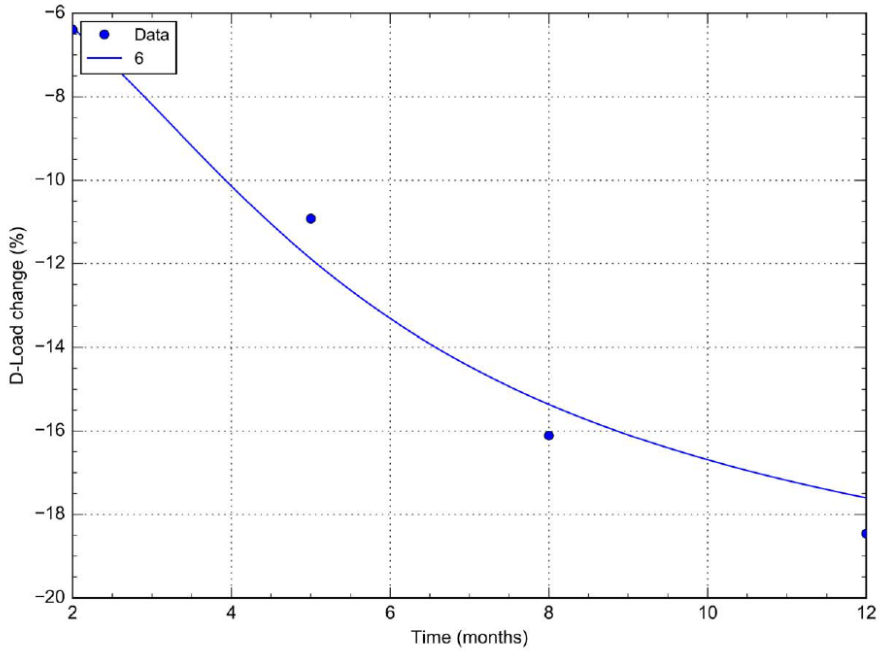

Figure 133. Curve fitting with $a \times e^{-x} + b \times \ln\left(1 + \frac{1}{x}\right) - 22.4053$ function

Based on the obtained results, it can be concluded that $a \times e^{-x} + b$ and $a \times Ln\left(1 + \frac{1}{x}\right) + b$ functions do not lead to an acceptable R^2,and they don't fit well on pH2-T25 results. On the other hand, $a \times e^{-x} + b \times \ln\left(1 + \frac{1}{x}\right) + c$ shows a perfect fit (R^2 = 0.99) on pH2-T50 data set and it fits well on pH4-T25 data (R^2 = 0.97). Considering all these findings, the following functions will be used for further analysis and extrapolation.

pH2-T50: $44.3771 \times e^{-x} + 21.9590 \times \ln\left(1 + \frac{1}{x}\right) - 22.4053$ *(Eq. 21)*

pH4-T25: $-61.0156 \times e^{-x} + 59.9776 \times \ln\left(1 + \frac{1}{x}\right) - 22.4053$ *(Eq. 22)*

Service life D-Load calculation

Using pH4-T25 equation and extrapolating the graph to 100 years will estimate the load bearing capacity change after 100 years. Figure 134 depicts the 100-year service life D-Load decrease pattern for SYNFRCPs in corrosive field environment (pH4-T25).

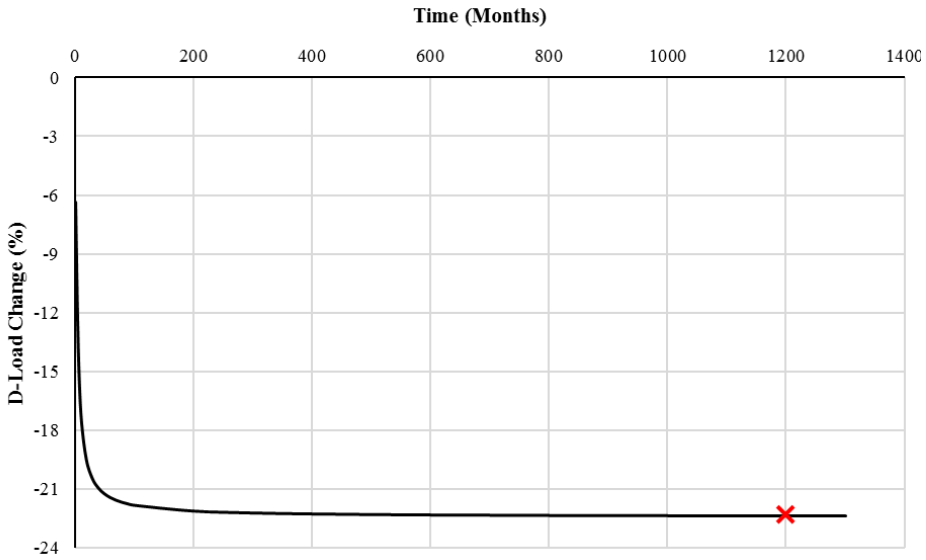

Figure 134. Service life load decrease pattern

Based on the graph shown in Figure 132, it can be concluded after being exposed to environments with pH level of 4 and 25°C ambient temperature for 100-years, the D-load of SYNFRCPs is predicted to decrease by 22.36%. Since this D-Load decrease is less than 33% service life criteria, it can be anticipated that SYNFRCPs would last longer than 100-years in these highly corrosive environments. These results are in agreement with the service life estimation of plain concrete pipes by the Florida Department of Transportation. As shown in Figure 123 and based on FDOT software calculations, plain concrete pipes will last longer than 200 years in this environment.

According to the findings of this research, SYNFRCPs meet the service life requirements of FDOT and other DOTs nationwide, and they can be used for infrastructural applications.

CHAPTER 7. SUMMARY AND CONCLUSION

In this research, a series of material and structural tests were conducted to determine the effects of corrosive acidic environments on SYNFRC specimens. The ultimate goal of this research was to determine the 100-year service life behavior of these pipes, and for this purpose, a series of mechanical and microscopic tests and analyses were conducted.

Initially, the effects of these environments were studied on SYNFRC cylindrical specimens. At this phase, 114 cylinders were made with two different fiber dosages and were immersed in pH 2.5 and pH 4.5 solutions with three different temperatures for four months. The specimens were tested at 1, 2, and 4 months intervals. Six of these cylinders were tested as control specimens, and the post-immersion test results were compared with these control compressive strength values. The control tests were conducted after 7 days of curing, and the results showed that:

- For specimens that were immersed in pH 2.5 solutions, after each immersion period the strength loss was higher in higher temperatures and this complies with the anticipated accelerating effect of elevated temperatures on the acid-concrete reactions.
- For pH 4.5, the temperature increase resulted in less compressive strength loss. This happened because hydration reactions and deterioration reactions were accelerated simultaneously, and the progress of hydration reactions neutralized the deteriorating effects of acid-concrete reactions.
- The compressive strength of the specimens that were immersed in pH2.5 solutions decreased by 1.87 times more than those which were soaked in pH4.5 baths.
- Immersion duration had a major deteriorating effect on the specimens. Specimens showed more than 30% compressive strength decrease after four months of immersion.

- Synthetic fibers were not deteriorated after four months of immersion in these harsh environments and this shows their acid resistivity.

At the second phase of this study, SYNFRCPs were cut into 2-ft. pieces and they were immersed in pH2 and pH4 solutions for a year. The baths' temperatures were 25°C and 50°C, and they were controlled with industrial temperature control systems. The control specimens of this set of tests were tested six months after production to eliminate the effect of hydration reactions on the accelerated aging test results in higher temperatures. Finally, from each of these environments, two specimens were tested after 2, 5, 8, and 12 months, and their D-load capacities were recorded and compared with control pipes.

- The D-load capacity of the specimens that were immersed in pH2 solutions decreased by 20% after one year, and pH4 specimens showed 18% D-load decrease after the same period.
- The shapes of the curves in these two environments (pH4 and pH2) were different. pH2 specimens' test results converged to a steady state load decrease value after five months, and the pattern continued for the rest of the immersion periods. For pH4, the results were continuously decreasing for all test intervals and based on the trend of the results; it can be predicted that the curve of pH4 specimens is going to converge to the pH2 plateau after a longer immersion period.

For further investigation of the results, microscopic analysis of the specimens was conducted to determine the microstructure alterations of the cement paste. For this purpose, a cylindrical core from each set of the specimens was extracted and tested with SEM, and the specimens were analyzed for their composition and microstructures. The results of this set support the outcomes of mechanical properties tests of the pipes.

- Elemental analysis showed that the surface of SYNFRCPs in pH4 acid contained 0.05% sulfur after two months of immersion. This shows that pH4 specimens have not deteriorated significantly before 2 months tests.
- The amount of sulfur in the pH2 specimens increased abruptly after two months of immersion, and it indicates that the deterioration reactions have already started in these pipes.
- The sulfur mass on the surface of the pH2 specimens didn't show any sign of considerable increase after 5 months of immersion. It was 11.25% at 5 months, 11.2% at 8 months, and 11.71% at 12 months tests. This means that the surface of these specimens were saturated with gypsum crystals gradually and the acid-concrete reactions reached to an equilibrium phase.
- For pH4 specimens, the amount of sulfur was negligible initially (0.05%), and it was constantly increasing after two months of immersion. The sulfur mass percentage was 7.74% at five months, 10.17 at 8 months, and 12.01 at 12 months tests.
- The normalized mass measurements of pH4 specimens showed a trend that was similar to the mechanical tests' results. In these tests, the amount of sulfur element on the surface of pH 4 specimens was converging to the steady state value of sulfur mass on the surface of the pH2 specimens.

Finally, to predict the 100-years behavior of SYNFRCPs, best functions that could be fitted to the pH2-T50 results were used to anticipate the service life behavior of pH4-T25 specimens. For this purpose, constantly decreasing and self-limiting functions were used for curve fitting.

After initial analysis, among three best-fitted functions, the function that was a combination of natural logarithm and exponential functions showed the best fit on the results of both environments. Using this function for service life prediction of specimens:

- It was predicted that after 100 years in the pH4 environment and the ambient temperature of 25°C, a SYNFRCP would lose 22.36% of its D-Load bearing capacity.
- Since 22.36% load decrease is less than the 33% service life criteria, it can be anticipated that SYNFRCPs will last longer than 100 years in these harsh and corrosive environments.
- Most of the DOTs require 100-year serviceability for major pipelines, and since it is predicted that SYNFRCPs will last longer than 100 years in highly corrosive environments, they can be used in the U.S. infrastructure systems with similar conditions, which require 100+ years of serviceability.
- For pH2-T50, which is a very harsh environment for concrete pipes, the load decrease is also predicted to converge to 22.36%, and this can ensure the long-term serviceability of SYNFRCPs in these environments.

APPENDIX I: THREE EDGE BEARING TEST RESULTS

Control tests:

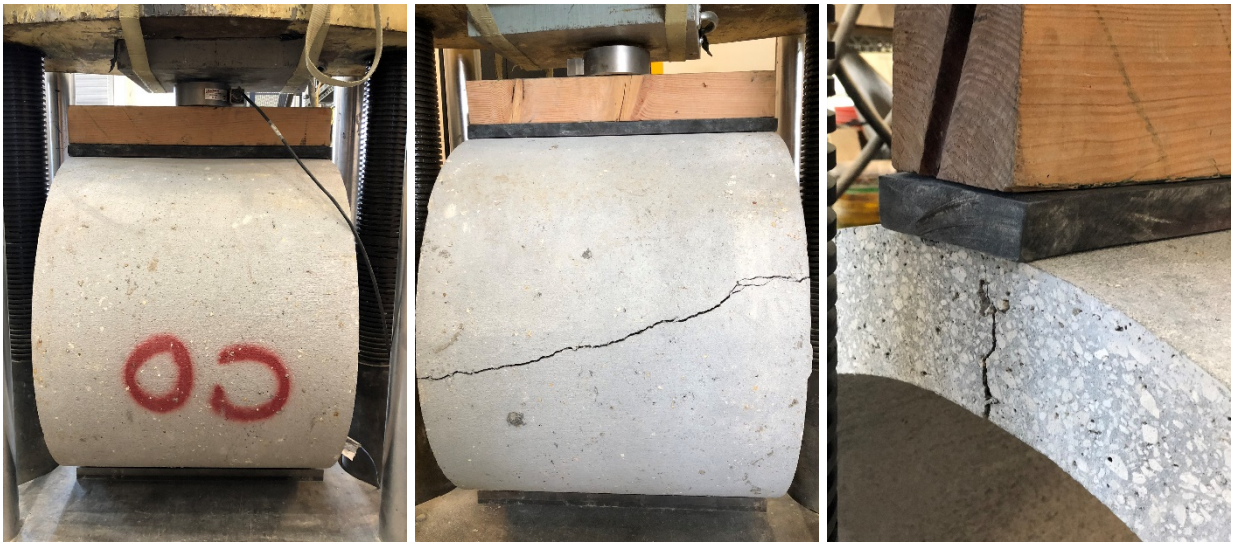

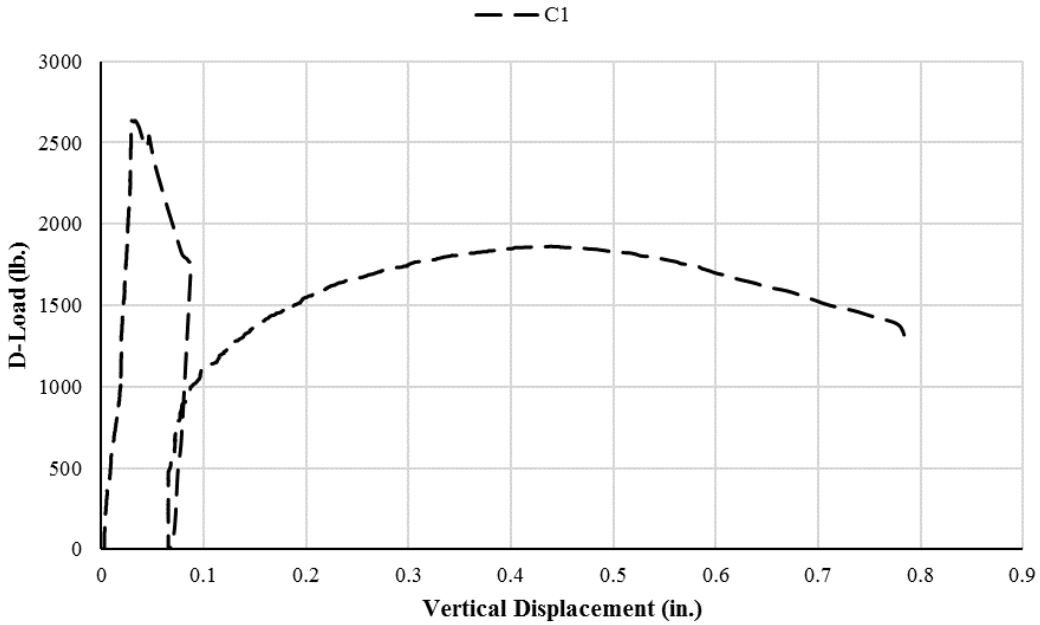
C1
3000
2500
2000
1500
1000
500
0
D-Load (lb.)
0
0.1
0.2
0.3
0.4
0.5
0.6
0.7
0.8
0.9
Vertical Displacement (in.)

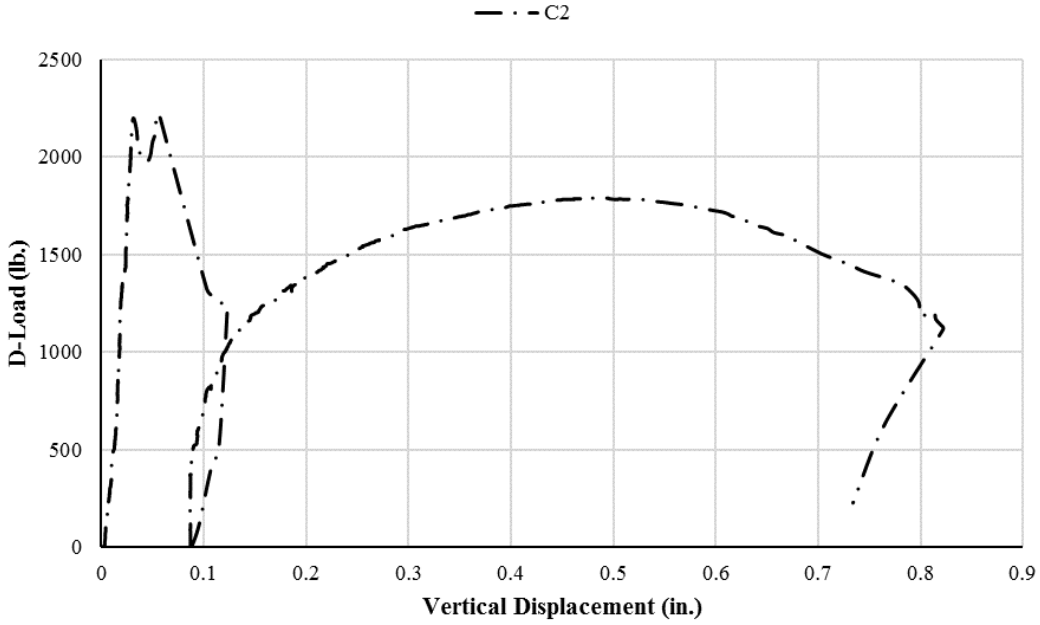
C2
2500
2000
1500
1000
500
0
D-Load (lb.)
0
0.1
0.2
0.3
0.4
0.5
0.6
0.7
0.8
0.9
Vertical Displacement (in.)

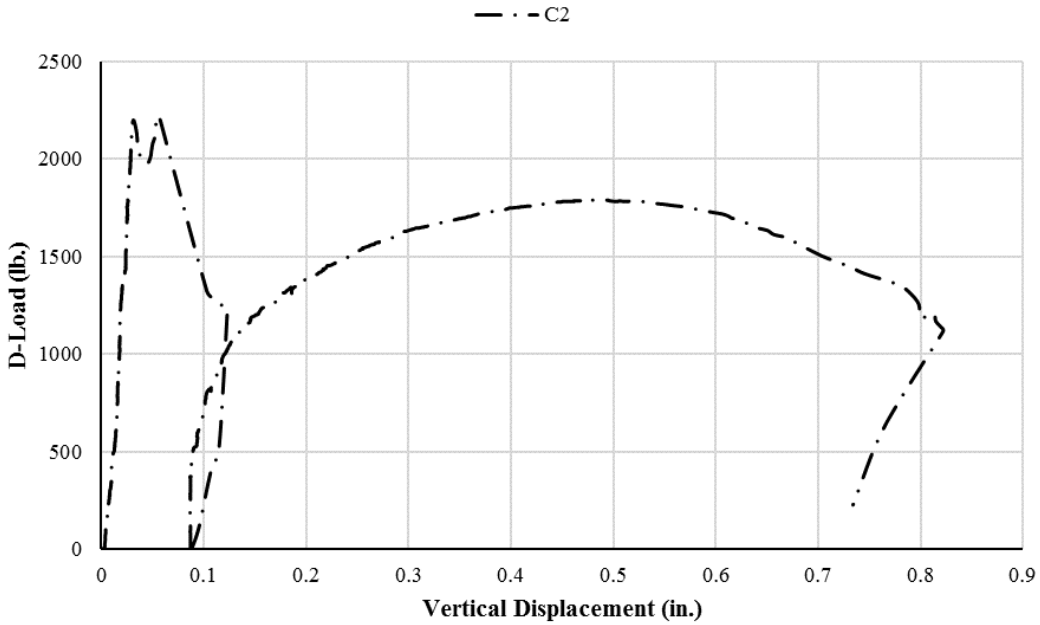
C2
2500
2000
1500
1000
500
0
D-Load (lb.)
0
0.1
0.2
0.3
0.4
0.5
0.6
0.7
0.8
0.9
Vertical Displacement (in.)

Two months tests:

pH 2 – T 50:

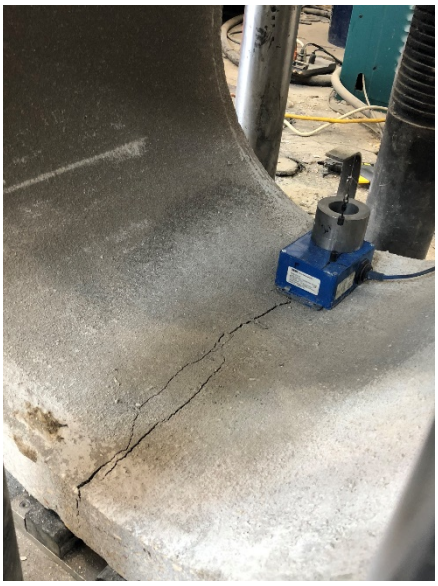

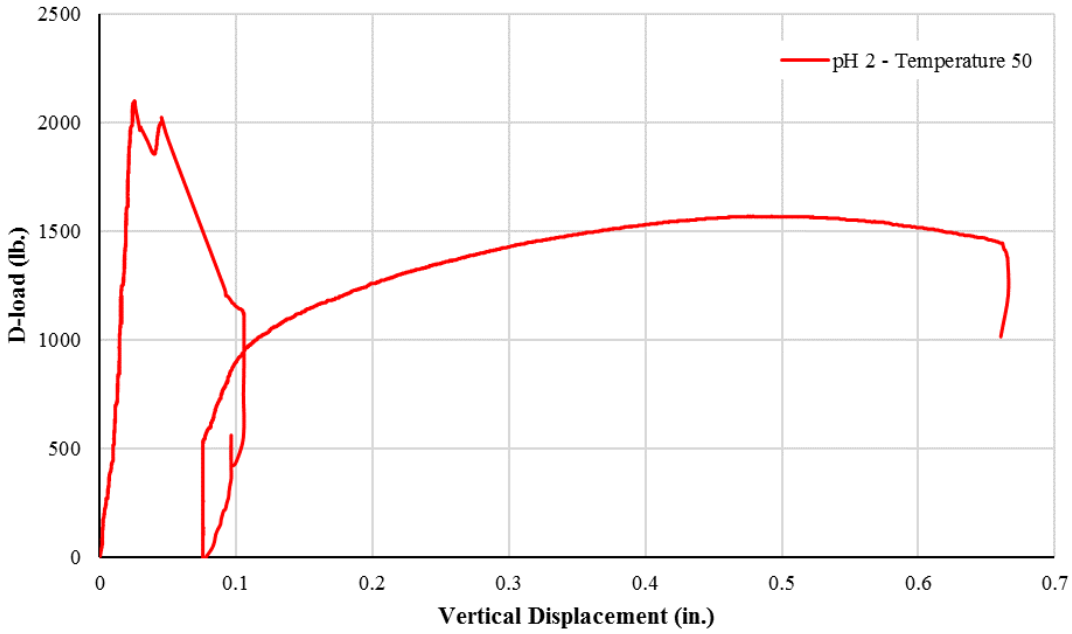
pH 2 - Temperature 50
D-load (lb.)
2500
2000
1500
1000
500
0
0
0.1
0.2
0.3
0.4
0.5
0.6
0.7
Vertical Displacement (in.)

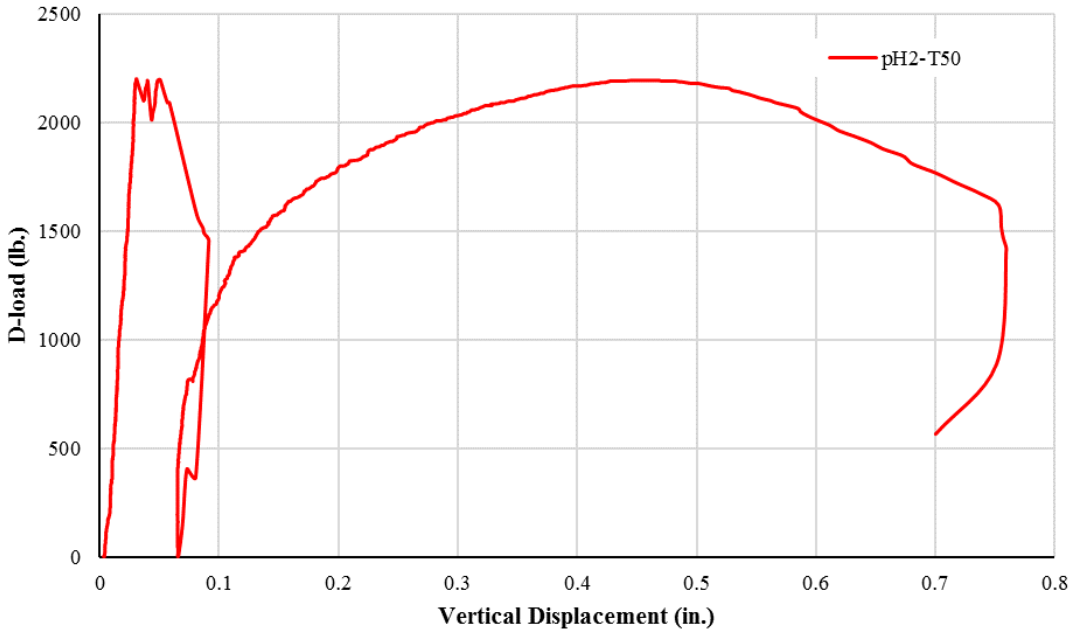
pH2-T50
D-load (lb.)
2500
2000
1500
1000
500
0
0
0.1
0.2
0.3
0.4
0.5
0.6
0.7
0.8
Vertical Displacement (in.)

pH 2 – T25:

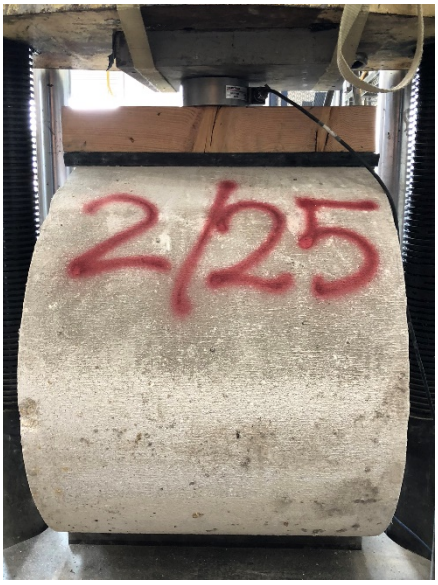

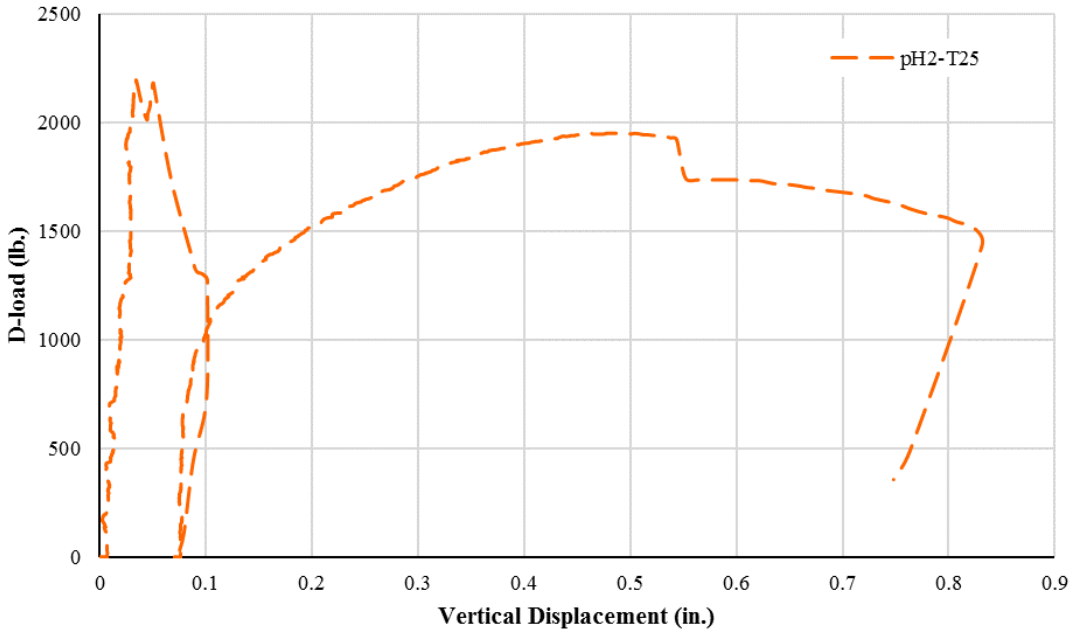
pH2-T25
D-load (lb.)
2500
2000
1500
1000
500
0
0
0.1
0.2
0.3
0.4
0.5
0.6
0.7
0.8
0.9
Vertical Displacement (in.)

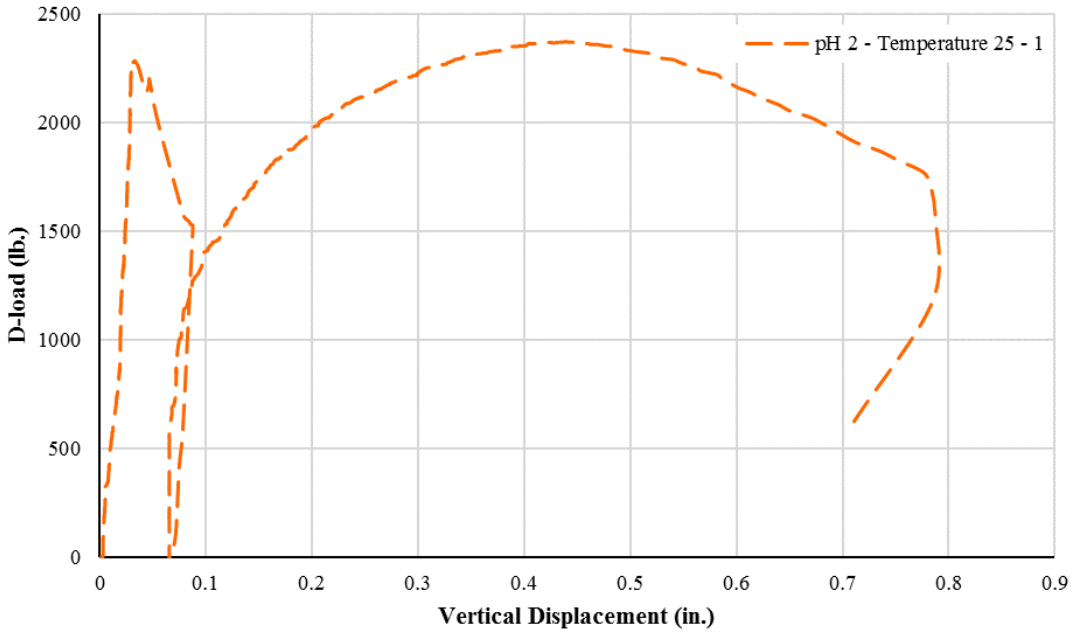
pH 2 - Temperature 25 - 1
D-load (lb.)
2500
2000
1500
1000
500
0
0
0.1
0.2
0.3
0.4
0.5
0.6
0.7
0.8
0.9
Vertical Displacement (in.)

pH 4 – T 50:

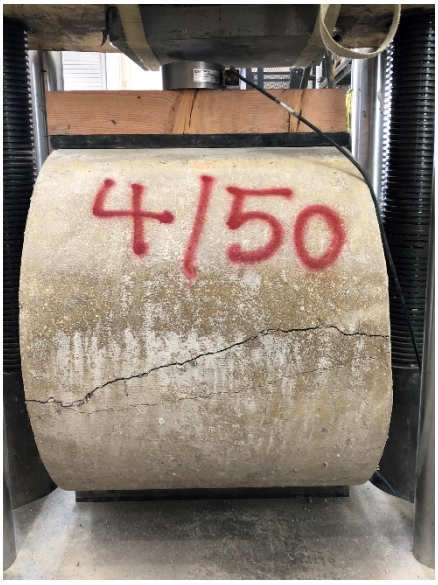

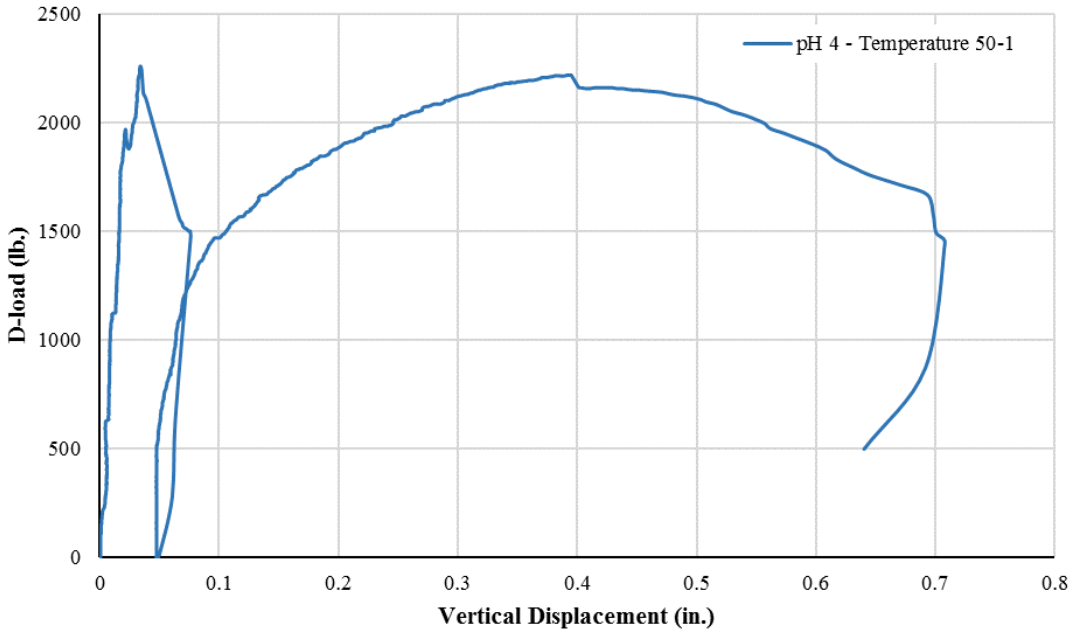
pH 4 - Temperature 50-1
D-load (lb.)
2500
2000
1500
1000
500
0
0
0.1
0.2
0.3
0.4
0.5
0.6
0.7
0.8
Vertical Displacement (in.)

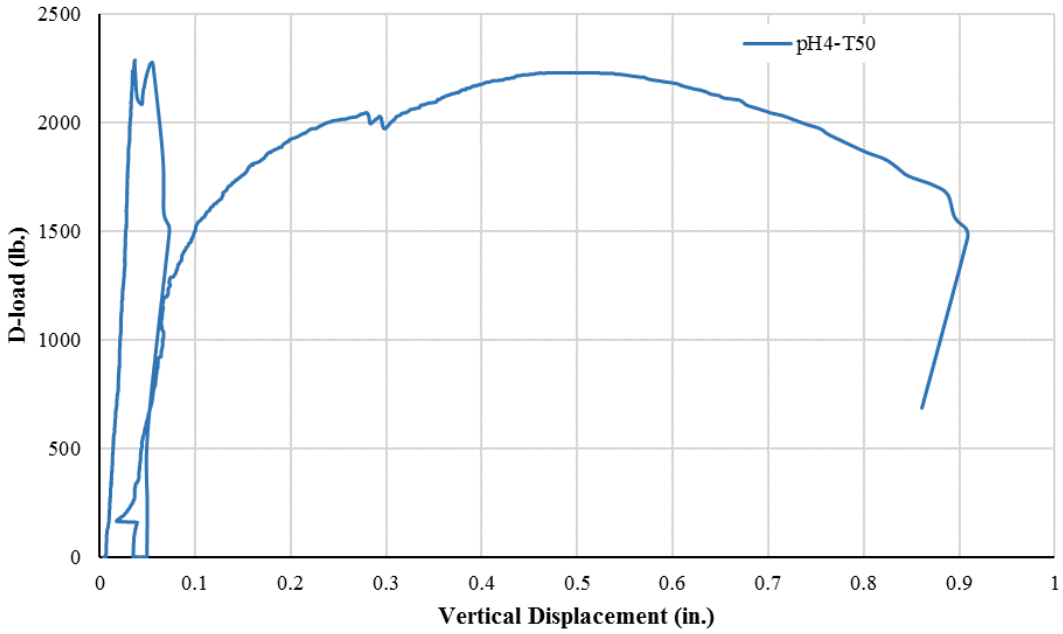
pH4-T50
D-load (lb.)
2500
2000
1500
1000
500
0
0
0.1
0.2
0.3
0.4
0.5
0.6
0.7
0.8
0.9
1
Vertical Displacement (in.)

pH 4 – T 25:

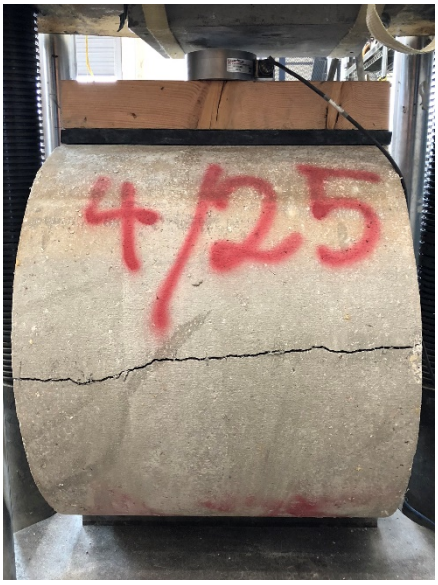

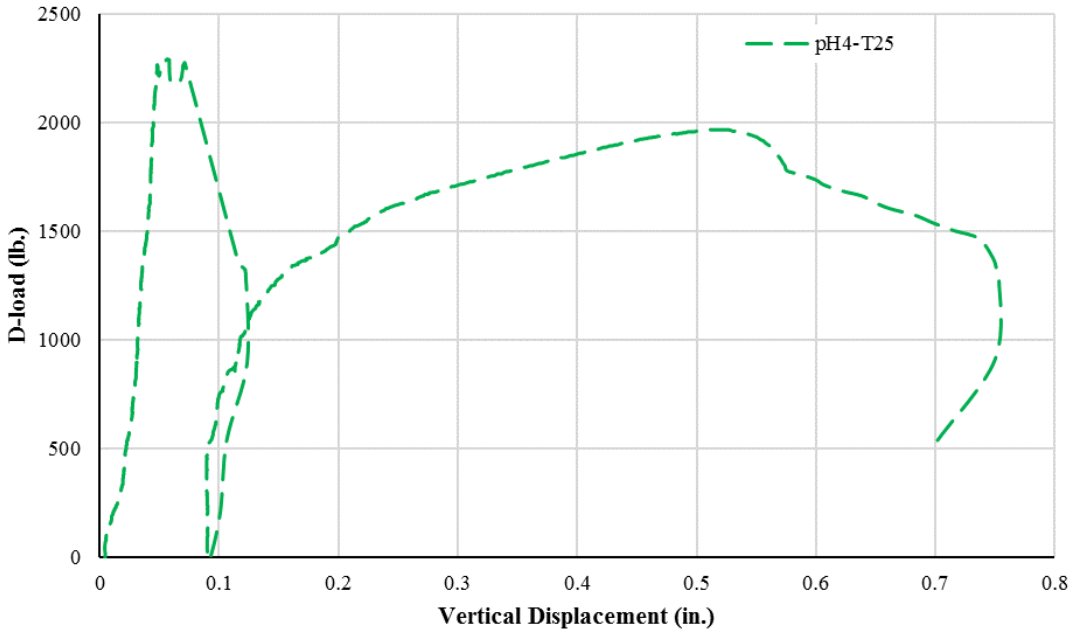
pH4-T25
D-load (lb.)
2500
2000
1500
1000
500
0
0
0.1
0.2
0.3
0.4
0.5
0.6
0.7
0.8
Vertical Displacement (in.)

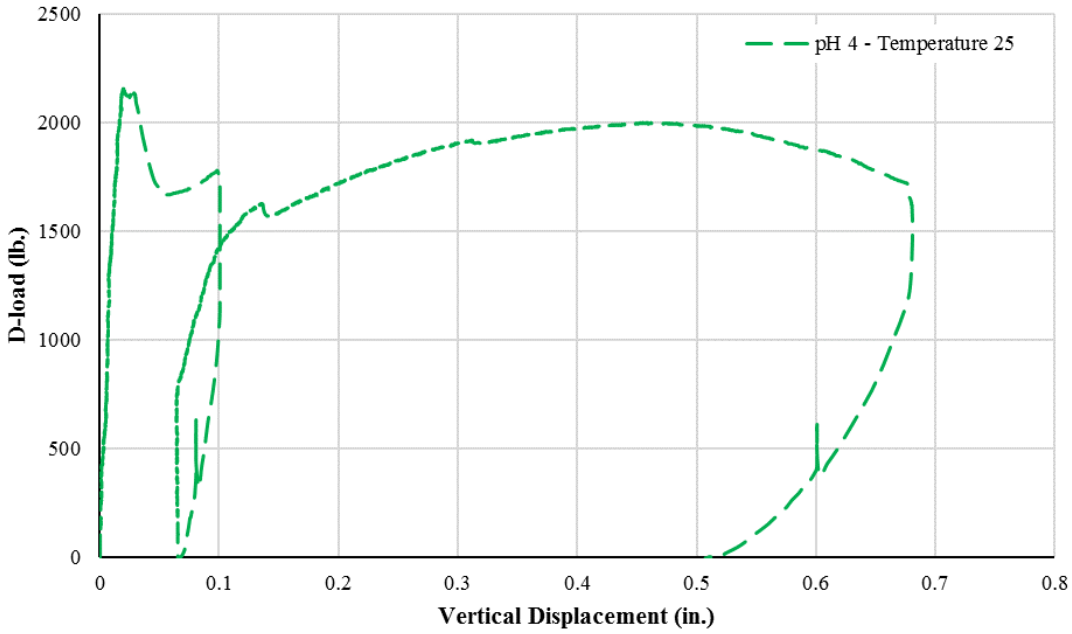
pH 4 - Temperature 25
D-load (lb.)
2500
2000
1500
1000
500
0
0
0.1
0.2
0.3
0.4
0.5
0.6
0.7
0.8
Vertical Displacement (in.)

Five months tests:

pH 2 – T 50:

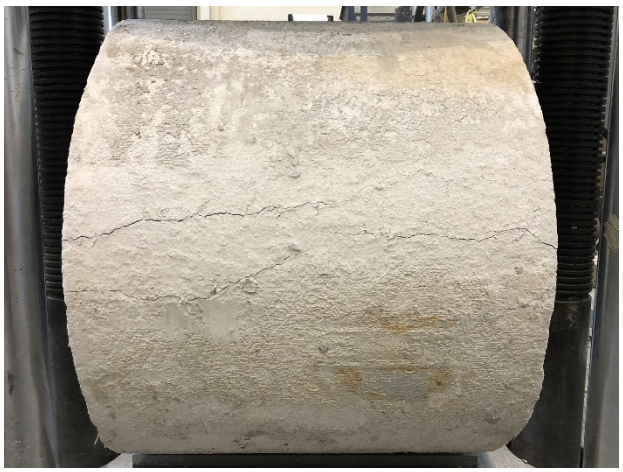

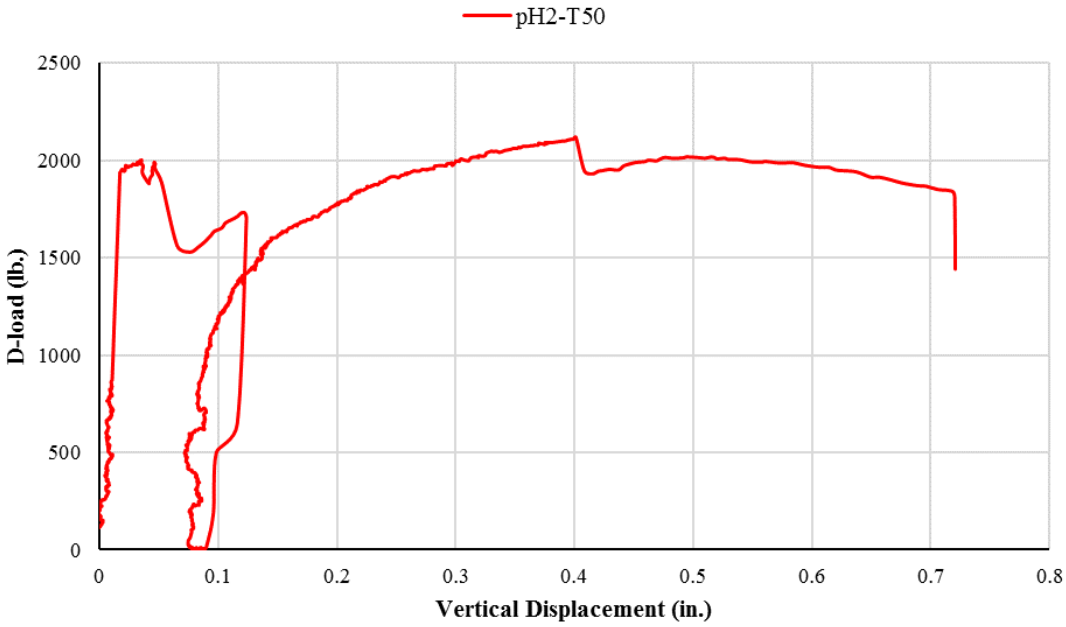
pH2-T50
2500
2000
1500
1000
500
0
D-load (lb.)
0
0.1
0.2
0.3
0.4
0.5
0.6
0.7
0.8
Vertical Displacement (in.)

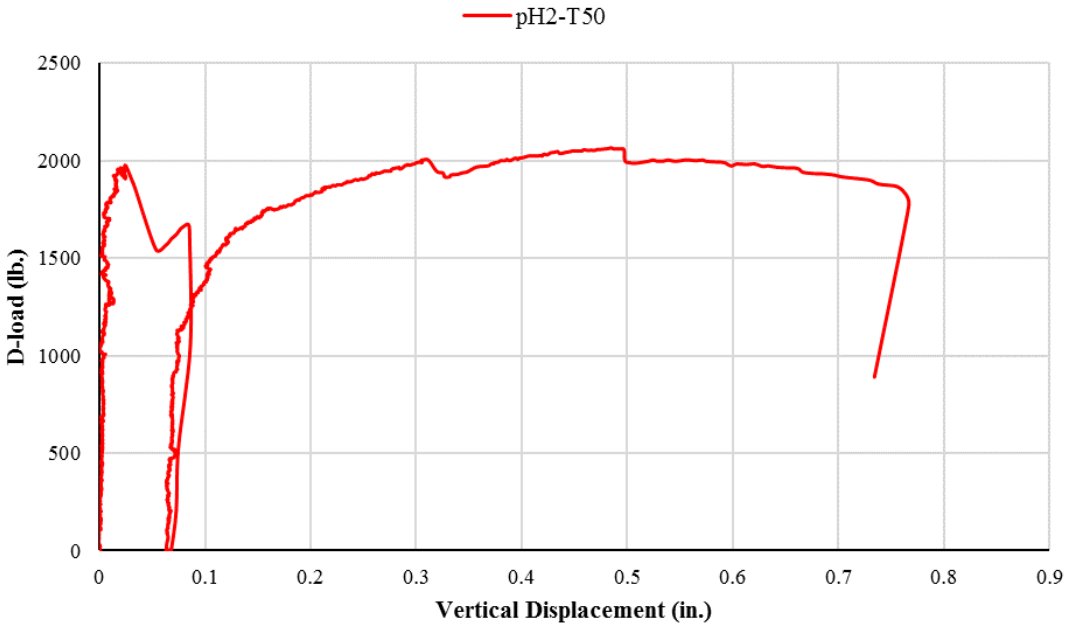
pH2-T50
2500
2000
1500
1000
500
0
D-load (lb.)
0
0.1
0.2
0.3
0.4
0.5
0.6
0.7
0.8
0.9
Vertical Displacement (in.)

pH 2 – T 25:

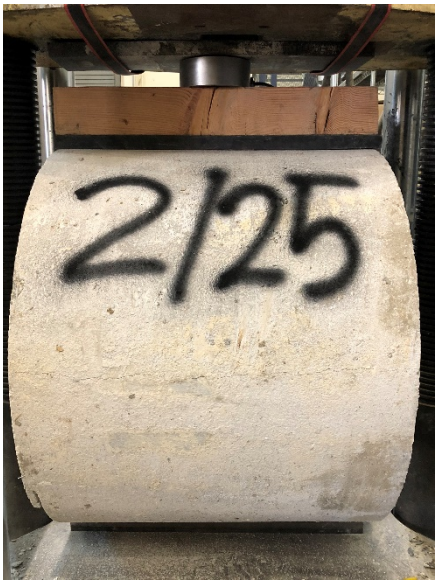

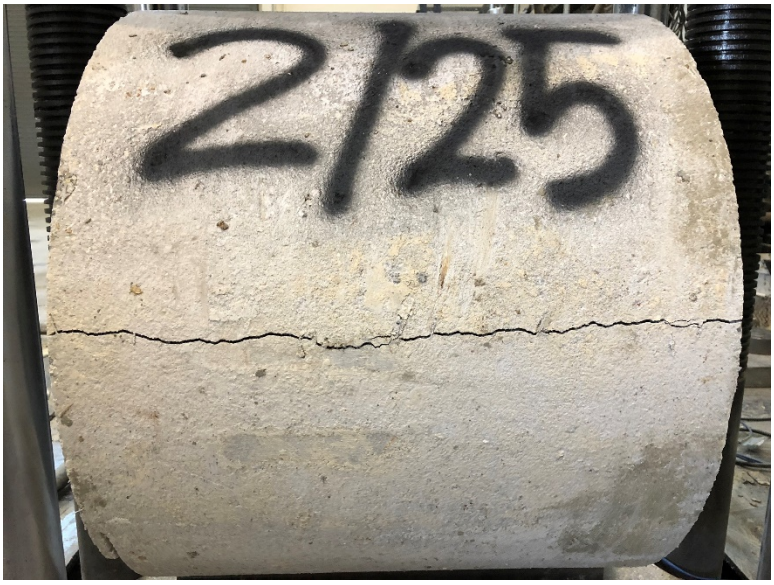

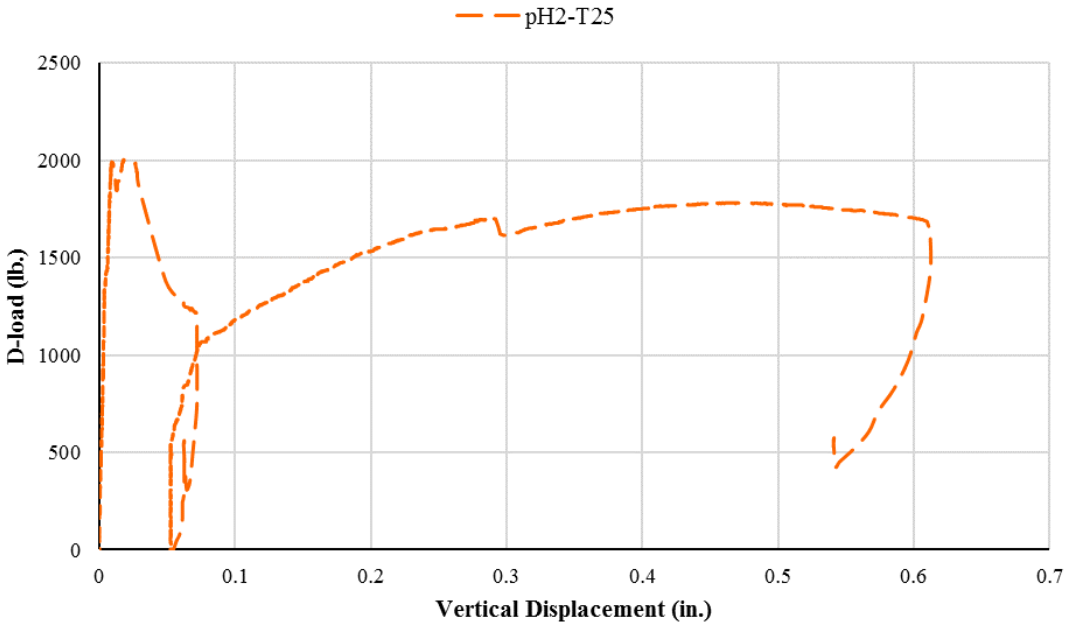
pH2-T25
2500
2000
1500
1000
500
0
D-load (lb.)
0
0.1
0.2
0.3
0.4
0.5
0.6
0.7
Vertical Displacement (in.)

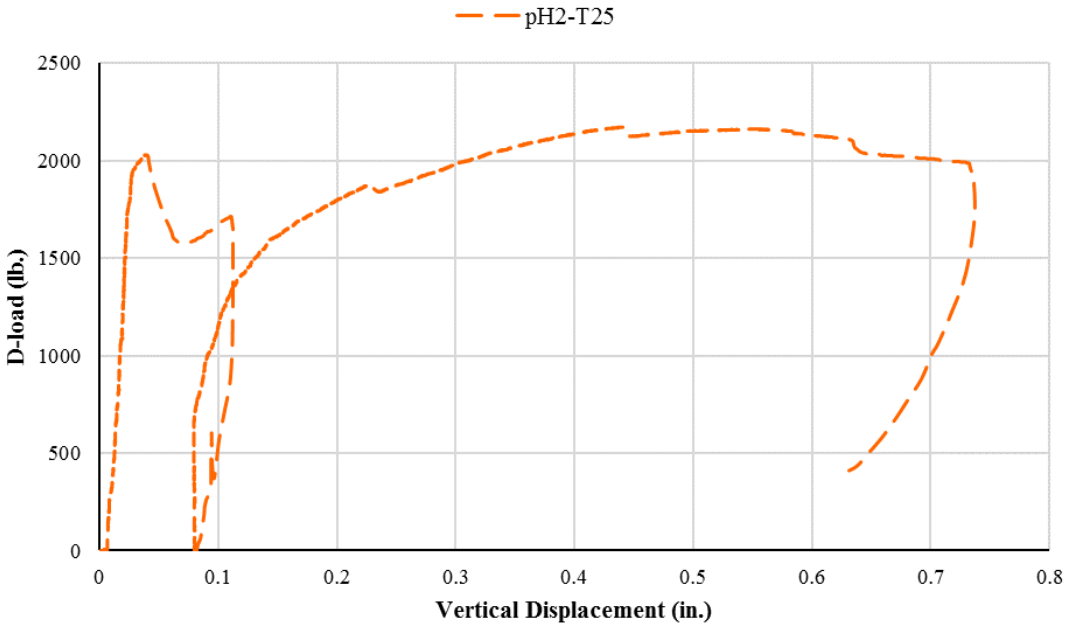
pH2-T25
2500
2000
1500
1000
500
0
D-load (lb.)
0
0.1
0.2
0.3
0.4
0.5
0.6
0.7
0.8
Vertical Displacement (in.)

pH 4 – T 50:

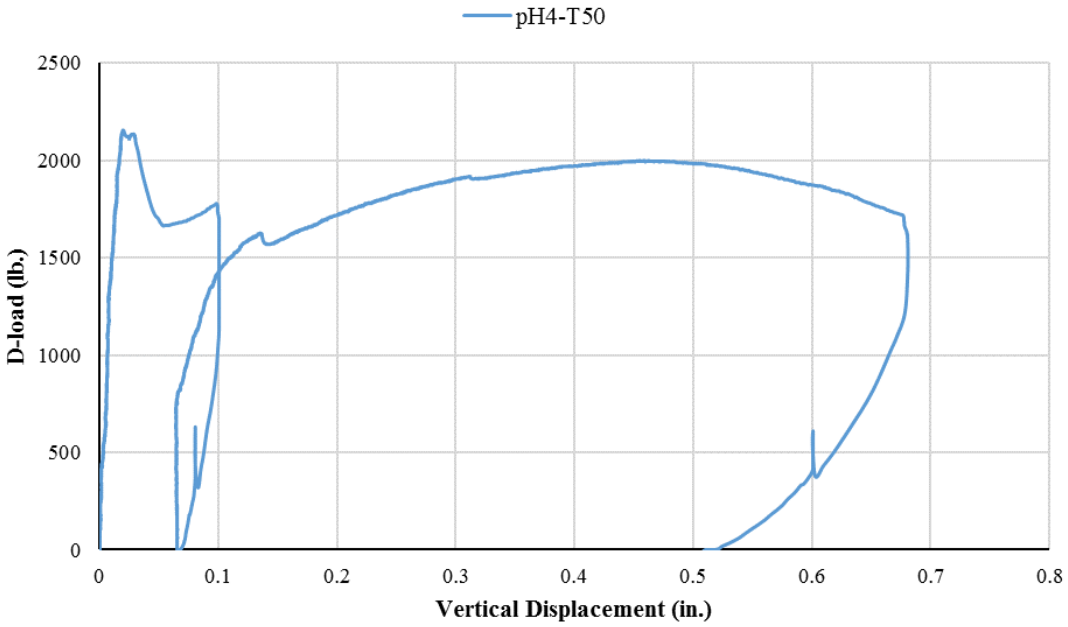
pH4-T50
2500
2000
1500
1000
500
0
D-load (lb.)
0
0.1
0.2
0.3
0.4
0.5
0.6
0.7
0.8
Vertical Displacement (in.)

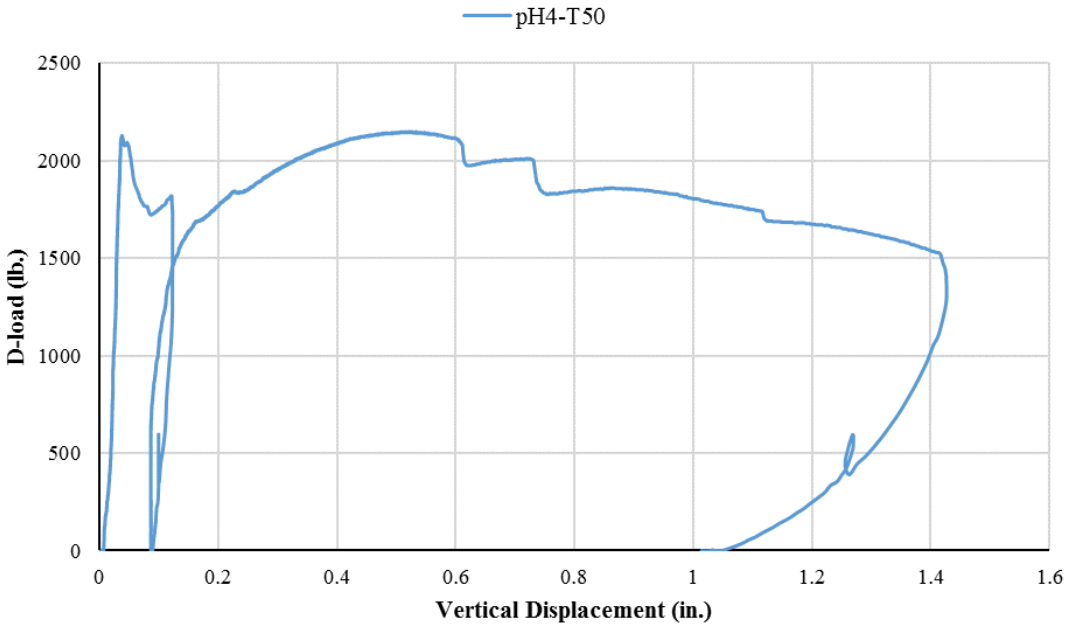
pH4-T50
2500
2000
1500
1000
500
0
D-load (lb.)
0
0.2
0.4
0.6
0.8
1
1.2
1.4
1.6
Vertical Displacement (in.)

pH 4 – T 25:


4/25

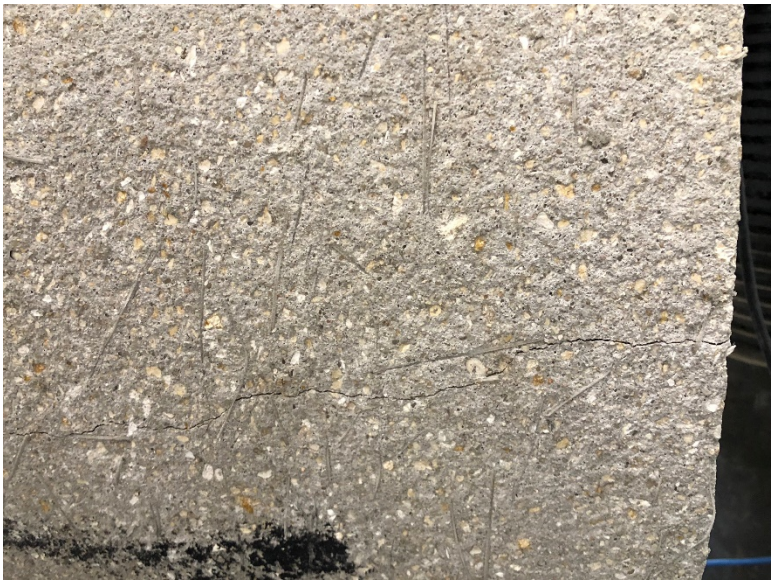

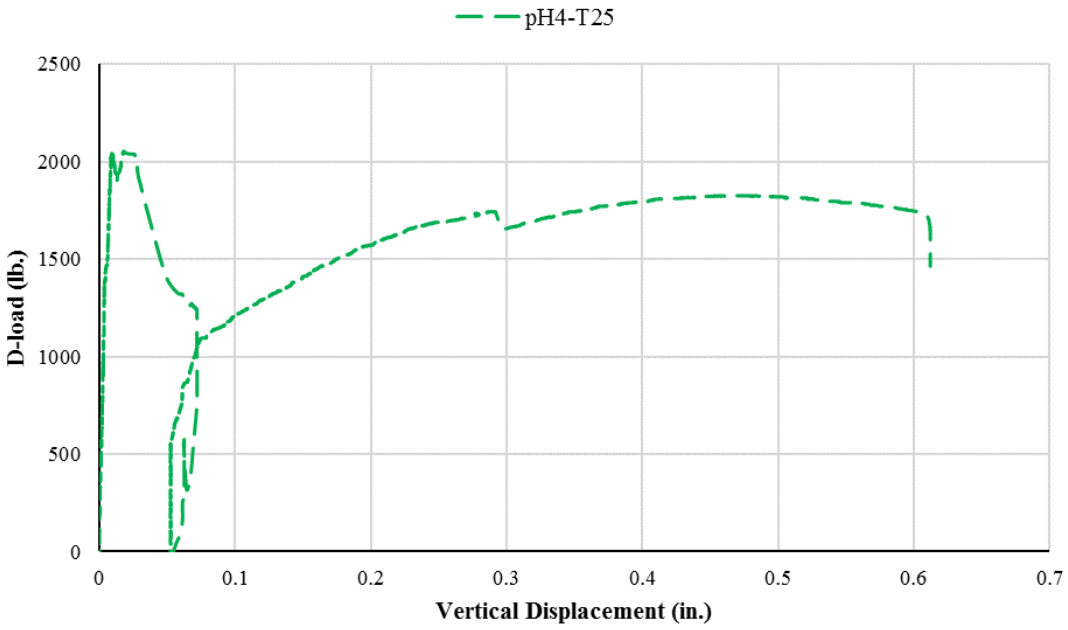
pH4-T25
2500
2000
1500
1000
500
0
D-load (lb.)
0
0.1
0.2
0.3
0.4
0.5
0.6
0.7
Vertical Displacement (in.)

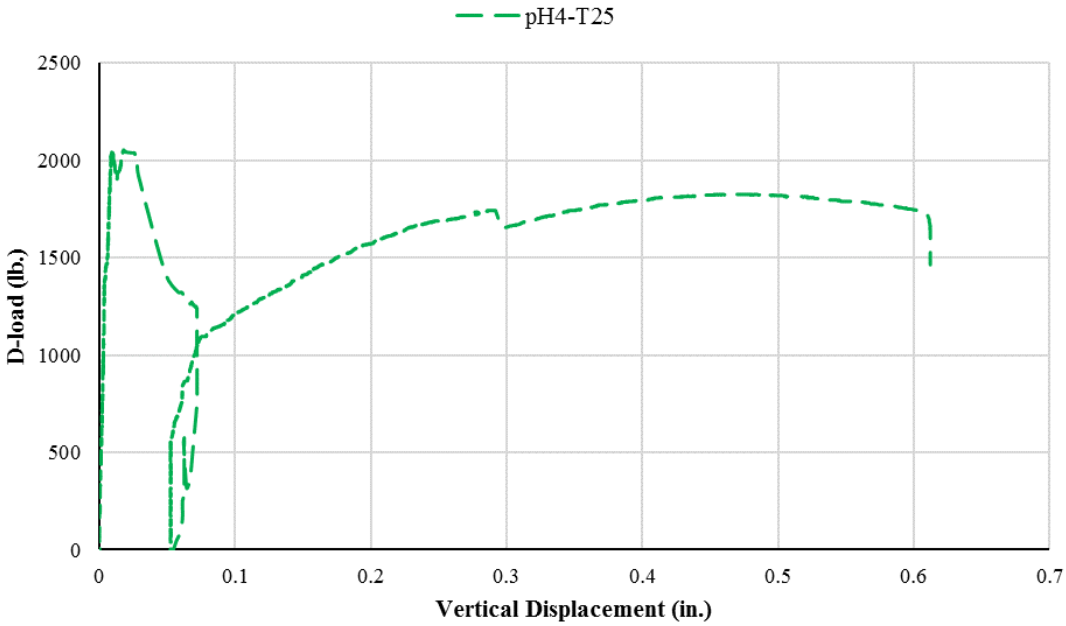
pH4-T25
2500
2000
1500
1000
500
0
D-load (lb.)
0
0.1
0.2
0.3
0.4
0.5
0.6
0.7
Vertical Displacement (in.)

Eight months tests:

pH 2 – T 50:

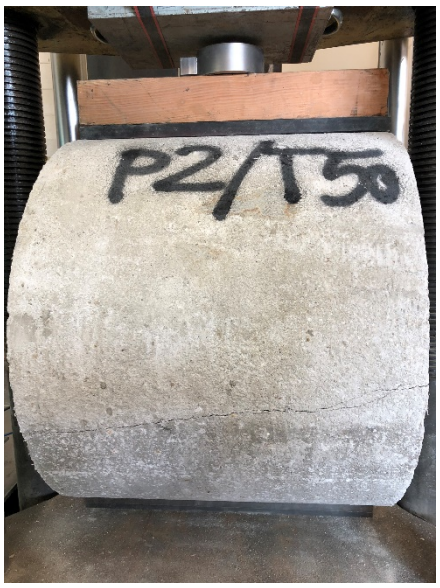

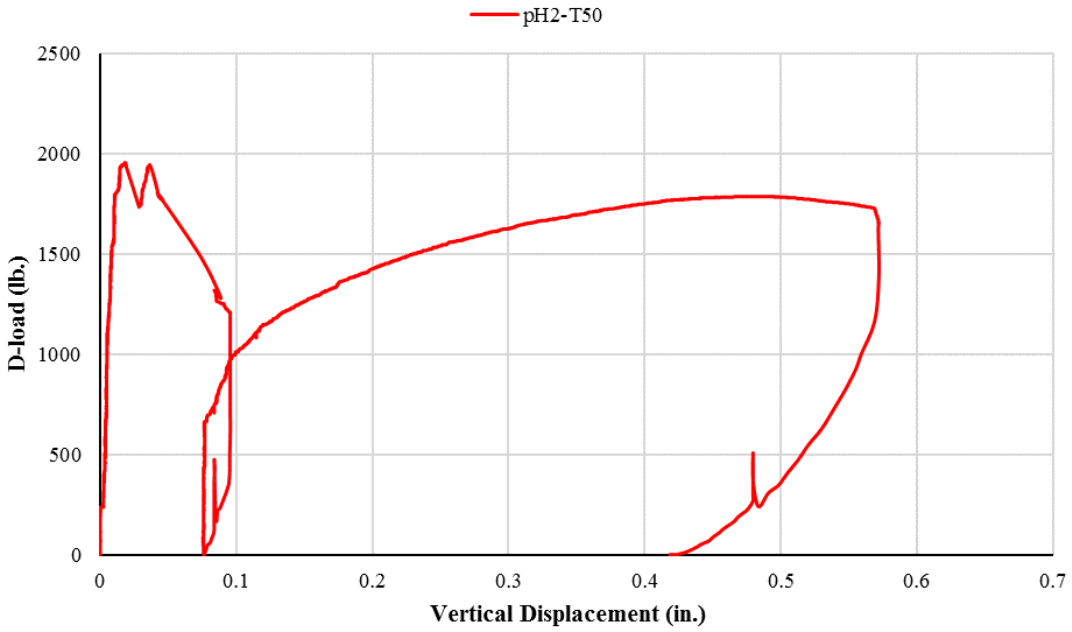
pH2-T50
2500
2000
1500
1000
500
0
D-load (lb.)
0
0.1
0.2
0.3
0.4
0.5
0.6
0.7
Vertical Displacement (in.)

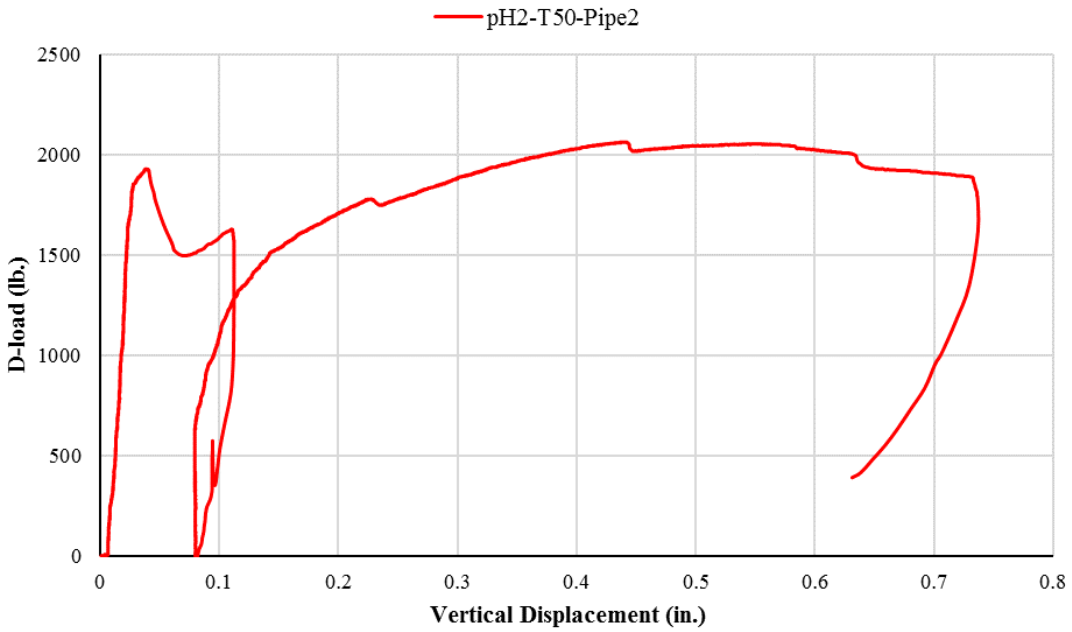
pH2-T50-Pipe2
2500
2000
1500
1000
500
0
D-load (lb.)
0
0.1
0.2
0.3
0.4
0.5
0.6
0.7
0.8
Vertical Displacement (in.)

pH 2 – T 25:

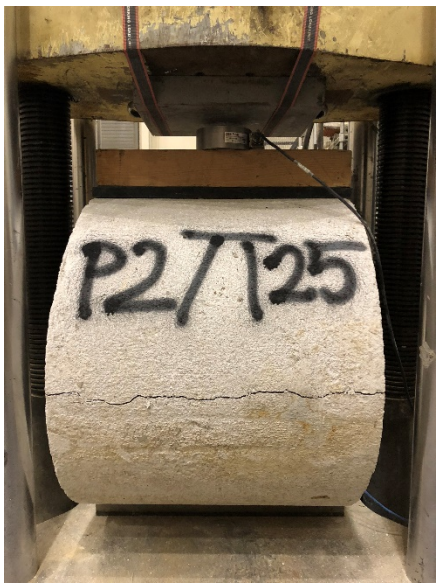

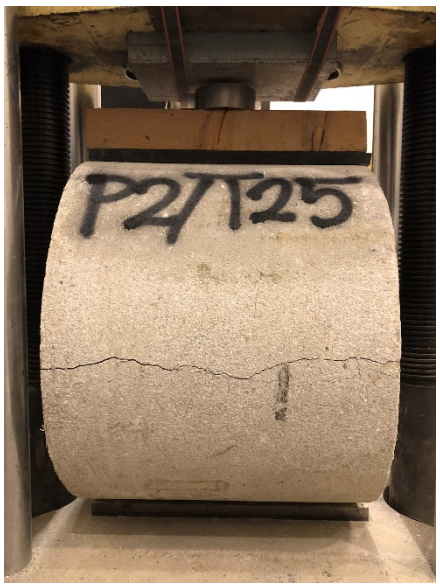

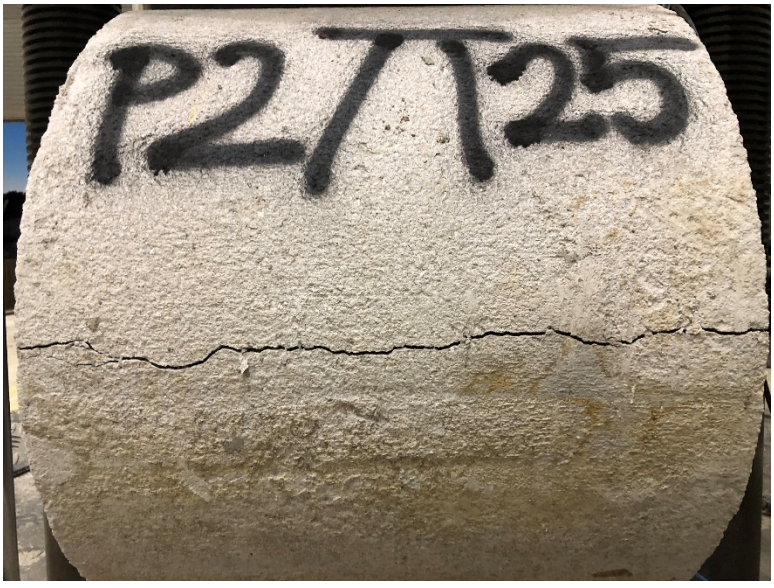

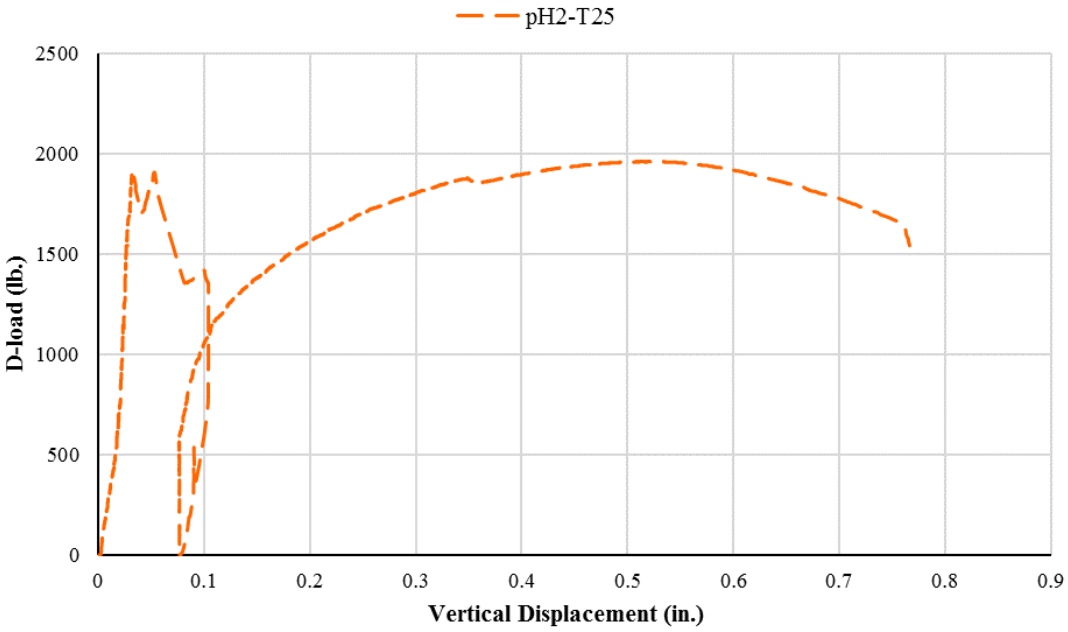
pH2-T25
2500
2000
1500
1000
500
0
D-load (lb.)
0
0.1
0.2
0.3
0.4
0.5
0.6
0.7
0.8
0.9
Vertical Displacement (in.)

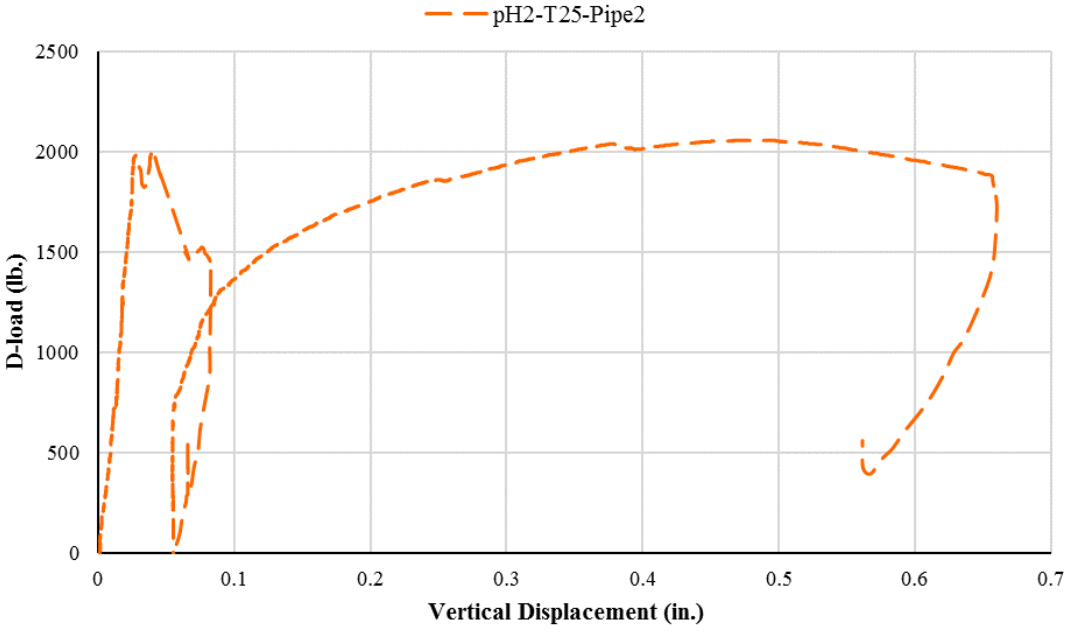
pH2-T25-Pipe2
2500
2000
1500
1000
500
0
D-load (lb.)
0
0.1
0.2
0.3
0.4
0.5
0.6
0.7
Vertical Displacement (in.)

pH 4 – T 50:

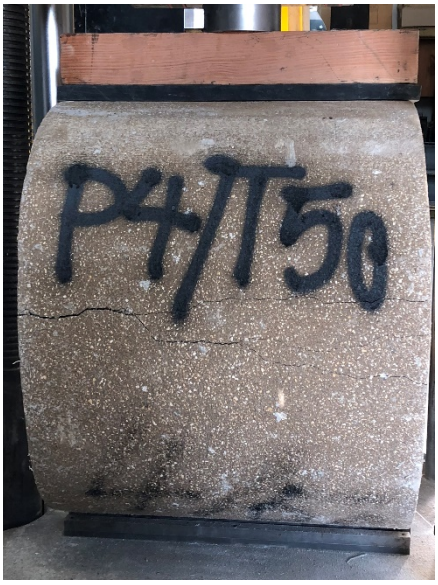

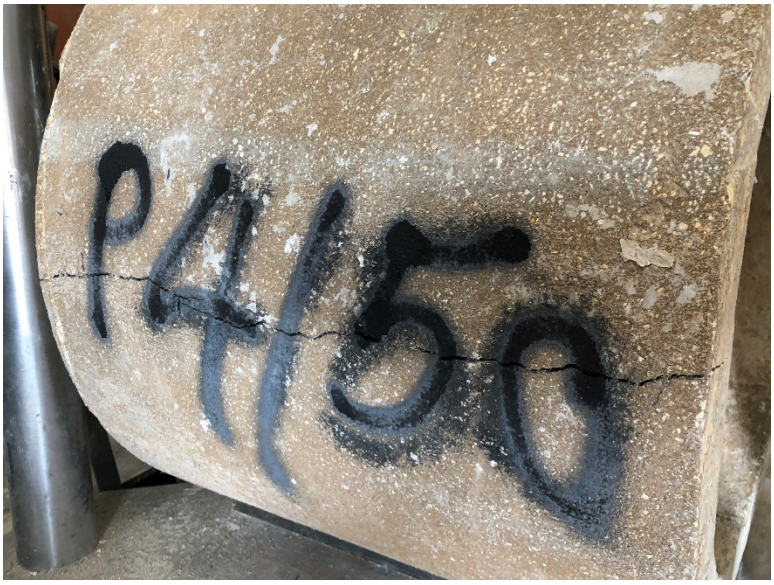

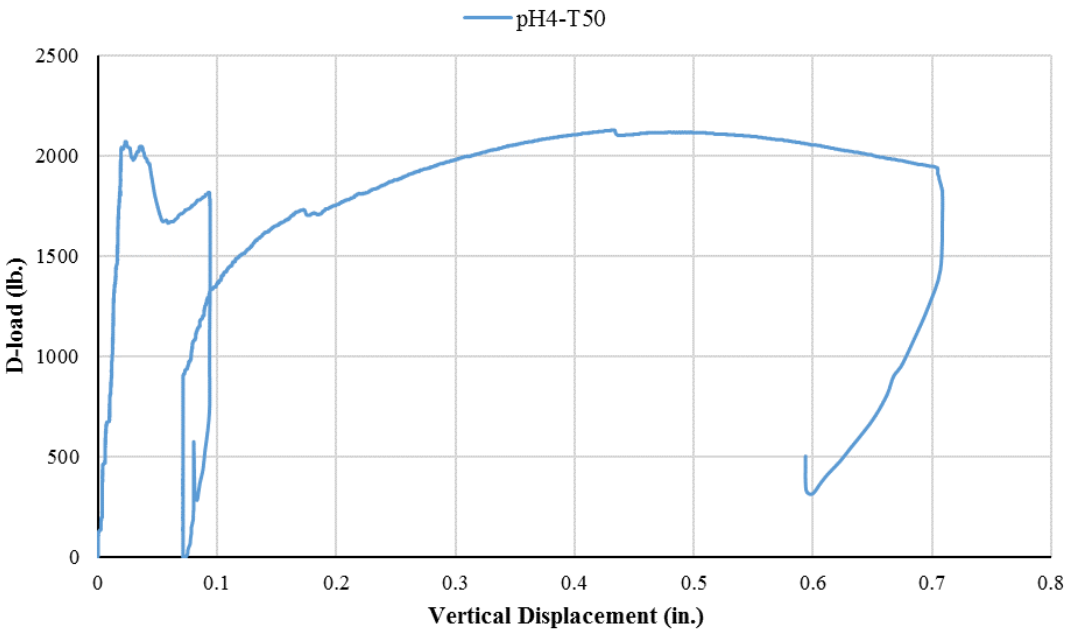
pH4-T50
2500
2000
1500
1000
500
0
D-load (lb.)
0
0.1
0.2
0.3
0.4
0.5
0.6
0.7
0.8
Vertical Displacement (in.)

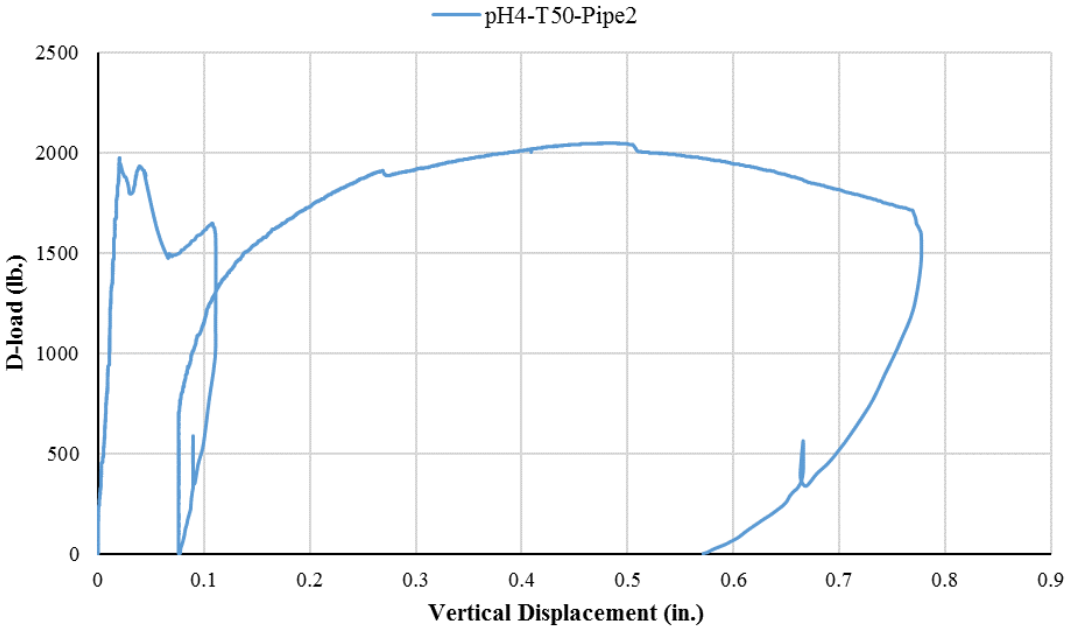
pH4-T50-Pipe2
2500
2000
1500
1000
500
0
D-load (lb.)
0
0.1
0.2
0.3
0.4
0.5
0.6
0.7
0.8
0.9
Vertical Displacement (in.)

pH 4 – T25:

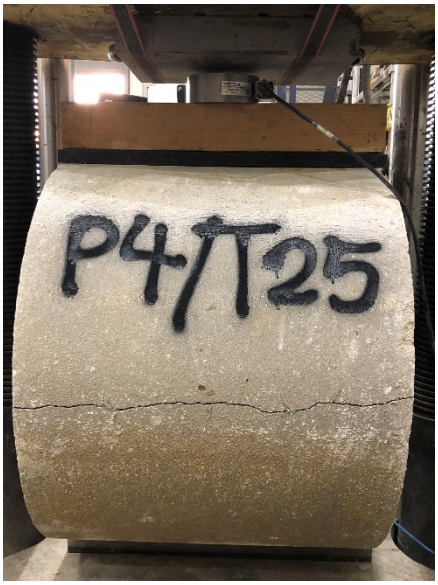

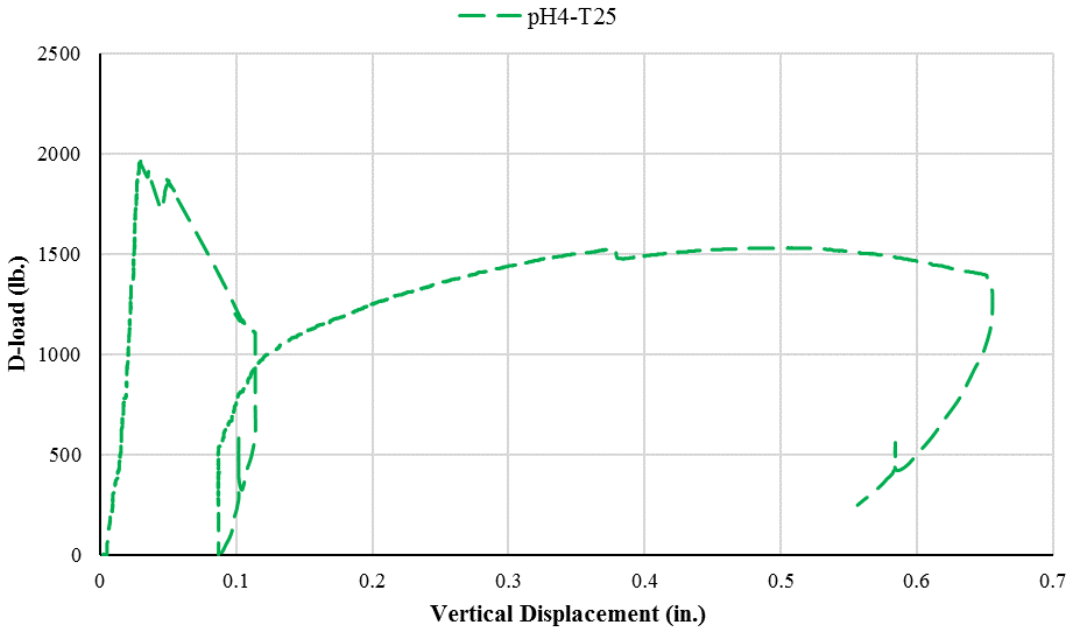
pH4-T25
2500
2000
1500
1000
500
0
D-load (lb.)
0
0.1
0.2
0.3
0.4
0.5
0.6
0.7
Vertical Displacement (in.)

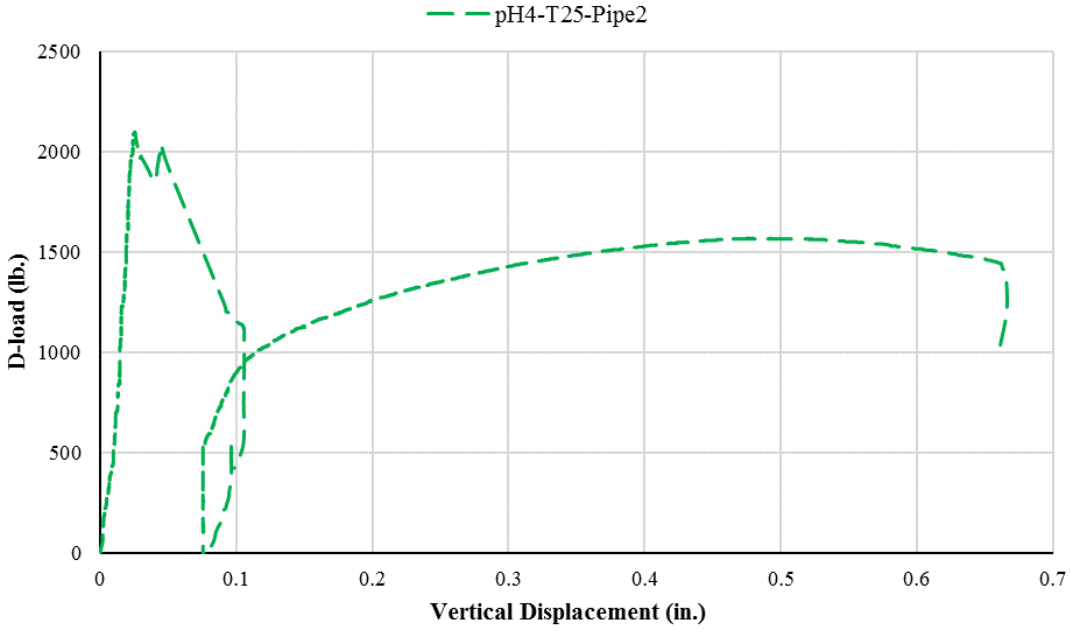
pH4-T25-Pipe2
2500
2000
1500
1000
500
0
D-load (lb.)
0
0.1
0.2
0.3
0.4
0.5
0.6
0.7
Vertical Displacement (in.)

Twelve months tests:

pH 2 – T50:

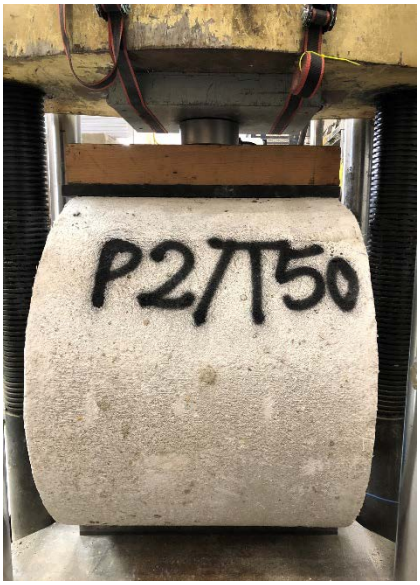

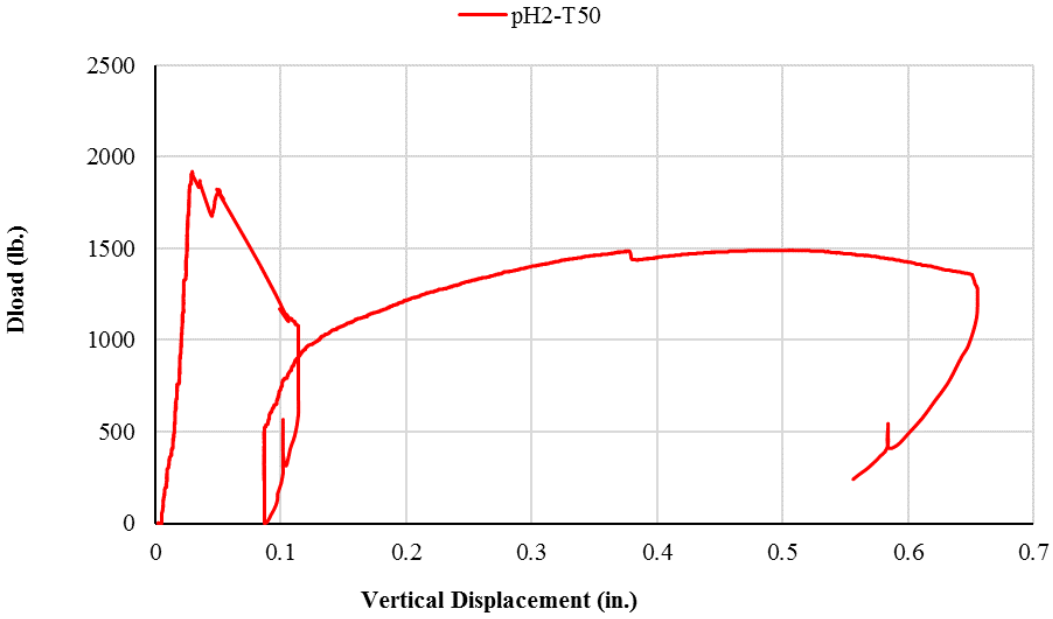
pH2-T50
2500
2000
1500
1000
500
0
Dload (lb.)
0
0.1
0.2
0.3
0.4
0.5
0.6
0.7
Vertical Displacement (in.)

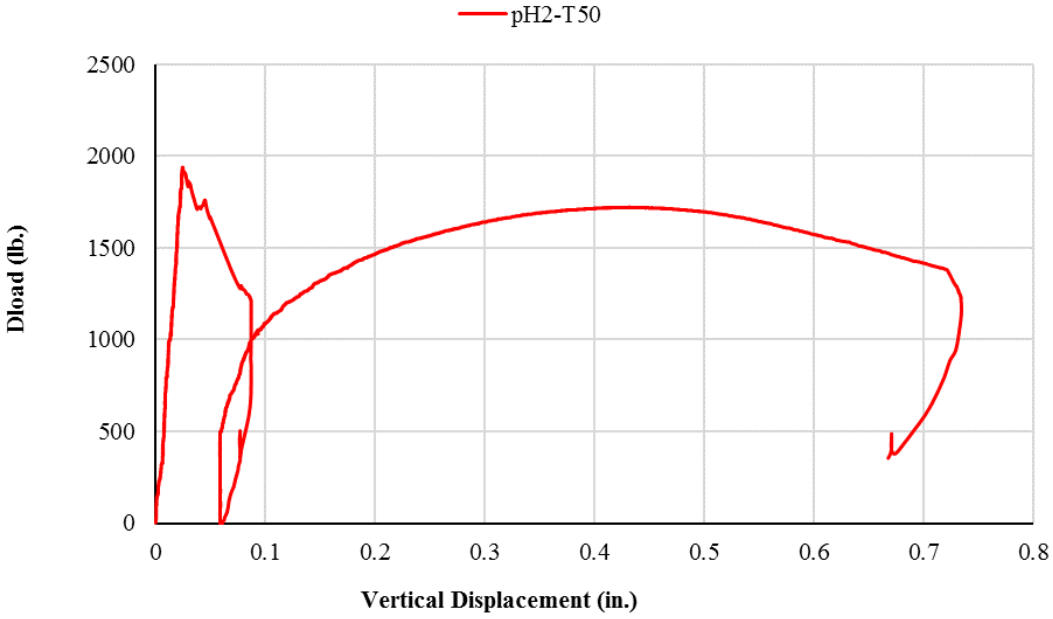
pH2-T50
2500
2000
1500
1000
500
0
Dload (lb.)
0
0.1
0.2
0.3
0.4
0.5
0.6
0.7
0.8
Vertical Displacement (in.)

pH 4 – T25:

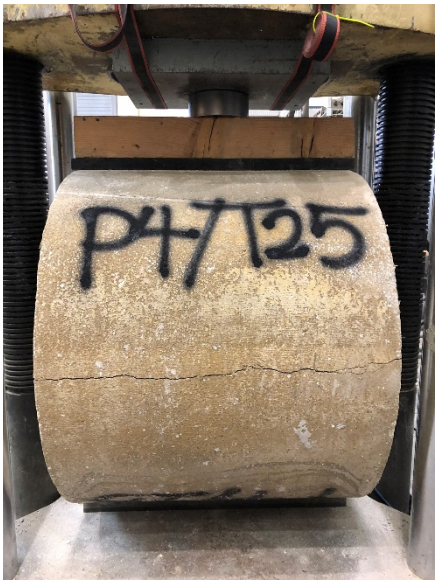
P4/T25


P4/T25

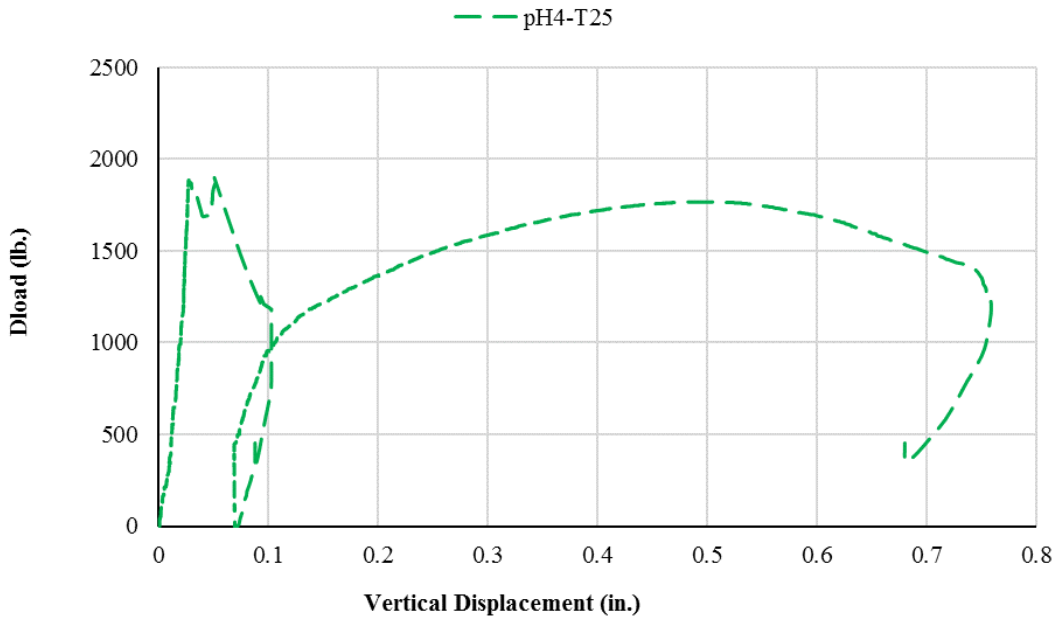
pH4-T25
2500
2000
1500
1000
500
0
Dload (lb.)
0
0.1
0.2
0.3
0.4
0.5
0.6
0.7
0.8
Vertical Displacement (in.)

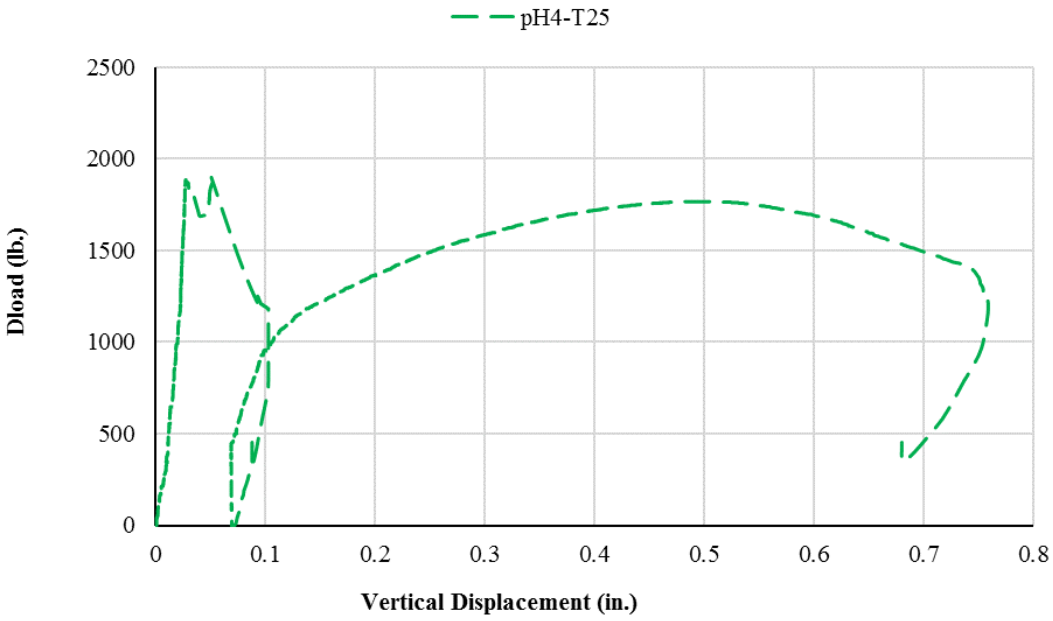
pH4-T25
2500
2000
1500
1000
500
0
Dload (lb.)
0
0.1
0.2
0.3
0.4
0.5
0.6
0.7
0.8
Vertical Displacement (in.)

APPENDIX II: EDX ANALYSIS RESULTS

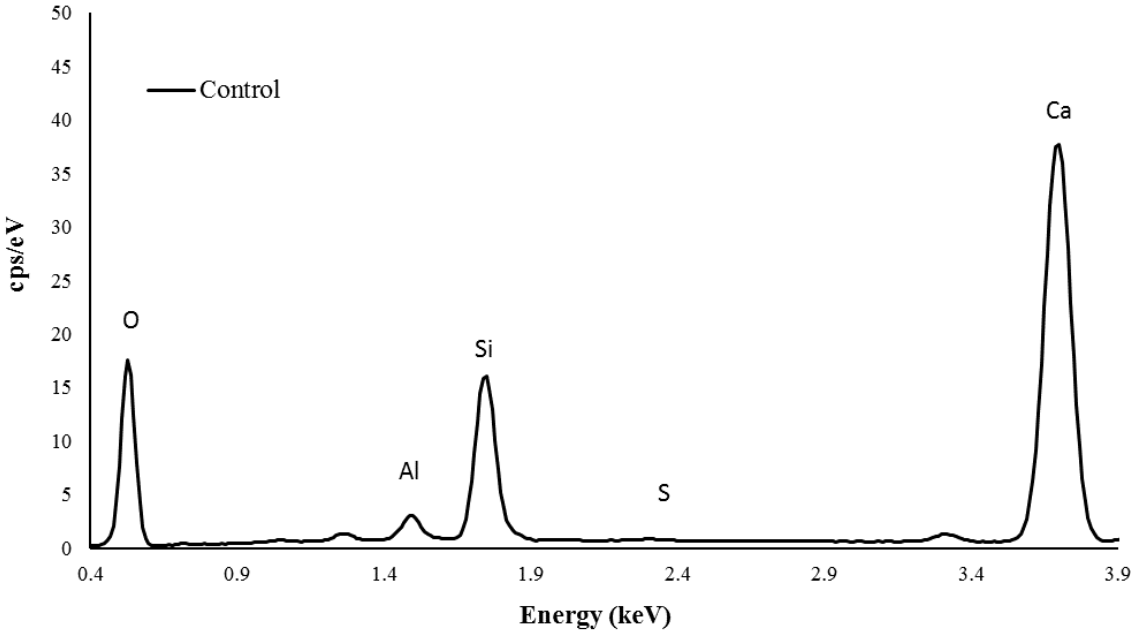

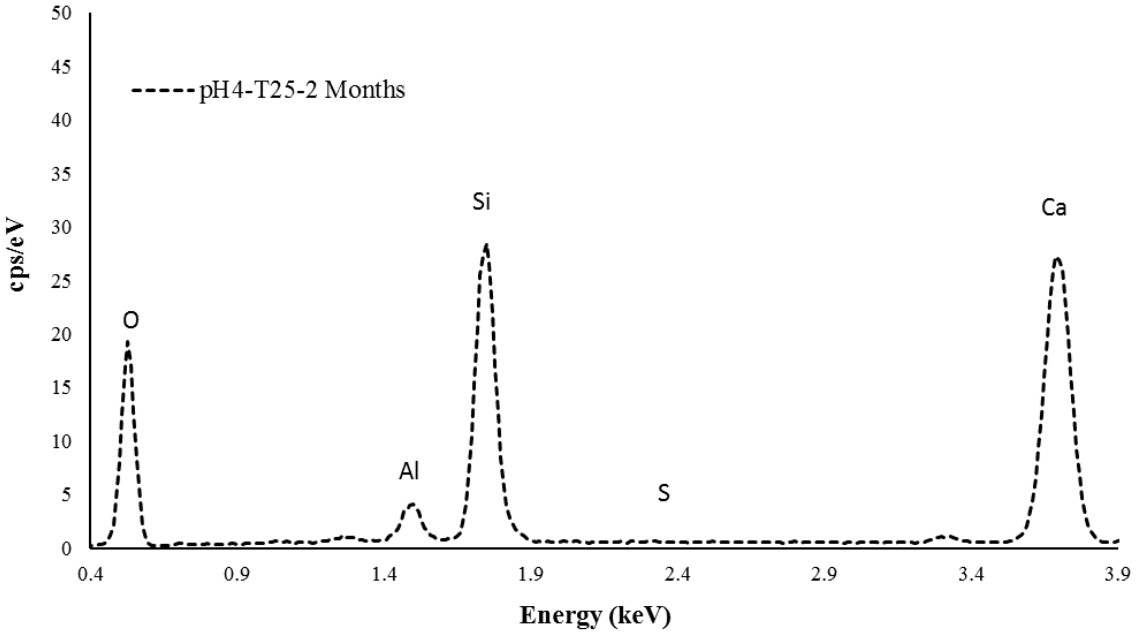

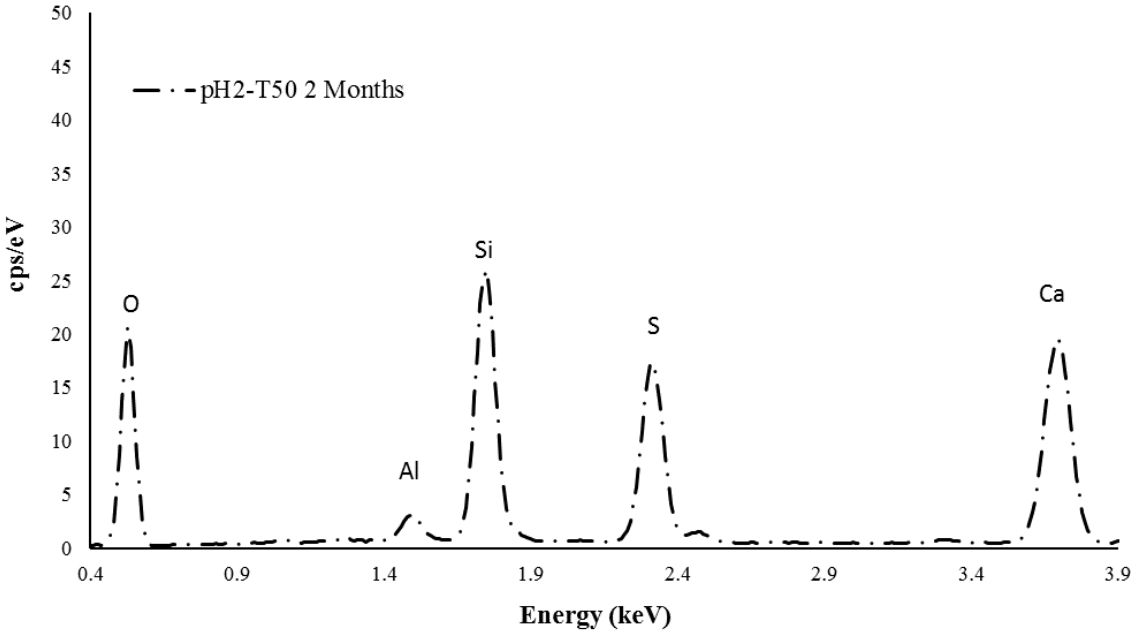
pH2-T50 2 Months
cps/eV
Energy (keV)
O
Al
Si
S
Ca

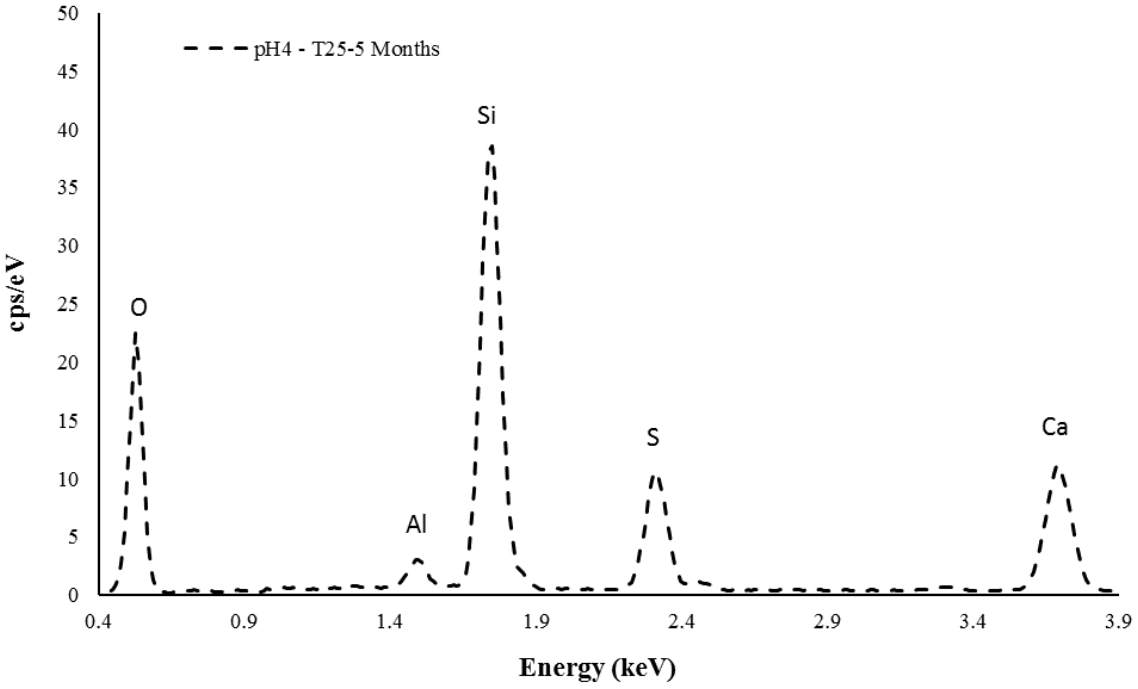
pH4 - T25-5 Months
cps/eV
Energy (keV)
O
Al
Si
S
Ca

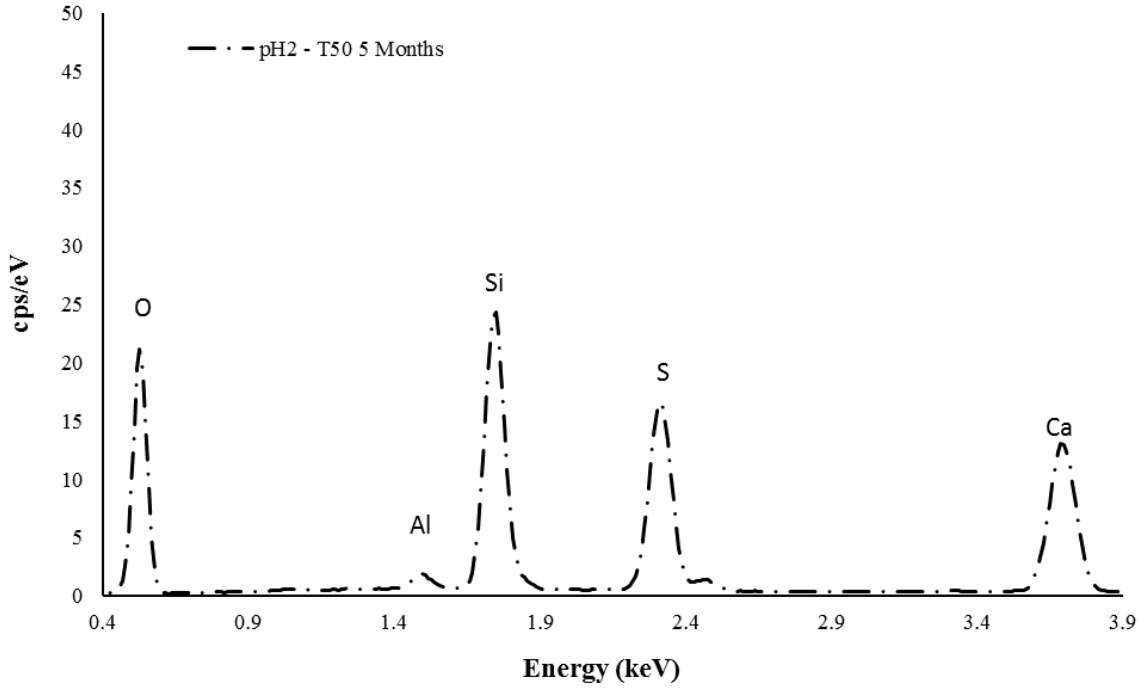
pH2 - T50 5 Months
cps/eV
Energy (keV)
O
Al
Si
S
Ca
0
5
10
15
20
25
30
35
40
45
50
0.4
0.9
1.4
1.9
2.4
2.9
3.4
3.9

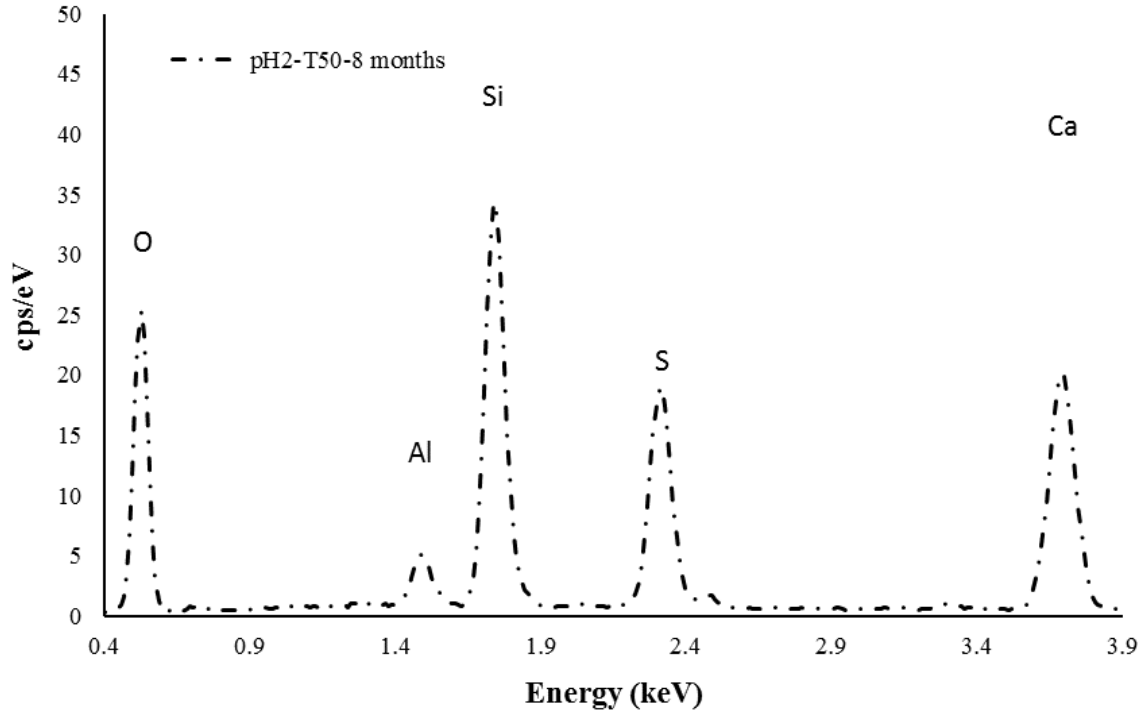
pH2-T50-8 months
cps/eV
Energy (keV)
O
Al
Si
S
Ca
0
5
10
15
20
25
30
35
40
45
50
0.4
0.9
1.4
1.9
2.4
2.9
3.4
3.9

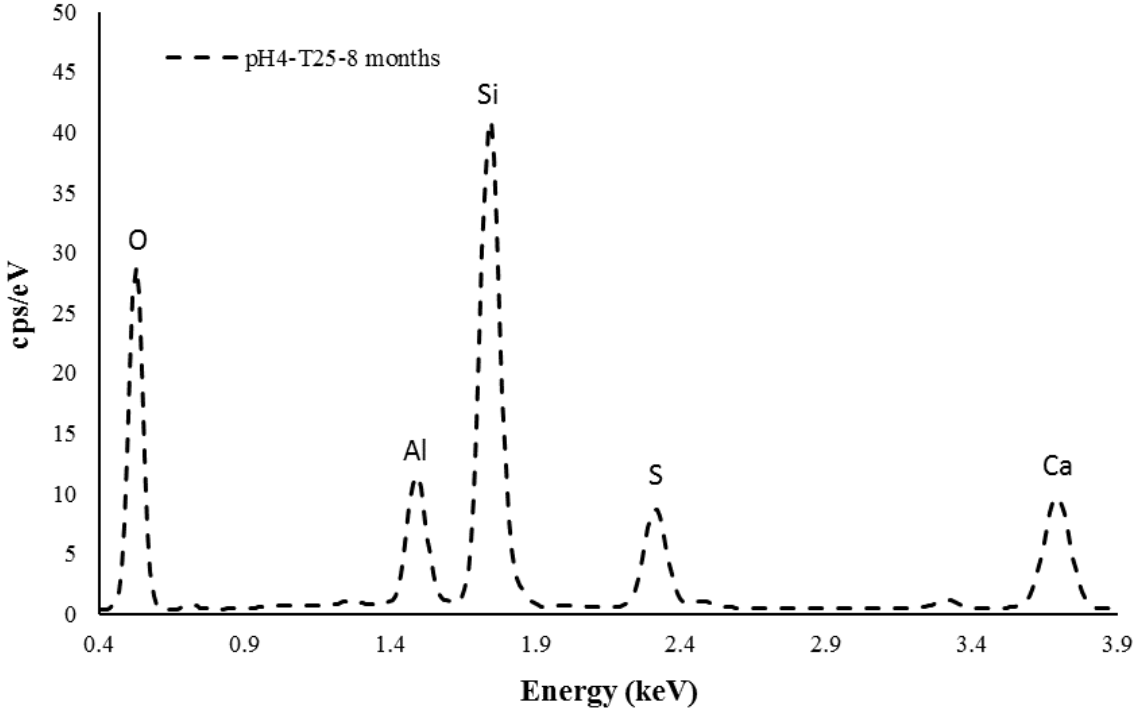
pH4-T25-8 months
cps/eV
Energy (keV)
O
Al
Si
S
Ca
0
5
10
15
20
25
30
35
40
45
50
0.4
0.9
1.4
1.9
2.4
2.9
3.4
3.9

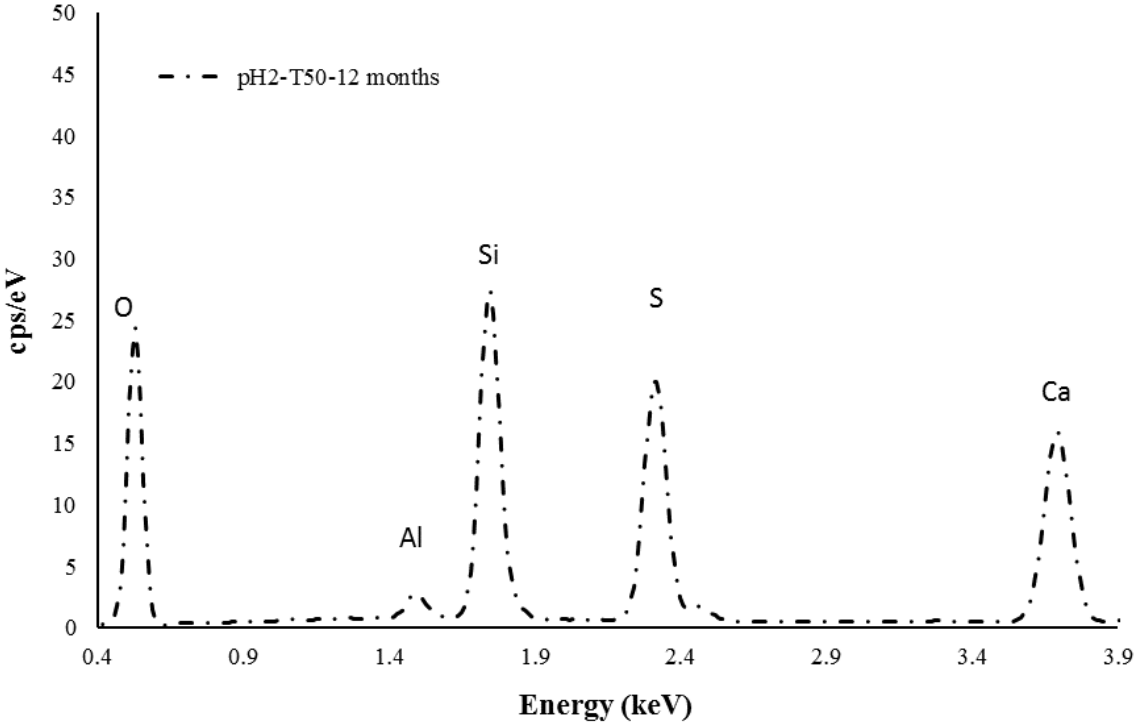
pH2-T50-12 months
cps/eV
Energy (keV)
O
Al
Si
S
Ca
0
5
10
15
20
25
30
35
40
45
50
0.4
0.9
1.4
1.9
2.4
2.9
3.4
3.9

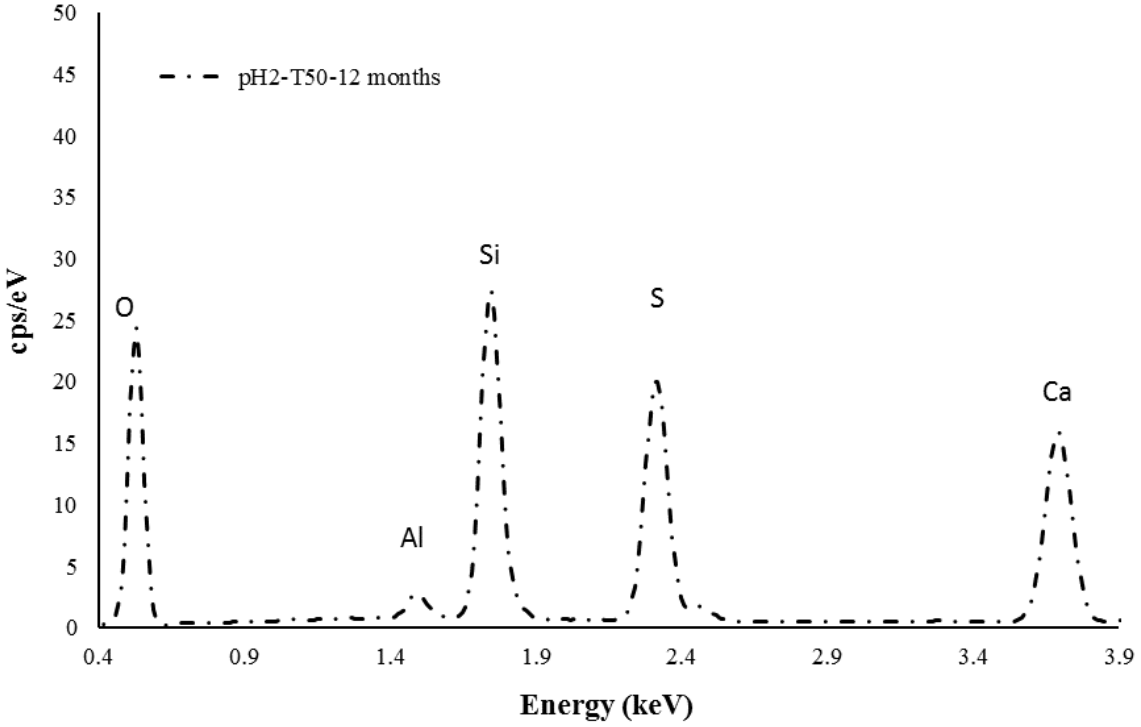
pH2-T50-12 months
cps/eV
Energy (keV)
O
Al
Si
S
Ca
50
45
40
35
30
25
20
15
10
5
0
0.4
0.9
1.4
1.9
2.4
2.9
3.4
3.9

REFERENCES

[1] Drainage Manual, Florida Department of Transportation, 2018.

[2] Culvert and Service Life Estimator, Version 5.5.1.0, Florida Department of Transportation Corrosion Research Laboratory, 2019.

[3] Davies, J.P., Clarke, B.A., Whiter, J.T. and Cunningham, R.J., “Factors influencing the structural deterioration and collapse of rigid sewer pipes,” Urban Water, Vol. 3, No. 1-2, 2001, pp. 73-89.

[4] Parande, A.K., Ramsamy, P.L., Ethirajan, S., Rao, C.R.K. and Palanisamy, N., “Deterioration of reinforced concrete in sewer environments”, Proceedings of the Institution of Civil Engineers-Municipal Engineer, Vol. 159, No. 1, 2006.

[5] Sulikowski, J., and Kozubal, J., “The durability of a concrete sewer pipeline under deterioration by sulphate and chloride corrosion”, Procedia Engineering, Vol.153, 2016, pp. 698-705.

[6] Busba, E., and Sagüés, A. A., "Localized corrosion of embedded steel in cracked reinforced concrete pipes" Corrosion, Vol. 69, No.4, 2013, pp. 403-416.

[7] Sagues, A.A., Peña, J., Cotrim, C., Pech-Canul, M. and Urdaneta, I., “Corrosion Resistance and Service Life of Drainage Culverts”, University of South Florida Tampa, Report No. WPI 0510756, 2001.

[8] Wilson, A., and Abolmaali, A., “Performance of synthetic fiber-reinforced concrete pipes”, Journal of Pipeline Systems Engineering and Practice, Vol. 5, No. 3, 2014, p. 04014002.

[9] Park, Y., Abolmaali, A., Kim, Y. H., & Ghahremannejad, M., “Compressive strength of fly ash-based geopolymer concrete with crumb rubber partially replacing sand”, Construction and Building Materials, Vol. 118, 2016, pp. 43-51.

[10] Rahmani, E., Dehestani, M., Beygi, M. H. A., Allahyari, H., and Nikbin, I. M., “On the mechanical properties of concrete containing waste PET particles”, Construction and Building Materials, Vol. 47, 2013, pp. 1302-1308.

[11] Park, Y., Abolmaali, A., Attiogbe, E., and Lee, S. H., “Time-Dependent Behavior of Synthetic Fiber-Reinforced Concrete Pipes under Long-Term Sustained Loading”, Transportation Research Record: Journal of the Transportation Research Board, No. 2407, 2014, pp. 71-79.

[12] ASTM International. ASTM C1818-18 Standard Specification for Synthetic Fiber Reinforced Concrete Culvert, Storm Drain, and Sewer Pipe. West Conshohocken, PA; ASTM International, 2018

[13] Wilson, Ashley, Ali Abolmaali, Yeonho Park, and Emmanuel Attiogbe. "Research and Concepts Behind the ASTM C1818 Specification for Synthetic Fiber Concrete Pipes." In Concrete Pipe and Box Culverts. ASTM International, 2017.

[14] Mostafazadeh, M., and Abolmaali, A., “Shear Behavior of Synthetic Fiber Reinforced Concrete”, Advances in Civil Engineering Materials, Vol. 5, No. 1, 2016, pp. 371-386.

[15] Ghahremannejad, Masoud, Maziar Mahdavi, Arash Emami Saleh, Sina Abhaee, and Ali Abolmaali. "Experimental investigation and identification of single and multiple cracks in synthetic fiber concrete beams." Case Studies in Construction Materials 9 (2018): e00182.

[16] Ghahremannejad, Masoud, Ali Abolmaali, and Maziar Mahdavi. "The Effects of pH and Temperature on Compressive Strength of Synthetic Fiber-Reinforced Concrete Cylinders Exposed to Sulfuric Acid." Advances in Civil Engineering Materials 7, no. 1 (2018): 403-413.

[17] Alcock, B., Cabrera, N. O., Barkoula, N. M., Reynolds, C. T., Govaert, L. E., and Peijs, T., "The effect of temperature and strain rate on the mechanical properties of highly oriented polypropylene tapes and all-polypropylene composites", Composites Science and Technology, Vol. 67, No. 10, 2007, pp. 2061-2070.

[18] Khajuria, A., Bohra, K., and Balaguru, P., "Long term durability of synthetic fibers in concrete", Special Publication, Vol. 126, 1991, pp. 851-868.

[19] Xiao, J., and Falkner, H., "On residual strength of high-performance concrete with and without polypropylene fibres at elevated temperatures", Fire Safety Journal, Vol. 41, No. 2, 2006, pp. 115-121.

[20] Bertron, A., Duchesne, J., and Escadeillas, G., "Accelerated tests of hardened cement pastes alteration by organic acids: analysis of the pH effect", Cement and Concrete Research, Vol. 35, No. 1, 2005, pp. 155-166.

[21] Kaufmann, J. P., "Durability performance of fiber reinforced shotcrete in aggressive environment", In World Tunnelling Congress, 2014.

[22] Araghi, H. J., Nikbin, I. M., Reskati, S. R., Rahmani, E., and Allahyari, H. "An experimental investigation on the erosion resistance of concrete containing various PET particles percentages against sulfuric acid attack", Construction and Building Materials, Vol. 77, 2015, pp. 461-471.

[23] Kim, B., Boyd, A. J., Kim, H. S., and Lee, S. H., “Steel and synthetic types of fibre reinforced concrete exposed to chemical erosion”, Construction and Building Materials, Vol. 93, 2015, pp. 720-728.

[24] Nematzadeh, M., and Fallah-Valukolaee, S., “Erosion resistance of high-strength concrete containing forta-ferro fibers against sulfuric acid attack with an optimum design”, Construction and Building Materials, Vol. 154, 2017, pp. 675-686.

[25] Rafieizonooz, Mahdi, Mohd Razman Salim, Jahangir Mirza, Mohd Warid Hussin, Rawid Khan, and Elnaz Khankhaje. "Toxicity characteristics and durability of concrete containing coal ash as substitute for cement and river sand." Construction and Building Materials 143 (2017): 234-246.

[26] Reynolds, Frederick H. "Thermally accelerated aging of semiconductor components." Proceedings of the IEEE 62, no. 2 (1974): 212-222.

[27] Naser, J. "Evaluating the effects of aging on electronic instrument and control circuit boards and components in nuclear power plants." Electric Power Research Institute: California, USA (2005).

[28] Pinto, R., S. Hobbs, and K. Hover. Accelerated aging of concrete: a literature review. No. FHWA-RD-01-073. Turner-Fairbank Highway Research Center, 2002.

[29] Diamond, Sidney. "The microstructure of cement paste and concrete—a visual primer." Cement and Concrete Composites 26, no. 8 (2004): 919-933.

[30] Mehta, P. Kumar, and Paulo JM Monteiro. "Concrete Microstructure, Properties and Materials." (2017).

[31] Qin, Xiao-chuan, Shao-ping Meng, Da-fu Cao, Yong-ming Tu, Natalia Sabourova, Niklas Grip, Ulf Ohlsson, Thomas Blanksvärd, Gabriel Sas, and Lennart Elfgren. "Evaluation of freeze-thaw damage on concrete material and prestressed concrete specimens." Construction and Building Materials 125 (2016): 892-904.

[32] Hartell, Julie Ann, Andrew J. Boyd, and Christopher C. Ferraro. "Sulfate attack on concrete: effect of partial immersion." Journal of Materials in Civil Engineering 23, no. 5 (2010): 572-579.

[33] Jewell, Robert B., Robert F. Rathbone, Tristana Y. Duvallet, T. L. Robi, and Kamyar C. Mahboub. "Fabrication and testing of low-energy calcium sulfoaluminate-belite cements that utilize circulating fluidized bed combustion by-products." Coal Combustion and Gasification Products Journal 7 (2015): 9-18.

[34] Joorabchian, Seyed M. "Durability of concrete exposed to sulfuric acid attack." Theses and dissertations. Presented to Ryerson University, Toronto, Ontario, Canada (2010).

[35] Upadhyay, Santosh K. Chemical kinetics and reaction dynamics. Springer Science & Business Media, 2007.

[36] ASTM C. 39, “Standard Method for Compressive Strength of Cylindrical Concrete Specimens”, ASTM International, West Conshohocken, PA, 2001.

[37] ASTM C76-19, “Standard Specification for Reinforced Concrete Culvert, Storm Drain, and Sewer Pipe”, West Conshohocken, PA; ASTM International, 2019.

[38] ASTM C497-19 Standard Test Methods for Concrete Pipe, Concrete Box Sections, Manhole Sections, or Tile. West Conshohocken, PA; ASTM International, 2019.

[39] National Academies of Sciences, Engineering, and Medicine. 2015. Service Life of Culverts. Washington, DC: The National Academies Press.

[40] Hurd, John Owen. "Service life model verification for concrete pipe culverts in Ohio." Transportation Research Record 1191 (1988): 118-131.

[41] Hadipriono, Fabian C., Richard E. Larew, and Oh-Young Lee. "Service life assessment of concrete pipe culverts." Journal of transportation engineering 114, no. 2 (1988): 209-220.

[42] Hyams, D. G. "CurveExpert Professional." See http://docs. curveexpert. net/curveexpert/pro (2012).

[43] Davoodi, Mohammad Reza, Maziar Mahdavi, and Seyed Amin Mostafavian. "Experimental and Analytical Determination of Dynamic Properties of a Steel Frame with Bolted Flange Joints." In Proceedings of International Conference on Engineering and Information Technology “ICEIT2012”, Toronto, Canada, Sep, pp. 17-18. 2012.

[43] Davoodi, Mohammad Reza, Maziar Mahdavi, and Seyed Amin Mostafavian. "Experimental and Analytical Determination of Dynamic Properties of a Steel Frame with Bolted Flange Joints." In Proceedings of International Conference on Engineering and Information Technology “ICEIT2012”, Toronto, Canada, Sep, pp. 17-18. 2012.